INVESTIGATING BLOOD CELL COMMUNICATION WITH NOVEL SAMPLE HANDLING AND MICROFLUIDIC TECHNOLOGY

By

Kari B. Anderson

A DISSERTATION

Submitted to
Michigan State University
in partial fulfillment of the requirements
for the degree of

Chemistry - Doctor of Philosophy

2013

ABSTRACT

INVESTIGATING BLOOD CELL COMMUNICATION WITH NOVEL SAMPLE HANDLING AND MICROFLUIDIC TECHNOLOGY

By

Kari B. Anderson

Puringergic receptor signaling events in platelets is a major determinant in platelet function. ADP binding to the P2Y-type receptors on platelet membranes, and the subsequent pathways evoked from this type of binding, is well-established. However, an understanding activity of the ATP-sensitive P2X1 platelet receptor is incomplete due to rapid receptor desensititzation. To circumvent this problem, most studies aimed at investigating P2X1 platelet activity require that the platelet samples contain apyrase in order to reduce already-existing levels of ATP. Of course, one drawback to this method is that the apyrase will also rapidly degrade any added ATP. Here, I describe a methoed that employs the reported P2X1 inhibitor NF449 to sensitize platelets in the absence of any added apyrase. Sensitization is verified by spectrofluorimetric determination of Ca^{2+} entry into the platelets after stimulation with concentrations of ATP ranging from 67 nM to 10 μM. Results suggest that sensitization of the P2X1 receptor by NF449 is not necessarily dependent upon the inhibitor concentration, but rather the ratio of the inhibitor and exogenously-added ATP concentrations. The sensitization by the NF449 was also found to be highly time-dependent.

A simple and inexpensive approach to fabricate polystyrene devices that is based upon molding polystyrene (PS) from Petri dishes against PDMS molds was developed. The ability to incorporate microchannels in polystyrene and integrate the resulting device

with standard laboratory equipment such as an optical plate reader for analyte readout and pipets for fluid propulsion is described. Integration of the microfluidic device with these off-chip functions (sample delivery and readout) enables high-throughput screens and analyses. Furthermore, this polystyrene device was used to monitor two endothelial cell processes. One experiment involved the fluorescence measurement of nitric oxide (NO) produced within an endothelial cell line following stimulation with ATP. The result was a four-fold increase in NO production (as compared to a control), with this receptor-based mechanism of NO production verifying the maintenance of cell receptors following immobilization onto the PS substrate. The ability to monitor cellular uptake was also demonstrated by optical determination of Ca^{2+} into endothelial cells following stimulation with the Ca^{2+} ionophore A20317. The result was a significant increase (42%) in the calcium uptake in the presence of the ionophore, as compared to a control (17%) ($p < 0.05$).

The PS device was further integrated with a polyester membrane in order to study drug transport across the membrane. However, significant absorption of drugs still occurred so a device made only of PS was fabricated using an epoxy mold and hydraulic press to embed channels and seal devices. The result was a device with millimeter sized channels, but the ability to rapidly fabricate these devices was lost. Thus, 3 Dimensional (3D) printing, commonly used for producing design prototypes in industry to fabricate a reusable, high throughput, 3D printed fluidic device that enables flow and incorporates a membrane above a channel in order to study drug transport and affect cells.

Catullus 85:

Odi et amo. Quare id faciam, fortasse requiris?

Nescio, sed fieri sentio et excrucior.

ACKNOWLEDGEMENTS

I would first like to thank the organizations without whom this research could not be funded including Michigan State University (MSU) for research and travel funding, the National Institutes of Health, the Cystic Fibrosis Foundation and Merck.

Secondly, I would like to thank my guidance committee Dr. A. Daniel Jones, Dr. Greg Swain and Dr. Weliky who were always willing to discuss research ideas. I would also like to thank Dr. Kathy Severin whom I taught for on numerous occasions. She was a great teaching mentor and always willing to assist graduate students through training or instrument usage.

The ability to collaborate with other departments at MSU has been crucial to moving certain projects forward. I would like to extend my thanks to the MSU RTSF Mass Spectrometry Core for instrument usage, Dr. Per Askeland in Engineering for help obtaining scanning electron microscopy images, Dr. Brian Rook in the Composite Materials and Structures Center for hydraulic press training, and Dr. Brian Wright in the Department of Electrical and Computer Engineering for assistance in 3 dimensional (3D) printing. Lastly, I would like to thank Tekna Inc. design firm in Kalamazoo, Mi for their assistance in creating the necessary 3D files for printing.

Collaboration has also been integral to my success within the Spence group so, I would like to specifically thank Dr. Stephen Halpin and Ms. Sarah Lockwood for help with the polystyrene and 3D printing projects, respectively. Additionally, I would also like to acknowledge members of the Spence research group from 2008 – 2013 for their knowledge and cooperation. Much of the work described herein entails blood draws,

buffer preparation, cell culture and device fabrication and to have a group willing to cooperate with one another on these aspects makes the work go a lot faster.

I would also like to thank Dr. Dana Spence for his role as advisor in this work. The research environment he creates fosters not only intellectual experimental design, but also creativity, which allows his graduate students to grow with every success and failure. I admire his devotion to his family and the graduate students that work for him, both past and present. I am happy at the end of my graduate career to call him mentor and friend.

Graduate school would be a hellish process to go through alone and I am grateful for the friends I made here as they made the process more enjoyable and their support made the hoops worth jumping through. Specifically, Suzanne Letourneau, my partner in crime from the beginning! Suzanne and I could always count on each other for early morning rabbit surgeries, late night study sessions and baking adventures. I would also like to thank Yimeng Wang (Meng Meng) for being such a good friend to me and becoming more in tune with American sarcasm every day that she can see through even the most offhand remarks. I could not ask for a better research group, five and forever!

Frankly, none of this would have been possible without the support of my family, specifically my parents, who have always been committed to my education and their support was invaluable over the course of my graduate career. Finally, I would like to thank Andy for his dedication to this work, his encouragement and willingness to let me figure out my path in life. His patience and love are unmatched and I appreciate his commitment to me now more than ever.

TABLE OF CONTENTS

LIST OF FIGURES

CHAPTER 1: INTRODUCTION

1.1 The Platelet and the Vascular System

The human body contains between 5-6 L of whole blood, 55% of which is comprised of plasma (water, glucose, proteins, electrolytes, hormones, clotting factors) and 45% consisting of red blood cells (RBCs), platelets and leukocytes. The RBC's primary role in the bloodstream is oxygen delivery throughout the body, while leukocytes protect the body from infection. In a blood vessel, RBCs flow in the middle of the vessel, which forces platelets towards the edge of the vessel wall due to their size. This allows for platelets to be closer to the site of potential vessel injuries. In general, platelets circulate in the bloodstream in an inactive state, but upon vessel wall injury, platelets are activated, initiating the clotting process, and forming a plug at the injury site. Platelets are discoid in shape, anucleate and are approximately 2-4 μm in size. A healthy individual will have 150-400 x 10^9 platelets per mL of whole blood[1] with the lifespan of a platelet being 7-10 days.

1.1.1 Blood Vessel Injury, Platelet Activation and Aggregation

A typical blood vessel contains an inner lining of endothelial cells that serve as a barrier between the whole blood and the outside tissue. On the outside of the vessel, smooth muscle cells control the contraction and relaxation of the vessel. As shown in figure 1.1, when a blood vessel is injured, sub endothelial cell collagen is exposed and subsequently, platelets adhere to the injury, become activated and undergo a shape

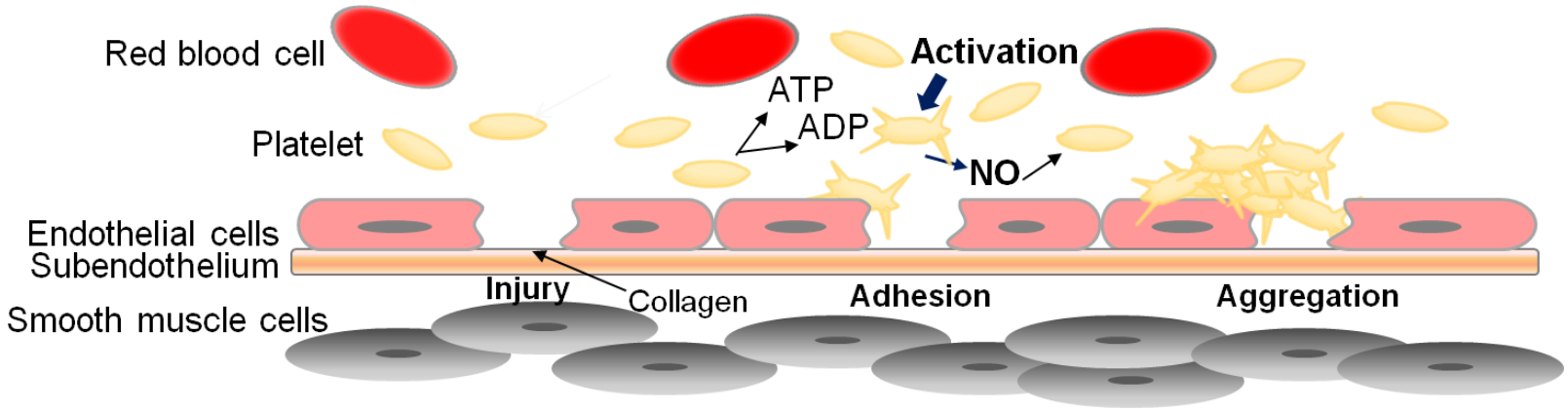

Figure 1.1: Blood vessel injury. For clarity only RBCs and platelets are pictured. A typical blood vessel is comprised of an inner layer of endothelial cells with smooth muscle cells lining the exterior. Upon blood vessel injury, subendothelial collagen is exposed and platelets that come into contact with the collagen become activated, undergo a shape change that results in adhesion, and release ATP and ADP into the bloodstream. As more platelets are recruited to the injury site, aggregation occurs and a plug over the injury site is formed. NO, a platelet inhibitor, is also released by platelets to inhibit further platelet recruitment to the injury site. For interpretation of the reference to color in this and all other figures, the reader is referred to the electronic version of this dissertation

change. Platelets initially bind to the newly exposed collagen (via the $\alpha_2\beta_1$ integrin) directly, as well as von Willebrand factor (vWF, via the GPIb-IX-V receptor), a plasma protein secreted by endothelial cells that binds collagen.[2] Once more platelets are recruited to the injury site; the platelets undergo a shape change where their normally smooth surface becomes adhesive and elongated with projections. During this process, activated platelets undergo granular secretion where additional molecules, released into the bloodstream, promote further aggregation of activated platelets.

Platelets have three types of granules: alpha, lysosomes and dense. The alpha granules secrete fibrinogen and vWF.[3] The alpha granules also contain many proteins involved in platelet adhesion, such as integrins and GPIb-IX-V.[4] The lysosomes contain enzymes involved in protein, lipid and carbohydrate breakdown. The contents of the dense granules are pro aggregatory and include thromboxane A2 (TXA2), adenosine diphosphate (ADP), adenosine triphosphate (ATP), calcium (Ca^{2+}), potassium (K^{+}) and serotonin.[5,6] Granular secretion is caused by an increase in cytosolic Ca^{2+}.[7]

Once secretion occurs and more platelets are recruited to the injury site, the combination of activating molecules, and increases in platelet Ca^{2+} results in conformational changes in integrins on the platelet surface that expose binding sites for fibrinogen.[8] Fibrinogen is what allows the platelets to adhere to one another, but fibrin, vWF, and fibronectin can also promote platelet aggregation. This is the start of the platelet plug, or clot, that will cover the entire injury site and prevent further blood loss.

1.2 Platelet Inhibitors

In the vasculature, there are two endothelial cell derived platelet inhibitors, prostacyclin (PGI2), and nitric oxide (NO), which result in elevated intraplatelet cyclic AMP and cyclic GMP, respectively, while another inhibitor is CD39, an ectonucleotidase.[9] Kinases dependent on cAMP and cGMP will affect several platelet signaling mechanisms, including Ca^{2+} mobilization.[10] Ca^{2+} is an important signaling molecule in platelets and is needed for cytoskeleton rearrangement necessary for shape change,[11] integrin activation necessary for aggregation,[12] and for NO production within the platelet.[13]

1.2.1 Nitric Oxide (NO)

NO is produced when endothelial nitric oxide synthase (eNOS) converts L-arginine to L-citrulline producing NO as a byproduct. Endothelial derived NO is not only a platelet inhibitor, but also promotes vasodilation, or widening of the blood vessel, via smooth muscle cell relaxation.[14,15] NO inhibits platelet function by binding to soluble guanylyl cyclase[16] resulting in elevated levels of cGMP,[17, 18] which activates protein kinase G (PKG).[9] PKG affects a mechanism called "store operated Ca^{2+} entry" where Ca^{2+} enters from the extracellular medium.[19] Elevated cGMP levels inhibit phosphodiesterase III (PDE III) and leads to an increase in cyclic adenosine monophosphate (cAMP) levels[20,21] causing activation of protein kinase A (PKA).[22] Elevated levels of PKA inhibit protein kinase C (PKC) and phospholipase C (PLC) activations and thus, intracellular Ca^{2+} mobilization.[23,24] This inhibition triggers a

decrease in cytosolic Ca^{2+},[25] which results in the inhibition of GPIIb-IIIa's ability to change conformations into its active form, which normally would allow for platelet interaction with fibrinogen.[26,27] Furthermore, the eNOS pathway for NO synthesis also occurs in platelets.[28] Platelet derived NO is also released into the bloodstream before platelets are activated[29] and during aggregation.[13,28] The platelet derived NO (micromolar) is released during aggregation and prevents further platelet aggregation and adhesion to the injury site.[13,30]

1.2.2 Prostacyclin (PGI2)

Prostacyclin binds to platelets via the prostacyclin receptor (IP receptor), which is only expressed on platelets[31] and smooth muscle cells.[32] It inhibits platelet activation induced by ADP, thrombin, collagen and TXA2, however, it primarily works through TXA_2.[33]

It has been suggested that P2X1-, a purinergic receptor on the platelet surface, evoked Ca^{2+} response may be less sensitive to PGI2 and NO inhibition by endothelial cells after agonist exposure[34] when compared to the store operated Ca^{2+} release.[**35**] This would explain why platelets are able to respond immediately to endothelial damage given their close proximity to endothelial cells and the inhibitors they release.

1.2.3 Ectonucleotidase CD39

The endothelial enzyme CD39 (NTPDase-1) is also able to inhibit platelet function by converting ATP and ADP to inert AMP[36] and eventually, adenosine by CD73.[37] CD39 does not

directly interact with the platelet itself, but it does interact with the ADP and ATP that platelets release from their granules.[36]

1.3 Purinergic Receptors on the Platelet Surface

Purinergic receptors on the platelet surface regulate activation by ATP or ADP binding. A simplified version of P2 receptor activation is shown in figure 1.2. Two receptors, P2Y1 and P2Y12 are G-protein coupled and bind ADP, while the third, P2X1, binds ATP, exclusively. ADP binds the P2Y1 receptor leading to G_q mediated activation of PLC, which leads to Ca^{2+} release intracellular stores, shape change, and reversible aggregation.[38,39] When ADP binds to G_i associated P2Y12, it leads to inhibition of adenylyl cyclase (AC) and enhanced aggregation.[38] PGI_2 inhibits platelet activation by increasing platelet cAMP levels via AC activation.[40] Since P2Y12 inhibits AC, this is in opposition to the endothelial cell release inhibitor PGI_2. Activation of both P2Y1 and P2Y12 are needed for platelets to exhibit a normal aggregation response. Inhibition of either receptor is enough to block ADP-induced platelet aggregation.[41]

The P2X1 receptor, one of seven sub types of P2X receptors[42], on the platelet surface is an ATP-gated cation channel that contains two transmembrane domains linked by a large extracellular loop.[43,44] The extracellular loop contains the binding site for ATP and competitive antagonists, while the transmembrane portion of the receptor forms the cation channel.[45] While there is not a solved structure for P2X1, X-ray crystallography has been used to determine the structure of P2X4 in the closed state[43] and with bound ATP.[46] P2X1 is the only P2X receptor

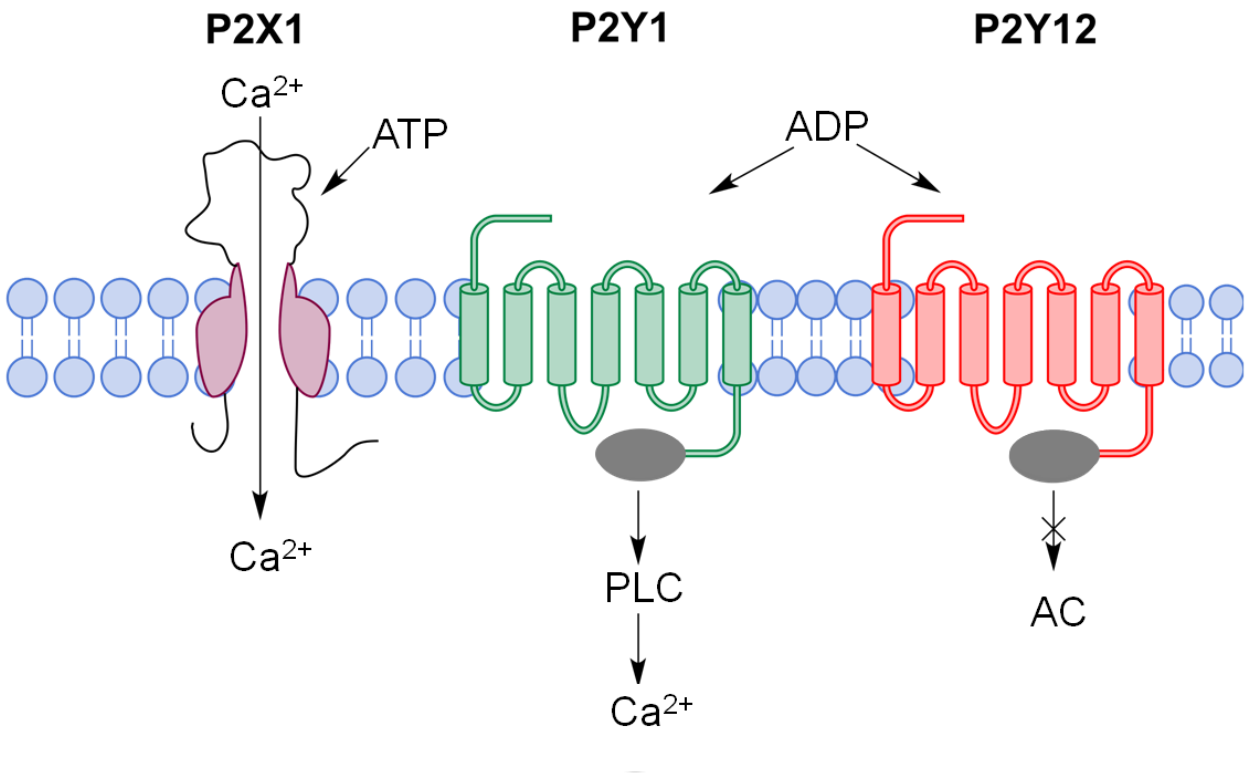

Figure 1.2: P2 receptors on platelet membrane. The platelet membrane has three purinergic receptors on its membrane surface. The P2X1 is a gated cation channel that is activated by ATP. Upon ATP binding there is a rapid Ca^{2+} influx into the platelet. P2Y1 and P2Y12 are both G-protein coupled receptors that bind ADP. When ADP binds P2Y1 it activates PLC, which causes intracellular Ca^{2+} release and subsequent platelet activation. When ADP binds P2Y12 it inhibits AC activity, thus, counteracting the inhibitory effects of PGI2. P2Y12 also enhances platelet aggregation and both P2Y1 and P2Y12 are required for full platelet aggregation.

found in significant quantities on the platelet surface[47] and since ATP binding is the only factor needed for channel opening, P2X1 is also a significant source of rapid Ca^{2+} influx into the platelet following activation.[48] Additionally, the Ca^{2+} influx also leads to membrane depolarization, which is thought to enhance signaling through P2Y1.[49] Previously, it was thought that P2X1 was not needed for proper platelet function,[50] although recent reports suggest this is not the case.[51-53]

Studying the P2X1 receptor's contribution to platelet function is difficult because it undergoes rapid desensitization during purification from whole blood due to spontaneously secreted ATP.[54] By combating the desensitization of P2X1 with a high dose of apyrase and using α,β-methylene-ATP (α,β-me-ATP) or β,γ-methylene ATP (β,γ-me-ATP) as the agonist, activation of P2X1 leads to rapid influx of Ca^{2+} and transient shape change.[54] The structures of ATP, α,β-me-ATP, and β,γ-me-ATP are shown in figure 1.3 where the difference from ATP is the replacement of oxygen with $–CH_2$ so that it cannot be broken down by apyrase. It has also been shown that ATP can stimulate NO production in the platelet and induce platelet aggregation.[51] Additionally, α,β-me-ATP has also been shown to desensitize the P2X1 receptor.[55] There is also literature that suggests a role for P2X1 in early activation of platelets with low concentrations of collagen.[52, 53] A number of disease states are associated with hyperactive platelets and coincidentally, also have bioavailability issues with regard to ATP.

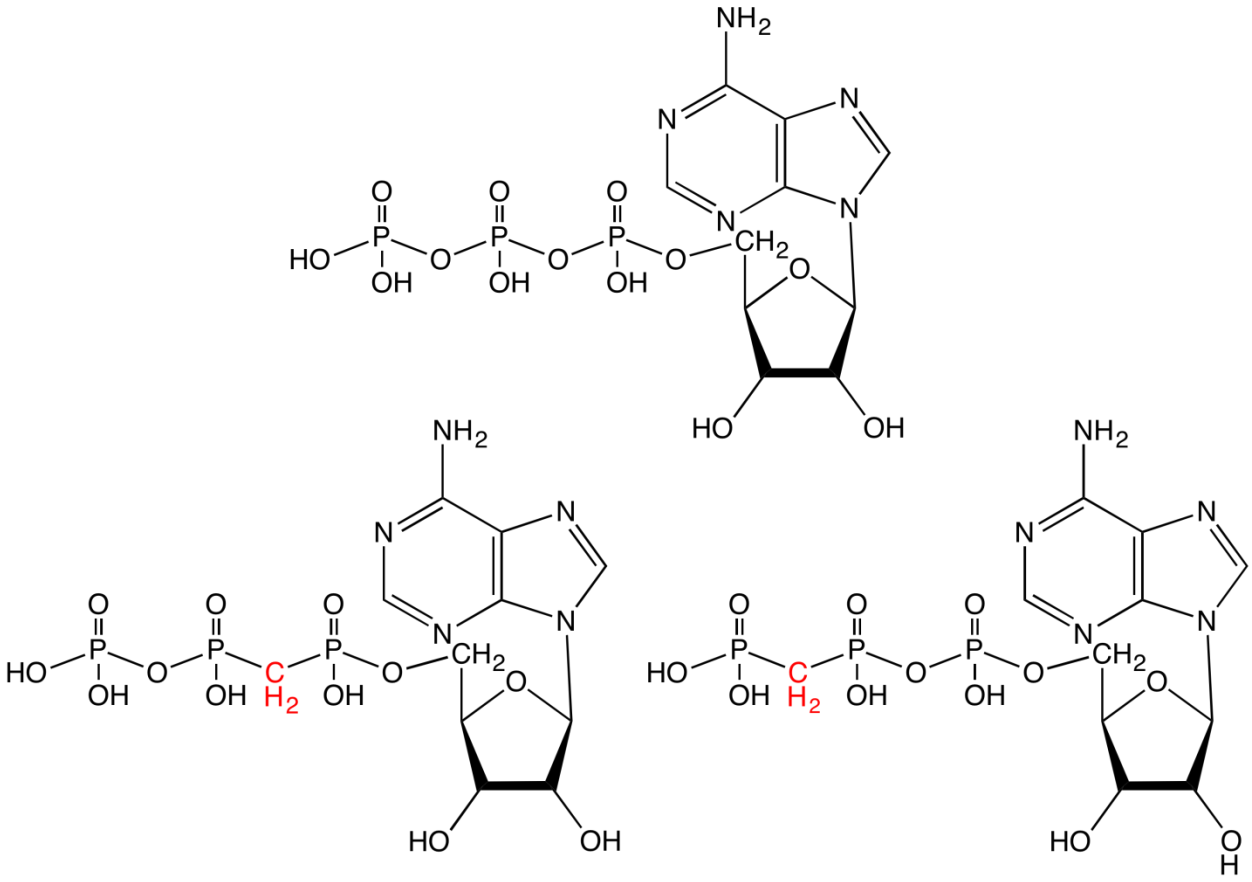

Figure 1.3: Structures of P2X1 agonists. The native structure of ATP is at the top of the image, whereas the modified structures of α,β-me-ATP and β,γ-me-ATP are shown at the bottom of the image. The differences in structure from ATP are highlighted in red on both structures.

1.4 Diseases with Hyperactive Platelets

It has been shown that platelets exhibit hyperactivity and are prone to excessive aggregation in certain disease states such as diabetes, pulmonary hypertension, cystic fibrosis (CF), sickle cell anemia and multiple sclerosis (MS). This hyperactivity can lead to unnecessary increased thrombus formation and subsequent blocking of blood vessels resulting in potential heart attack or stroke**.**

1.4.1 Diabetes

Patients with diabetes have been described as having hyperactive platelets. Diabetes is characterized by either lack of insulin secretion (type 1 diabetes) or a resistance to insulin (type 2 diabetes). Insulin is produced and stored in beta cells present in the islets of Langerhans region of the pancreas. In response to such stimuli as elevated glucose levels, exocytosis of insulin occurs depositing insulin in the bloodstream.[56] Patients with diabetes experience complications associated with blood flow, heart disease and stroke.[57] The problems with blood flow may be associated with hyperactive platelets. It has been shown that diabetic platelet activation is enhanced with response to epinephrine, ADP and thrombin.[58,59,60] Diabetic platelets have also been shown to be resistant to inhibition by NO[61] and PGI2.[62] Patients with diabetes also have high platelet turnover, which results in more circulating reticulated, or young, platelets. These reticulated platelets are larger and more reactive to activation stimuli than regular platelets.[63] Additionally, the reticulated platelets are resistant to the effects of aspirin and clopidogrel, which are two common antiplatelet drugs.[64,65]

1.4.2 Hypertension

Hypertension, or high blood pressure, is another condition that is characterized by hyperactive platelets. Platelets from patients with hypertension exhibit increased *in vivo* aggregation in response to ADP, epinephrine and collagen[66] as well as high intracellular free Ca^{2+} [67] and losses in NO bioavailability.[67] The susceptibility of platelets in hypertensive patients to aggregate can lead to increased risk of heart attack, as well as stroke.

1.4.3 Cystic Fibrosis

Cystic fibrosis (CF) is one of the most common hereditary disorders, especially in the Caucasian population.[68] CF is a genetic disorder, which results in dysfunctional cystic fibrosis transmembrane conductance regulator (CFTR) protein.[68] The CFTR protein is identified as a chloride channel present in the cell membrane.[69] Certain mutations of the CFTR protein make it inactive, which affects its functions, including chloride and ATP conductance.[70]

RBCs express the CFTR protein while platelets do not and CF platelets have been described as having increased aggregability *ex vivo*.[71,72] Additionally, it has been reported that platelets from CF patients have increased TXA_2 release[73] and do not respond well to prostaglandin E_1 (PGE_1), a platelet inhibitor.[74] Furthermore, it has been shown that CF plasma causes activation of CF platelets as well as healthy platelets, though activation of the CF platelets was higher than that of the normal.[71]

1.4.4 Sickle Cell Anemia

Sickle cell anemia is a blood disorder where RBCs sickle under deoxygenated conditions obstructing capillaries and restricting blood flow.[75] Sickle cell disease has been described as a "hypercoaguable state",[76] where platelet activation is abnormal. Plasma samples taken from sickle cell patients during steady state (non-sickled RBCs) and crisis (sickled RBCs) show increased levels of thrombin and depletion of anticoagulant proteins suggesting that the platelets are hyperactive.[77]

1.4.5 Multiple Sclerosis

A final disease state where patients exhibit platelet hyperactivity is in multiple sclerosis (MS). MS is a neurological disease that results in demyelination and scarring of nerves in the brain and spinal cord, which can lead to loss of nerve function, muscle weakness, and problems speaking.[78] Abnormalities in platelets from patients with MS were first described in 1965 as increased platelet stickiness.[79] It has been studied furthered and has been determined that MS platelets exhibit increased platelet microparticles (PMP) and P-selectin expression when compared to healthy controls. Both PMP and P-selectin are recognized indicators of platelet activation.[80]

1.4.6 Defects in RBC ATP release

In addition to hyperactive platelets, the diseases mentioned above all have defects in RBC derived ATP release. RBCs from patients with CF[81], diabetes[82] and hypertension[83] all exhibit

decreased ATP release while those RBCs from MS[84] and sickle cell patients[85] have increased ATP levels in the extracellular space due to RBC release and cell lysis, respectively. Platelets circulate throughout the body in the presence of RBCs and it has been shown that RBC derived ATP release does have an effect on platelet adhesion to an adhered endothelium at both low and high concentrations of ATP.[51] Since P2X1 is the only ATP receptor on the platelet, it is possible that RBC derived ATP may influence platelet activity via P2X1. The Spence group has shown through platelet aggregation studies on washed platelets and PRP that ATP can induce platelet aggregation; however, it is difficult to distinguish the effects of ATP from ADP, the immediate hydrolyzed product of ATP. Ectonucleotidases in the plasma and on the platelet surface convert ADP to ATP so; isolating the platelet response to ATP, ADP, or both is a challenge. Non hydrolysable forms of ATP are often used to study the P2X1 receptor's response, but these forms of ATP do not interact with the receptor in the same manner as native ATP. Additionally, in order to prove that hyperactive platelets may be a result of abnormal RBC derived ATP release affecting the platelet P2X1 receptor it is necessary to consider each component of the vasculature (RBCs, platelets, endothelial cells) and how each component contributes to platelet activation. Consequently, it is important to have methods to study platelets in an *in vitro* setting where each component of the vasculature can be isolated and probed.

1.5 Measuring Platelet Activity *in Vitro*

1.5.1 Aggregometry

One of the most common ways to study platelet function is by using light transmission aggregometry (LTA). In its simplest form, LTA measures changes in optical density of platelet solutions when exposed to individual agonists. Platelets are usually suspended in plasma, but

measurements can also be performed on suspensions of washed platelets. Measurements are carried out in a clear cuvette, with stirring at 37 ˚C.[86] For setting the lower and upper limits for LTA using samples in PRP, the 0% and 100% aggregation are calibrated to the PRP and platelet poor plasma (PPP), respectively. Aggregation is then monitored by changes in light transmission before and after addition of an agonist.[87].

Another form of aggregometry involves whole blood samples where changes in electrical impedance (Ohms) are measured. In principle, a single layer of platelets attach to the electrodes prior to aggregation and after an agonist is added, aggregating platelets attach at the electrodes thus causing changes in impedance at the electrode.[88, 89] The inherent advantage to using whole blood aggregometry is that all blood cells are present during the experiment, which more reflects an *in vivo* situation.

For both the whole blood aggregometry and the LTA, dense granule release from platelets can also be simultaneously monitored, specifically, ATP via a chemiluminescent reaction with D-luciferin/firefly luciferase. The emitted light can be compared to ATP standards for quantification purposes.[90] This technique is useful because it monitors both the morphological changes that platelets undergo and granular release, which can further activate platelets.

1.5.2 Flow Cytometry and Fluorescence

Flow cytometry is a powerful tool for studying platelets as it can measure multiple assays and various cell types at once. Before analysis by flow cytometry, cells are labeled with the desired fluorescent tag, which is often conjugated to a cell or protein specific antibody. Then the

cells in suspension flow one by one through a laser beam where the fluorophores are excited, and the emitted light collected. The intensity of the emission is directly proportional to the antigen or cell type being studied, as well as size and granularity of the cell.

One of the biggest advantages of flow cytometry is that platelets can be analyzed in the presence of other blood components, such as RBCs and leukocytes, which can affect platelet activation.[91,92] Furthermore, there are a number of antibodies available that bind activated platelets and not resting platelets. A few examples include 2G5[93] (receptor site on bound fibrinogen), IAC-1[94] (collagen binding site exposure), and S12[95] (P-selectin exposure on the membrane).

Ca^{2+}, an important signaling molecule in the platelet, is also studied using flow cytometry and fluorescence techniques. One of the most widely used probes to study Ca^{2+} is Fura-2, a ratiometric dye used as an intracellular Ca^{2+} probe.[96] When Ca^{2+} binds Fura-2, its absorption shifts to a shorter wavelength, thus, the ratio of unbound to bound Fura-2 can be used to calculate the concentration of Ca^{2+}.[97] Other commonly used Ca^{2+} probes include Fluo-3 AM[98] and Fluo-4 AM[99] where the AM ester group allows the dye to be loaded into the cell and subsequently, cleaved by intracellular esterases and the resulting dye is able to bind intracellular Ca^{2+}.

1.5.3 Microfluidic Devices

One of the inherent disadvantages of *in vitro* assays performed on platelet activity is the lack of a flow component and presence of other cells common to the vasculature. Through the use of microfluidic devices it is possible to remedy this disadvantage. Flow perfusion chambers were the first *in vitro* flow devices used to study platelets, where, typically, a glass coverslip is coated with a platelet activator or endothelial cells and thrombus formation at that interface can be monitored at various shear rates.[100] Simple devices such as this have been used to study thrombus formation[101], as well as integrin activation[102] in the platelet. These flow chambers have some disadvantages, including, lack of standardization in chamber fabrication[103] and the need for large volumes of blood (> 5 mL) to perform multiple assays.[104] Microfluidic technology is one way to overcome these disadvantages.

Typically, microfluidic devices are fabricated using photolithography and soft lithography with the end device being made of polydimethylsiloxane and having channel dimensions anywhere from 2-100 μm. PDMS is easy to use, inexpensive and biologically compatible so, it can be used to research thrombus formation. In brief, a master is created by photolithography, where a polymerizable SU-8 photoresist is spin coated onto a silicon wafer, a transparent mask with a pattern of channels is placed on the coated wafer, and exposed to UV light. The SU-8 that is exposed to the light polymerizes and the wafer developed to remove excess photoresist resulting in a master with positive features. A mixture of PDMS and curing agent is then poured over the master, allowed to cure, and peeled off resulting in negative features on the PDMS. These features tend to be the channels and any inlets, access ports, or

waste wells are typically punched right into the PDMS. The final PDMS channel layer can be sealed with glass or a blank layer of PDMS and the end device is able to incorporate flow across a single or multiple channel(s).[105]

Single channel microfluidic devices have been used to study collagen induced-thrombus formation under flow conditions,[106] anti-platelet drugs and shear gradients with a stenosis mimic,[107,108] and measurement of platelet size.[109] Microfluidics can also be used in a high throughput manner where multiple channels are used to monitor platelet activity. Devices with multiple channels have been used to study platelet adhesion to an endothelium,[110,51] platelet adhesion/signaling under flow conditions,[111] collagen induced thrombus formation,[112] and the effect of anti-platelet drugs during flow.[113] These microfluidic devices are designed to study various aspects of thrombus formation on an *in vitro* platform.

1.5.4 Apyrase and α,β-me-ATP in Platelet Preparation and Analysis

As mentioned previously, the platelet P2X1 receptor is prone to rapid desensitization *in vitro* due to spontaneously secreted ATP.[54] In order to reduce the effect of desensitization, researchers generally employ apyrase, which is derived from potato and acts as an ADPase and ATPase. In order for apyrase to protect the P2X1 receptor from desensitization, concentrations of 0.3-1 U/ml are used during sample preparation.[53] A higher concentrations of apyrase, 5 U/mL, was used in order to study platelet shape change with α,β-me-ATP as the agonist.[114] Since apyrase is most often used when studying the P2X1 receptor, agonists that are resistant to

hydrolysis must be employed to probe receptor function. Typically, α,β-me-ATP and β,γ methylene ATP (β,γ-me-ATP) are used as P2X1 agonists, however, neither α,β-me-ATP or β,γ-me-ATP are as potent as native ATP when it comes to P2X1 response.[115,116]

One of the inherent disadvantages in using apyrase in platelet solutions is that it breaks down ATP/ADP, which is what forces researchers to use α,β-me-ATP or β,γ-me-ATP as these analogues cannot be broken down by apyrase. However, these molecules do not represent the true *in vivo* activation of the P2X1 receptor. It is possible that the contribution of the P2X1 receptor to platelet activation and aggregation has previously been underestimated.

In order to study the P2X1 receptor a method that uses native ATP, without the presence of added apyrase is necessary. Furthermore, the role of RBC derived ATP (a significant source of ATP in the bloodstream) has not been fully investigated as a platelet regulator via the P2X1 receptor. Thus, a novel way to investigate P2X1 will be investigated, as well as novel microfluidic technology capable of probing these cellular responses and further analyzing the role of RBC derived ATP release in platelet activation.

REFERENCES

REFERENCES

1. A. D. Michelson, How Platelets Work: Platelet Function and Dysfunction. *J. Thromb. Thrombolysis* 2004, *16*. 7-12.

2. V. T. Turitto, H. J. Weiss, T. S. Zimmerman, I. I. Sussman, Factor VIII/von Willebrand factor in subendothelium mediates platelet adhesion. *Blood* 1985, *65*. 823-31.

3. H. R. Gralnick, S. B. Williams, L. P. Mckeown, D. M. Krizek, B. C. Shafer, M. E. Rick, Platelet Vonwillebrand-Factor - Comparison with Plasma Vonwillebrand-Factor. *Thromb. Res.* 1985, *38*. 623-633, DOI: Doi 10.1016/0049-3848(85)90205-1.

4. D. M. Maynard, H. F. G. Heijnen, M. K. Horne, J. G. White, W. A. Gahl, Proteomic analysis of platelet alpha-granules using mass spectrometry. *J. Thromb. Haemostasis* 2007, *5*. 1945-1955, DOI: DOI 10.1111/j.1538-7836.2007.02690.x.

5. H. Holmsen, H. J. Weiss, Secretable storage pools in platelets. *Annu. Rev. Med.* 1979, *30*. 119-34.

6. C. S. Mckinney, E. D. Ozkan, R. Zafar, P. M. Kelley, D. Njus, D. A. Walz, Characterization of Serotonin Transport in Human Platelet Dense Granules. *Thromb Haemost* 1993, *69*. 549-549.

7. D. E. Knight, M. C. Scrutton, Direct Evidence for a Role for Ca2+ in Amine Storage Granule Secretion by Human-Platelets. *Thromb. Res.* 1980, *20*. 437-446, DOI: Doi 10.1016/0049-3848(80)90282-0.

8. S. J. Shattil, C. Kim, M. H. Ginsberg, The final steps of integrin activation: the end game. *Nat. Rev. Mol. Cell Biol. 11*. 288-300.

9. U. R. Schwarz, U. Walter, M. Eigenthaler, Taming platelets with cyclic nucleotides. *Biochemical Pharmacology* 2001, *62*. 1153-1161.

10. D. Varga-Szabo, A. Braun, B. Nieswandt, Calcium signaling in platelets. *J. Thromb. Haemostasis* 2009, *7*. 1057-1066.

11. D. R. Hathaway, R. S. Adelstein, Human platelet myosin light chain kinase requires the calcium-binding protein calmodulin for activity. *Proceedings of the National Academy of Sciences of the United States of America* 1979, *76*. 1653-7.

12. S. J. Shattil, L. F. Brass, Induction of the fibrinogen receptor on human platelets by intracellular mediators. *Journal of Biological Chemistry* 1987, *262*. 992-1000.

13. J. E. Freedman, J. Loscalzo, M. R. Barnard, C. Alpert, J. F. Keaney, Jr., A. D. Michelson, Nitric oxide released from activated platelets inhibits platelet recruitment. *Journal of Clinical Investigation* 1997, *100*. 350-356.

14. L. J. Ignarro, G. M. Buga, K. S. Wood, R. E. Byrns, G. Chaudhuri, Endothelium-derived relaxing factor produced and released from artery and vein is nitric oxide. *Proceedings of the National Academy of Sciences of the United States of America* 1987, *84*. 9265-9.

15. L. J. Ignarro, R. E. Byrns, G. M. Buga, K. S. Wood, Endothelium-derived relaxing factor from pulmonary artery and vein possesses pharmacologic and chemical properties identical to those of nitric oxide radical. *Circ. Res.* 1987, *61*. 866-79.

16. T. C. Bellamy, J. Garthwaite, The receptor-like properties of nitric oxide-activated soluble guanylyl cyclase in intact cells. *Molecular and Cellular Biochemistry* 2002, *230*. 165-176, DOI: Doi 10.1023/A:1014204426331.

17. F. Murad, C. K. Mittal, W. P. Arnold, S. Katsuki, H. Kimura, Guanylate cyclase: activation by azide, nitro compounds, nitric oxide, and hydroxyl radical and inhibition by hemoglobin and myoglobin. *Adv Cyclic Nucleotide Res* 1978, *9*. 145-58.

18. T. D. Warner, Influence of endothelial mediators on the vascular smooth muscle and circulating platelets and blood cells. *International angiology : a journal of the International Union of Angiology* 1996, *15*. 93-9.

19. J. A. Rosado, S. Jenner, S. O. Sage, A role for the actin cytoskeleton in the initiation and maintenance of store-mediated calcium entry in human platelets. Evidence for conformational coupling. *Journal of Biological Chemistry* 2000, *275*. 7527-7533.

20. J. A. Beavo, Cyclic nucleotide phosphodiesterases: functional implications of multiple isoforms. *Physiological Reviews* 1995, *75*. 725-48.

21. H. H. Schmidt, S. M. Lohmann, U. Walter, The nitric oxide and cGMP signal transduction system: regulation and mechanism of action. *Biochimica et Biophysica Acta* 1993, *1178*. 153-75.

22. D. A. Wink, J. B. Mitchell, Chemical biology of nitric oxide: Insights into regulatory, cytotoxic, and cytoprotective mechanisms of nitric oxide. *Free Radical Biology & Medicine* 1998, *25*. 434-56.

23. D. R. Riddell, J. S. Owen, Nitric oxide and platelet aggregation. *Vitam Horm* 1999, *57*. 25-48.

24. R. Feil, S. M. Lohmann, H. de Jonge, U. Walter, F. Hofmann, - Cyclic GMP-dependent protein kinases and the cardiovascular system. *Circ Res* 2003, *93*. 907-16.

25. G. H. Rao, S. Krishnamurthi, L. Raij, J. G. White, Influence of nitric oxide on agonist-mediated calcium mobilization in platelets. *Biochemical Medicine and Metabolic Biology* 1990, *43*. 271-5.

26. M. E. Mendelsohn, S. Oneill, D. George, J. Loscalzo, Inhibition of Fibrinogen Binding to Human Platelets by S-Nitroso-N-Acetylcysteine. *Journal of Biological Chemistry* 1990, *265*. 19028-19034.

27. A. D. Michelson, S. E. Benoit, M. I. Furman, W. L. Breckwoldt, M. J. Rohrer, M. R. Barnard, J. Loscalzo, Effects of nitric oxide/EDRF on platelet surface glycoproteins. *Am J Physiol* 1996, *270*. H1640-8.

28. M. W. Radomski, R. M. Palmer, S. Moncada, An L-arginine/nitric oxide pathway present in human platelets regulates aggregation. *Proceedings of the National Academy of Sciences of the United States of America* 1990, *87*. 5193-7.

29. Q. S. Zhou, G. R. Hellermann, L. P. Solomonson, Nitric-Oxide Release from Resting Human Platelets. *Thromb. Res.* 1995, *77*. 87-96, DOI: Doi 10.1016/0049-3848(95)90868-G.

30. J. E. Freedman, R. Sauter, E. M. Battinelli, K. Ault, C. Knowles, P. L. Huang, J. Loscalzo, Deficient platelet-derived nitric oxide and enhanced hemostasis in mice lacking the NOSIII gene. *Circ. Res.* 1999, *84*. 1416-1421.

31. A. K. Dutta-Roy, A. K. Sinha, Purification and properties of prostaglandin E1/prostacyclin receptor of human blood platelets. *J Biol Chem* 1987, *262*. 12685-91.

32. R. L. Jones, Y. M. Qian, H. N. C. Wong, H. W. Chan, A. P. C. Yim, Prostanoid action on the human pulmonary vascular system. *Clinical and Experimental Pharmacology and Physiology* 1997, *24*. 969-972, DOI: DOI 10.1111/j.1440-1681.1997.tb02730.x.

33. J. M. Manganello, Y. Djellas, C. Borg, K. Antonakis, G. C. Le Breton, Cyclic AMP-dependent phosphorylation of thromboxane A2 receptor-associated GÎ±13. *Journal of Biological Chemistry* 1999, *274*. 28003-28010.

34. C. Y. E. Fung, S. Jones, A. Ntrakwah, K. M. Naseem, R. W. Farndale, M. P. Mahaut-Smith, Platelet Ca2+ responses coupled to glycoprotein VI and Toll-like receptors persist in the presence of endothelial-derived inhibitors: roles for secondary activation of P2X1 receptors and release from intracellular Ca2+ stores. *Blood 119*. 3613-3621.

35. J. Geiger, C. Nolte, E. Butt, S. O. Sage, U. Walter, Role of cGMP and cGMP-dependent protein kinase in nitrovasodilator inhibition of agonist-evoked calcium elevation in human platelets. *Proceedings of the National Academy of Sciences of the United States of America* 1992, *89*. 1031-5.

36. A. J. Marcus, M. J. Broekman, J. H. F. Drosopoulos, N. Islam, T. N. Alyonycheva, L. B. Safier, K. A. Hajjar, D. N. Posnett, M. A. Schoenborn, K. A. Schooley, R. B. Gayle, C. R. Maliszewski, The endothelial cell ecto-ADPase responsible

for inhibition of platelet function is CD39. *Journal of Clinical Investigation* 1997, *99*. 1351-1360.

37. H. Zimmermann, 5'-Nucleotidase: molecular structure and functional aspects. *Biochem J* 1992, *285 (Pt 2)*. 345-65.

38. M. Cattaneo, The P2 receptors and congenital platelet function defects. *Semin. Thromb. Hemostasis* 2005, *31*. 168-173.

39. S. O. Sage, R. Reast, T. J. Rink, ADP evokes biphasic calcium influx in fura-2-loaded human platelets. Evidence for calcium entry regulated by the intracellular calcium store. *Biochemical Journal* 1990, *265*. 675-80.

40. M. Cattaneo, A. Lecchi, Inhibition of the platelet P2Y12 receptor for adenosine diphosphate potentiates the antiplatelet effect of prostacyclin. *J. Thromb. Haemostasis* 2007, *5*. 577-582.

41. J. Jin, S. P. Kunapuli, Coactivation of two different G protein-coupled receptors is essential for ADP-induced platelet aggregation. *Proceedings of the National Academy of Sciences of the United States of America* 1998, *95*. 8070-8074.

42. R. A. North, Molecular physiology of P2X receptors. *Physiological Reviews* 2002, *82*. 1013-1067.

43. T. Kawate, J. C. Michel, W. T. Birdsong, E. Gouaux, Crystal structure of the ATP-gated P2X4 ion channel in the closed state. *Nature (London, United Kingdom)* 2009, *460*. 592-598.

44. A. J. Brake, M. J. Wagenbach, D. Julius, New structural motif for ligand-gated ion channels defined by an ionotropic ATP receptor. *Nature (London, United Kingdom)* 1994, *371*. 519-23.

45. L. E. Browne, L.-H. Jiang, R. A. North, New structure enlivens interest in P2X receptors. *Trends in Pharmacological Sciences 31*. 229-237.

46. M. Hattori, E. Gouaux, Molecular mechanism of ATP binding and ion channel activation in P2X receptors. *Nature (London, United Kingdom) 485*. 207-212.

47. L. Wang, O. Oestberg, A. K. Wihlborg, H. Brogren, S. Jern, D. Erlinge, Quantification of ADP and ATP receptor expression in human platelets. *J. Thromb. Haemostasis* 2003, *1*. 330-336.

48. S. O. Sage, T. J. Rink, The kinetics of changes in intracellular calcium concentration in fura-2-loaded human platelets. *Journal of Biological Chemistry* 1987, *262*. 16364-9.

49. J. Martinez-Pinna, I. S. Gurung, C. Vial, C. Leon, C. Gachet, R. J. Evans, M. P. Mahaut-Smith, Direct Voltage Control of Signaling via P2Y1 and Other GÎ±q-coupled Receptors. *Journal of Biological Chemistry* 2005, *280*. 1490-1498.

50. S. Takano, J. Kimura, I. Matsuoka, T. Ono, No requirement of P2X1 purinoceptors for platelet aggregation. *European Journal of Pharmacology* 1999, *372*. 305-309.

51. W. Karunarathne, C. J. Ku, D. M. Spence, The dual nature of extracellular ATP as a concentration-dependent platelet P2X1 agonist and antagonist. *Integr Biol* 2009, *1*. 655-663, DOI: Doi 10.1039/B909873a.

52. C. Y. Fung, C. A. Brearley, R. W. Farndale, M. P. Mahaut-Smith, A major role for P2X1 receptors in the early collagen-evoked intracellular Ca2+ responses of human platelets. *Thromb Haemost* 2005, *94*. 37-40.

53. C. Y. E. Fung, C. Cendana, R. W. Farndale, M. P. Mahaut-Smith, Primary and secondary agonists can use P2X1 receptors as a major pathway to increase intracellular Ca2+ in the human platelet. *J. Thromb. Haemostasis* 2007, *5*. 910-917.

54. M. G. Rolf, C. A. Brearley, M. P. Mahaut-Smith, Platelet shape change evoked by selective activation of P2X1 purinoceptors with alpha ,beta -methylene ATP. *Thromb Haemost* 2001, *85*. 303-308.

55. H. H. Dalziel, G. A. Gray, R. M. Drummond, B. L. Furman, P. Sneddon, Investigation of the selectivity of alpha , beta -methylene ATP in inhibiting vascular responses of the rat in vivo and in vitro. *Br J Pharmacol* 1990, *99*. 820-4.

56. F. Chimienti, A. Favier, M. Seve, ZnT-8, a pancreatic beta-cell-specific zinc transporter. *Biometals* 2005, *18*. 313-317, DOI: DOI 10.1007/s10534-005-3687-9.

57. A. I. Vinik, T. Erbas, T. S. Park, R. Nolan, G. L. Pittenger, Platelet dysfunction in type 2 diabetes. *Diabetes Care* 2001, *24*. 1476-1485.

58. D. J. Betteridge, K. E. El Tahir, J. P. Reckless, K. I. Williams, Platelets from diabetic subjects show diminished sensitivity to prostacyclin. *Eur J Clin Invest* 1982, *12*. 395-8.

59. H. E. Harrison, A. H. Reece, M. Johnson, Effect of insulin treatment on prostacyclin in experimental diabetes. *Diabetologia* 1980, *18*. 65-8.

60. J. Kutti, H. Wadenvik, B. Henestam, G. Stenstrom, Evaluation of platelet reactivity in diabetes mellitus. *Acta Med Scand* 1986, *219*. 195-9.

61. N. N. Chan, P. Vallance, H. M. Colhoun, Nitric oxide and vascular responses in Type I diabetes. *Diabetologia* 2000, *43*. 137-47.

62. G. Davi, G. B. Rini, M. Averna, S. Novo, G. Difede, A. Pinto, A. Notarbartolo, A. Strano, Thromboxane-B2 Formation and Platelet Sensitivity to Prostacyclin in Insulin-Dependent and Insulin-Independent Diabetics. *Thromb. Res.* 1982, *26*. 359-370, DOI: Doi 10.1016/0049-3848(82)90254-7.

63. D. Tschoepe, P. Roesen, J. Esser, B. Schwippert, H. K. Nieuwenhuis, B. Kehrel, F. A. Gries, Large Platelets Circulate in an Activated State in Diabetes-Mellitus. *Semin. Thromb. Hemostasis* 1991, *17*. 433-438, DOI: DOI 10.1055/s-2007-1002650.

64. S. Guthikonda, E. I. Lev, R. Patel, T. Delao, A. L. Bergeron, J. F. Dong, N. S. Kleiman, Reticulated platelets and uninhibited COX-1 and COX-2 decrease the antiplatelet effects of aspirin. *J. Thromb. Haemostasis* 2007, *5*. 490-496, DOI: DOI 10.1111/j.1538-7836.2007.02387.x.

65. C. L. Alviar, M. Vaduganathan, A. Tellez, K. Rammohan, B. Nure, T. Delao, M. Arikan, J. F. Granada, E. I. Lev, N. S. Kleiman, S. Guthikonda, Role of reticulated platelets and platelet size in modifying anti-platelet effects of aspirin and clopidogrel in patients with stable coronary artery disease. *Circ. Res.* 2007, *101*. 1210-1210.

66. L. Somova, J. Mufunda, Platelet activity and salt sensitivity in the pathogenesis of systemic (essential) hypertension in black Africans. *Clin Exp Hypertens* 1993, *15*. 781-96.

67. M. El Haouari, J. A. Rosado, Platelet function in hypertension. *Blood Cells, Mol., Dis.* 2009, *42*. 38-43.

68. G. R. Cutting, Cystic fibrosis: using genetic association to identify modifiers of disease variability in cystic fibrosis. *European Journal of Human Genetics* 2006, *14*. 890-891.

69. M. R. Knowles, M. J. Stutts, A. Spock, N. Fischer, J. T. Gatzy, R. C. Boucher, Abnormal ion permeation through cystic fibrosis respiratory epithelium. *Science (Washington, DC, United States)* 1983, *221*. 1067-70.

70. P. M. Quinton, Chloride impermeability in cystic fibrosis. *Nature* 1983, *301*. 421-2.

71. B. P. O'Sullivan, M. D. Linden, A. L. Frelinger, III, M. R. Barnard, M. Spencer-Manzon, J. E. Morris, R. O. Salem, M. Laposata, A. D. Michelson, Platelet activation in cystic fibrosis. *Blood* 2005, *105*. 4635-4641.

72. R. J. Stead, M. A. Barradas, D. P. Mikhailidis, J. Y. Jeremy, M. E. Hodson, J. C. Batten, P. Dandona, Platelet hyperaggregability in cystic fibrosis. *Prostaglandins Leukot Med* 1987, *26*. 91-103.

73. D. P. Mikhailidis, R. J. Stead, M. A. Barradas, M. E. Hodson, J. C. Batten, P. Dandona, Platelet abnormalities in patients with cystic fibrosis and obligate heterozygotes. *Haematologica* 1990, *75*. 137-40.

74. G. Agam, M. Aviram, M. Zilberman-Kaufman, A. Rothstein, A. A. Livne, Cyclic AMP-related and cation-affected human platelet chloride transport regulation. *Eur J Clin Chem Clin Biochem* 1995, *33*. 329-35.

75. P. A. Lane *Sickle cell disease*; Department of Pediatrics, University of Colorado School of Medicine, Denver, USA: United States, 1996.

76. R. B. Francis, Jr., Platelets, coagulation, and fibrinolysis in sickle cell disease: their possible role in vascular occlusion. *Blood Coagul Fibrinolysis* 1991, *2*. 341-53.

77. K. I. Ataga, E. P. Orringer, Hypercoagulability in sickle cell disease: a curious paradox. *Am. J. Med.* 2003, *115*. 721-728.

78. A. Compston, A. Coles, Multiple sclerosis. *Lancet* 2008, *372*. 1502-1517, DOI: Doi 10.1016/S0140-6736(08)61620-7.

79. H. P. Wright, R. H. Thompson, K. J. Zilkha, Platelet adhesiveness in multiple sclerosis. *Lancet* 1965, *2*. 1109-10.

80. W. A. Sheremata, W. Jy, L. L. Horstman, Y. S. Ahn, J. S. Alexander, A. Minagar, Evidence of platelet activation in multiple sclerosis. *J. Neuroinflammation* 2008, *5*. No pp given.

81. R. S. Sprague, M. L. Ellsworth, A. H. Stephenson, M. E. Kleinhenz, A. J. Lonigro, Deformation-induced ATP release from red blood cells requires CFTR activity. *American Journal of Physiology* 1998, *275*. H1726-H1732.

82. J. Carroll, M. Raththagala, W. Subasinghe, S. Baguzis, T. D. a. Oblak, P. Root, D. Spence, An altered oxidant defense system in red blood cells affects their ability to release nitric oxide-stimulating ATP. *Mol. BioSyst.* 2006, *2*. 305-311.

83. R. S. Sprague, A. H. Stephenson, M. L. Ellsworth, C. Keller, A. J. Lonigro, Impaired release of ATP from red blood cells of humans with primary pulmonary hypertension. *Exp. Biol. Med. (Maywood, NJ, U. S.)* 2001, *226*. 434-439.

84. S. Letourneau, L. Hernandez, A. N. Faris, D. M. Spence, Evaluating the effects of estradiol on endothelial nitric oxide stimulated by erythrocyte-derived ATP using a microfluidic approach. *Anal. Bioanal. Chem.* *397*. 3369-3375.

85. A. Dorn-Beineke, T. Frietsch, Sickle cell disease - pathophysiology, clinical and diagnostic implications. *Clin. Chem. Lab. Med.* 2002, *40*. 1075-1084.

86. G. V. Born, Aggregation of blood platelets by adenosine diphosphate and its reversal. *Nature* 1962, *194*. 927-9.

87. G. V. Born, M. J. Cross, The Aggregation of Blood Platelets. *J Physiol* 1963, *168*. 178-95.

88. D. C. Cardinal, R. J. Flower, Electronic Aggregometer - Novel Device for Assessing Platelet Behavior in Blood. *J Pharmacol Methods* 1980, *3*. 135-158, DOI: Doi 10.1016/0160-5402(80)90024-8.

89. D. L. McGlasson, G. A. Fritsma, Whole Blood Platelet Aggregometry and Platelet Function Testing. *Semin. Thromb. Hemostasis* 2009, *35*. 168-180, DOI: DOI 10.1055/s-0029-1220325.

90. R. D. Feinman, J. Lubowsky, I. Charo, M. P. Zabinski, Iumi-Aggregometer - New Instrument for Simultaneous Measurement of Secretion and Aggregation by Platelets. *Journal of Laboratory and Clinical Medicine* 1977, *90*. 125-129.

91. M. T. Santos, J. Valles, A. J. Marcus, L. B. Safier, M. J. Broekman, N. Islam, H. L. Ullman, A. M. Eiroa, J. Aznar, Enhancement of platelet reactivity and modulation of eicosanoid production by intact erythrocytes. A new approach to platelet activation and recruitment. *J Clin Invest* 1991, *87*. 571-80, DOI: 10.1172/JCI115032.

92. M. R. Barnard, L. A. Krueger, A. L. Frelinger, 3rd, M. I. Furman, A. D. Michelson, Whole blood analysis of leukocyte-platelet aggregates. *Curr Protoc Cytom* 2003, *Chapter 6*. Unit 6 15, DOI: 10.1002/0471142956.cy0615s24.

93. C. Zamarron, M. H. Ginsberg, E. F. Plow, Monoclonal antibodies specific for a conformationally altered state of fibrinogen. *Thromb Haemost* 1990, *64*. 41-6.

94. A. Schoolmeester, K. Vanhoorelbeke, S. Katsutani, H. Depraetere, H. B. Feys, J. M. Heemskerk, M. F. Hoylaerts, H. Deckmyn, Monoclonal antibody IAC-1 is specific for activated alpha2beta1 and binds to amino acids 199 to 201 of the integrin alpha2 I-domain. *Blood* 2004, *104*. 390-6, DOI: 10.1182/blood-2003-12-4224.

95. E. Larsen, A. Celi, G. E. Gilbert, B. C. Furie, J. K. Erban, R. Bonfanti, D. D. Wagner, B. Furie, PADGEM protein: a receptor that mediates the interaction of activated platelets with neutrophils and monocytes. *Cell* 1989, *59*. 305-12.

96. R. Y. Tsien, M. Poenie, Fluorescence Ratio Imaging - a New Window into Intracellular Ionic Signaling. *Trends in Biochemical Sciences* 1986, *11*. 450-455, DOI: Doi 10.1016/0968-0004(86)90245-8.

97. R. Y. Tsien, T. Pozzan, T. J. Rink, Measuring and Manipulating Cytosolic Ca-2+ with Trapped Indicators. *Trends in Biochemical Sciences* 1984, *9*. 263-266, DOI: Doi 10.1016/0968-0004(84)90160-9.

98. A. Minta, J. P. Kao, R. Y. Tsien, Fluorescent indicators for cytosolic calcium based on rhodamine and fluorescein chromophores. *J Biol Chem* 1989, *264*. 8171-8.

99. K. R. Gee, K. A. Brown, W. N. U. Chen, J. Bishop-Stewart, D. Gray, I. Johnson, Chemical and physiological characterization of fluo-4 Ca2+-indicator dyes. *Cell Calcium* 2000, *27*. 97-106, DOI: DOI 10.1054/ceca.1999.0095.

100. K. S. Sakariassen, R. Muggli, H. R. Baumgartner, Measurements of platelet interaction with components of the vessel wall in flowing blood. *Methods in Enzymology* 1989, *169*. 37-70.

101. S. P. Jackson, W. S. Nesbitt, E. Westein, Dynamics of platelet thrombus formation. *Journal of thrombosis and haemostasis : JTH* 2009, *7 Suppl 1*. 17-20, DOI: 10.1111/j.1538-7836.2009.03401.x.

102. J. M. Cosemans, B. F. Iserbyt, H. Deckmyn, J. W. Heemskerk, Multiple ways to switch platelet integrins on and off. *Journal of thrombosis and haemostasis : JTH* 2008, *6*. 1253-61, DOI: 10.1111/j.1538-7836.2008.03041.x.

103. M. Roest, A. Reininger, J. J. Zwaginga, M. R. King, J. W. Heemskerk, Flow chamber-based assays to measure thrombus formation in vitro: requirements for standardization. *Journal of thrombosis and haemostasis : JTH* 2011, *9*. 2322-4, DOI: 10.1111/j.1538-7836.2011.04492.x.

104. R. Van Kruchten, J. M. Cosemans, J. W. Heemskerk, Measurement of whole blood thrombus formation using parallel-plate flow chambers - a practical guide. *Platelets* 2012, *23*. 229-42, DOI: 10.3109/09537104.2011.630848.

105. D. C. Duffy, J. C. McDonald, O. J. A. Schueller, G. M. Whitesides, Rapid Prototyping of Microfluidic Systems in Poly(dimethylsiloxane). *Analytical Chemistry* 1998, *70*. 4974-4984.

106. D. P. Sarvepalli, D. W. Schmidtke, M. U. Nollert, Design Considerations for a Microfluidic Device to Quantify the Platelet Adhesion to Collagen at Physiological Shear Rates. *Ann Biomed Eng* 2009, *37*. 1331-1341, DOI: DOI 10.1007/s10439-009-9708-z.

107. W. S. Nesbitt, E. Westein, F. J. Tovar-Lopez, E. Tolouei, A. Mitchell, J. Fu, J. Carberry, A. Fouras, S. P. Jackson, A shear gradient-dependent platelet aggregation mechanism drives thrombus formation. *Nat. Med. (N. Y., NY, U. S.)* 2009, *15*. 665-673.

108. F. J. Tovar-Lopez, G. Rosengarten, E. Westein, K. Khoshmanesh, S. P. Jackson, A. Mitchell, W. S. Nesbitt, A microfluidics device to monitor platelet aggregation dynamics in response to strain rate micro-gradients in flowing blood. *Lab on a Chip* 2010, *10*. 291-302, DOI: 10.1039/b916757a.

109. D. W. Inglis, K. J. Morton, J. A. Davis, T. J. Zieziulewicz, D. A. Lawrence, R. H. Austin, J. C. Sturm, Microfluidic device for label-free measurement of platelet activation. *Lab Chip* 2008, *8*. 925-931.

110. C.-J. Ku, T. D'Amico Oblak, D. M. Spence, Interactions between Multiple Cell Types in Parallel Microfluidic Channels: Monitoring Platelet Adhesion to an Endothelium in the Presence of an Anti-Adhesion Drug. *Anal. Chem. (Washington, DC, U. S.)* 2008, *80*. 7543-7548.

111. E. Gutierrez, B. G. Petrich, S. J. Shattil, M. H. Ginsberg, A. Groisman, A. Kasirer-Friede, Microfluidic devices for studies of shear-dependent platelet adhesion. *Lab Chip* 2008, *8*. 1486-1495.

112. K. B. Neeves, S. F. Maloney, K. P. Fong, A. A. Schmaier, M. L. Kahn, L. F. Brass, S. L. Diamond, Microfluidic focal thrombosis model for measuring murine platelet deposition and stability: PAR4 signaling enhances shear-resistance of platelet aggregates. *J Thromb Haemost* 2008, *6*. 2193-201.

113. S. F. Maloney, L. F. Brass, S. L. Diamond, P2Y12 or P2Y1 inhibitors reduce platelet deposition in a microfluidic model of thrombosis while apyrase lacks efficacy under flow conditions. *Integr Biol 2*. 183-192.

114. C. Oury, E. Toth-Zsamboki, C. Thys, J. Tytgat, J. Vermylen, M. F. Hoylaerts, The ATP-gated P2X1 ion channel acts as a positive regulator of platelet responses to collagen. *Thromb Haemost* 2001, *86*. 1264-1271.

115. R. A. North, A. Surprenant, Pharmacology of cloned P2X receptors. *Annual Review of Pharmacology and Toxicology* 2000, *40*. 563-580.

116. M. P. Mahaut-Smith, S. Jones, R. J. Evans, The P2X1 receptor and platelet function. *Purinergic Signal*. DOI: 10.1007/s11302-011-9224-0.

CHAPTER 2: PLATELET P2X1 RECEPTOR FUNCTION IN THE ABSENCE OF EXOGENOUS APYRASE

2.1 Platelet P2X1 receptor

Purinergic receptors on the surface of the platelet are important in mediating the clotting process that occurs after vascular injury, most notably the ADP-sensitive receptors, P2Y1/P2Y12, and the ATP-sensitive, P2X1 receptor.[1-4] Though the roles for P2Y-type receptors in platelet activation and thrombus formation are well established, the role of the P2X1 receptor in platelet function is less clear. For example, P2X1 activation has been shown to induce transient platelet shape change,[5] and is also involved with collagen-induced aggregation events.[6-9] It has also been shown that ATP acting through the P2X1 receptor is important as a secondary platelet agonist in the activation process.[10] Conversely, other studies report a minimal role for P2X1 in platelet activation.[11] Activation of the P2X1 receptor by ATP is responsible for extracellular Ca^{2+} entry into the platelet. Not only is Ca^{2+} important for P2X1 response, but also ADP dependent P2Y response where extracellular Ca^{2+} dependent ectonucleotidases affect ADP induced platelet aggregation.[12]

A review on the P2X1 receptor stresses its importance in thrombotic events and the need to study the receptor as a potential therapeutic target.[13] More specifically, an *in vitro* study performed on platelets from P2X1 receptor-deficient mice showed that collagen-induced platelet aggregation and adhesion to a collagen coated surface were

reduced. The collagen coated surface was mimicking a vascular injury and thrombus growth on that coated region was also reduced in the P2X1 deficient platelets.[7] Additionally, in an *in vivo* study on these P2X1 deficient mice, bleeding times were normal, but there was reduced thrombus formation following laser induced vascular injury and reduced mortality in models of thromboembolism.[7] With the information garnered from both *in vitro* and *in vivo* studies on platelet P2X1 receptor activity, it is possible that P2X1 is a potential therapeutic target for anti-thrombotic drugs.

2.1.1 Difficulties in measuring P2X1 receptor activity

The P2X1 receptor is difficult to study because it is rapidly desensitized during *in vitro* experimentation, especially when the platelets have been separated from plasma and washed.[14-15] In order to overcome this rapid receptor desensitization,[16-18] apyrase, which catalyzes the dephosphorylation of adenine nucleotides, is commonly used during platelet purification from whole blood to reduce the number of phosphate-containing nucleotides already present in the bulk solution. Unfortunately, the addition of apyrase to the bulk solution results in the breakdown of exogenously added ATP to ADP, which is unable to activate the P2X1 receptor.

Another factor contributing to the complexity of platelet P2X1 activation is distinguishing effects due to ATP from those arising from ADP, especially after dephosphorylation from ATP to ADP. For example, when P2X1 is stimulated with ATP, Ca^{2+} enters the platelet from the sample matrix and can be measured with a fluorescent probe such as Fura-2 or Fluo-4 AM. However, ADP can also contribute to this Ca^{2+}

signal, as ADP binding to the P2Y1 receptor results in the release of Ca^{2+} from granules contained within the platelet.[19-21] Therefore, the degradation of ATP to ADP, or ADP contamination in the ATP agonist, leads to inconclusive results regarding the source of the increased platelet Ca^{2+}. However, there are techniques that can be used to distinguish the two receptors. For example, in the case of measuring Ca^{2+}, one can simply perform the studies in a Ca^{2+}-free buffer. Such a system would prevent Ca^{2+} entering the platelet due to P2X1 activation by ATP, but not P2Y activation, since the Ca^{2+} release would be intracellular. In other words, any measured Ca^{2+} signal during experiments with a Ca^{2+}-free buffer would likely be due to release of Ca^{2+} from intracellular stores. This release is indicative of ADP binding to the platelet.

In addition to using Ca^{2+}-free buffers to differentiate receptor activity, many investigators employ the use of α,β-methylene-ATP (α,β-me-ATP), a stable ATP analogue that cannot be enzymatically dephosphorylated to ADP. The use of such a stable ATP analogue ensures that any measured Ca^{2+} flux into the platelet is due to P2X1. However, α,β-me-ATP leads only to transient platelet shape change[5] and low levels of aggregation[22] and could potentially be under representing P2X1 activity that would be measured with authentic ATP as discussed in Chapter 1.

2.1.2 NF449 as a P2X1 receptor inhibitor

To facilitate the understanding of receptor action and response, inhibitors of the platelet purinergic receptors can be employed. Suramin was one of the first P2X antagonists described[23] and subsequent derivatives of suramin have also been synthesized.[24-27] One of those derivatives, 4,4',4'',4'''-(carbonyl(imino-5,1,3-benzenetriyl-bis(carbonylimino)))tetrakis-benzene-1,3-disulphonic acid or more commonly, NF449, has been shown to be a potent and specific antagonist of P2X1.[27] The structure of NF449 is shown in figure 2.1. Previously, the structure of the P2X4 receptor from zebrafish had been solved in the absence of bound ATP[28], but more recently, the structure of P2X4 with bound ATP has been solved[29], giving more information about the ATP binding pocket on P2X type receptors. The mechanism of activation involves ATP binding in the extracellular loop, which induces conformational changes that prompts flexing of the transmembrane domains and allowing for "lateral fenestration" of cations.[29] It is proposed that NFF49 binds at or near the ATP binding site on P2X receptors[30], and due to steric hindrance, prevents the channel pore form opening.[29] However, structural studies involving P2X-bound NF449 have yet to be performed.

NF449 is one of the most widely used platelet P2X1 inhibitors and it has been shown to reduce Ca^{2+} influx and reduce activation of the receptor by both ATP and α,β-me-ATP.[25, 31-32] Interestingly, in contrast to its inhibitory actions on the P2X1 receptor, NF449 has been reported to enhance P2X1 sensitization in frog oocytes.[25] A detailed

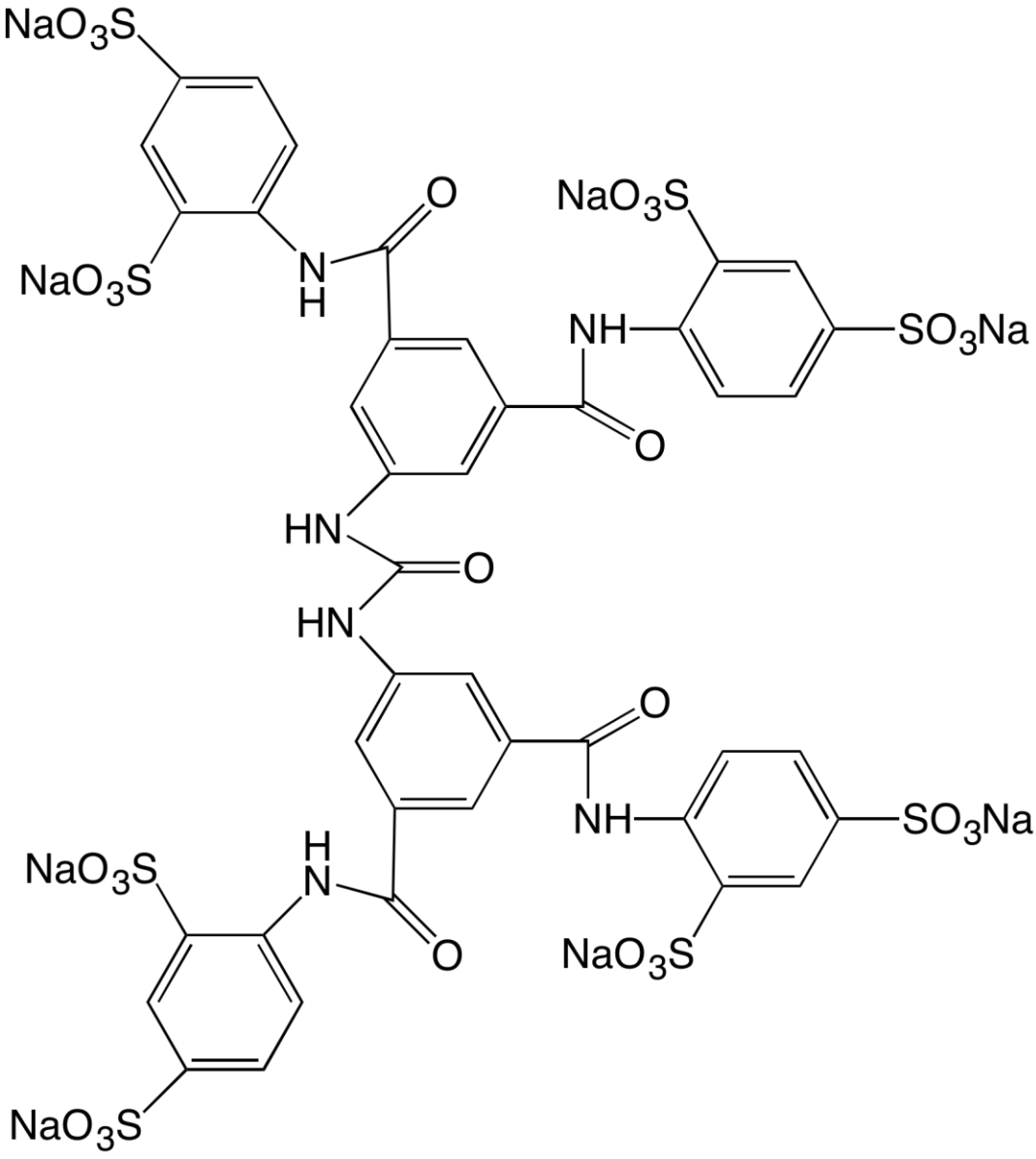

Figure 2.1: Structure of NF449. The P2X1 inhibitor, NF449, is pictured with coordinating sodium ions (Na^+), but in solution the polysulphonates are negatively charged.

examination of these reports involving NF449 inhibition and sensitization reveals that the conditions (concentrations of NF449, number of cells used in the studies and incubation time of the NF449 with the cells prior to measurement) differed greatly. These reports led me to the hypothesis that NF449 may exhibit sensitizing and inhibitory actions on the platelet P2X1 receptor that are dependent upon the ratio of agonist and inhibitor employed during platelet preparation. This is important because if NF449 can be used to sensitize platelets, instead of apyrase, there would not be a need to use a non-hydrolysable form of ATP during experiments, enabling the effects of ATP versus ADP to be distinguished with regard to platelet activity. This is significant, as discussed in Chapter 1; because certain diseases (cystic fibrosis, diabetes, hypertension, sickle cell anemia) have defects in RBC derived ATP release, as well as increased platelet activity. The correlation between these two cell types would be the ATP activation of P2X1 receptor on the platelets so, a method to study platelet response to ATP that does not involve apyrase or α,β-me-ATP would be extremely useful.

2.2 Methods

2.2.1 Isolation of platelets from human whole blood

Whole blood was obtained via venipuncture under consent from donors and collected into heparinized tubes. In general, 10 tubes of whole blood were collected from each donor (~30 mL). After the whole blood was centrifuged at 500 *g* for 10 min at room temperature, the platelet-rich plasma (PRP) was decanted for subsequent platelet purification.

Platelets were isolated from the PRP by adding 1 mL of acid citrate dextrose (ACD; in mM, 41.6 citric acid anhydrous, 76.7 monosodium citric acid anhydrous, 122.1 dextrose) to every 9 mL of PRP and centrifuging at 1500 *g* for 10 min at room temperature. The harvested platelets were then washed twice with 10% ACD calcium free Modified Tyrodes Buffer (MTB; in mM, 12 $NaHCO_3$, 0.32 NaH_2PO_4, 10 HEPES, 137 NaCl, 2.7 KCl, 0.5 $MgCl_2$, and 5.5 dextrose, Sigma-Aldrich, St. Louis, MO) solution with centrifugation in between each wash. The washed platelets were then re-suspended in 10% ACD calcium free MTB. No apyrase was used in this purification. The washed platelets were counted using a hemacytometer and adjusted to a concentration of 2.0 x 10^9 platelets mL^{-1} in 1 mL 10% ACD calcium free MTB. Platelet samples were prepared and investigated the same day as isolation.

2.2.2 Fluo-4 AM probe and NF449 platelet sample preparation

A 2.3 mM stock of the Ca^{2+} specific probe Fluo-4 AM (Molecular Probes/Invitrogen Eugene, OR) was prepared by dissolving 50 μg of the probe in 20 μL of anhydrous DMSO. A 5 μL aliquot of the stock was mixed with 5 μL of a 200 mg/mL pluronic F-127 surfactant (Molecular Probes/Invitrogen Eugene, OR) solution to enhance the probe's penetration capacity. Finally, this probe solution was diluted to 1 mL in 10% ACD calcium free MTB to create an 11.4 μM working solution. This 1 mL solution of the fluorescent probe was then added to the 1 mL platelet solution for a final concentration of 5.7 μM Fluo 4 AM and incubated on ice for 30 min. The platelet solution containing the probe was then centrifuged at 1500 *g* for 5 min at room

temperature and washed twice with 10% ACD calcium free MTB to remove any excess probe. Finally, the platelets were resuspended in 2 mL of 10% ACD calcium free MTB.

Aliquots of the Fluo-4 AM loaded platelet solution (1.0×10^9 platelets mL^{-1}) were incubated for 30 min on ice with NF449 (Tocris Bioscience, Ellisville, MO) at final concentrations ranging from 0-40 μM, or MRS 2179 (Tocris Bioscience) at final concentrations ranging from 0-60 μM.

2.2.3 Fluorescence determination of intracellular platelet Ca^{2+}

Calcium measurements were performed with a spectrofluorometer (HORIBA Jobin Yvon, Edison, NJ) having 2 nm slit widths using excitation at 496 nm and emission at 516 nm. The sample was contained in a 4 mL 21N-Q-10 far UV quartz cuvette. A 40 μL aliquot of platelet sample was added to 1940 μL of MTB with calcium (2 mM Ca^{2+}) at 37 °C and a fluorescence baseline was collected for 15 s prior to the addition of 20 μL of agonist prepared in Ca^{2+} free MTB. Agonists included ATP, ADP and α,β-methylene ATP (Sigma-Aldrich, St. Louis, MO) at stock concentrations ranging from 0-1000 μM resulting in final concentrations of 0-10 μM in the cuvette. Fluorescence measurements were collected for an additional 90 s; samples were stirred throughout the measurement. A schematic of sample preparation and subsequent fluorescence measurement is shown in figure 2.2.

2.2.4 Data analysis

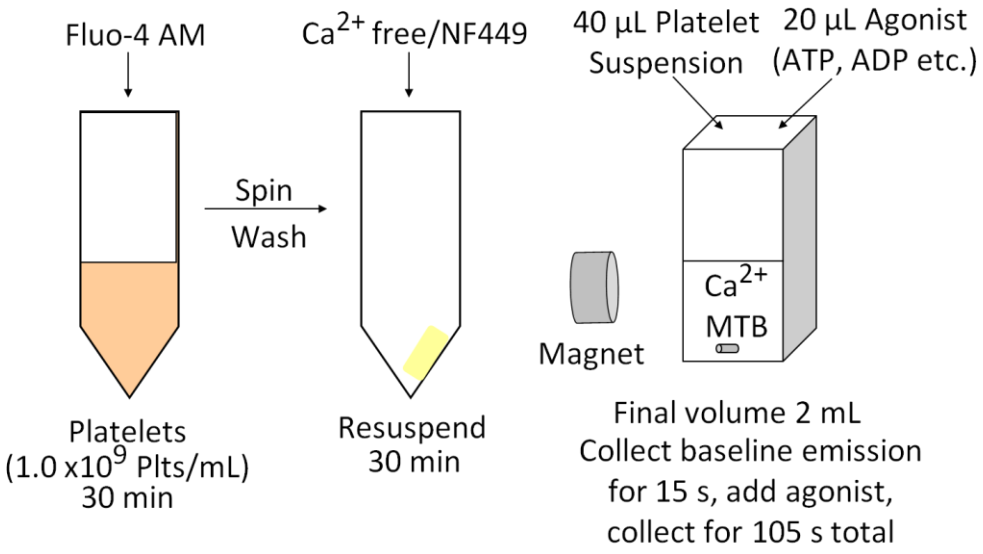

Figure 2.2: Schematic representation of experimental setup. Platelets were incubated with the Ca^{2+} probe Fluo-4 AM for 30 min, then the excess probe was washed off and the platelets incubated with either buffer or NF449. Finally, measurements of Ca^{2+} influx were performed using a spectrofluorometer with a magnet setup so that samples could be stirred during measurement. Samples were kept in a Ca^{2+} free environment until measurement.

Included in the results and discussions section are spectra that represent raw fluorescence data collected over time, whereas the summarized data are represented as a percent change in fluorescence. This percent change was calculated by subtracting the quotient of the average baseline fluorescence intensity and average peak fluorescence intensity from 1 and multiplying by 100 to obtain a percent. N = human blood draws.

2.4 Results

2.4.1. NF449 sensitizes ATP-induced Ca^{2+} Influx

ATP was added as an agonist to platelets, in the presence and absence of NF449, to evaluate its effect on P2X1 mediated Ca^{2+} influx. Shown in figure 2.3 (left), adding CaMTB to platelets alone has no effect on the fluorescence signal. Furthermore, the addition of ATP to the platelet sample resulted in no significant increase in fluorescence signal (compared to baseline) due to Ca^{2+} entry into the platelets. However, there was a significant increase in Ca^{2+} entry when ATP was added to platelets containing 0.5 μM NF449. Furthermore, as shown in figure 2.3 (right), Ca^{2+} entry into the platelets containing 2.5 μM NF449 increased as the concentration of ATP was increased from 67 nM to 5 μM, although the first significant change in signal (in comparison to baseline) did not occur until the ATP concentration reached 310 nM. Thus, activation of the P2X1 receptor and subsequent Ca^{2+} influx is ATP concentration dependent under NF449 sensitizing conditions.

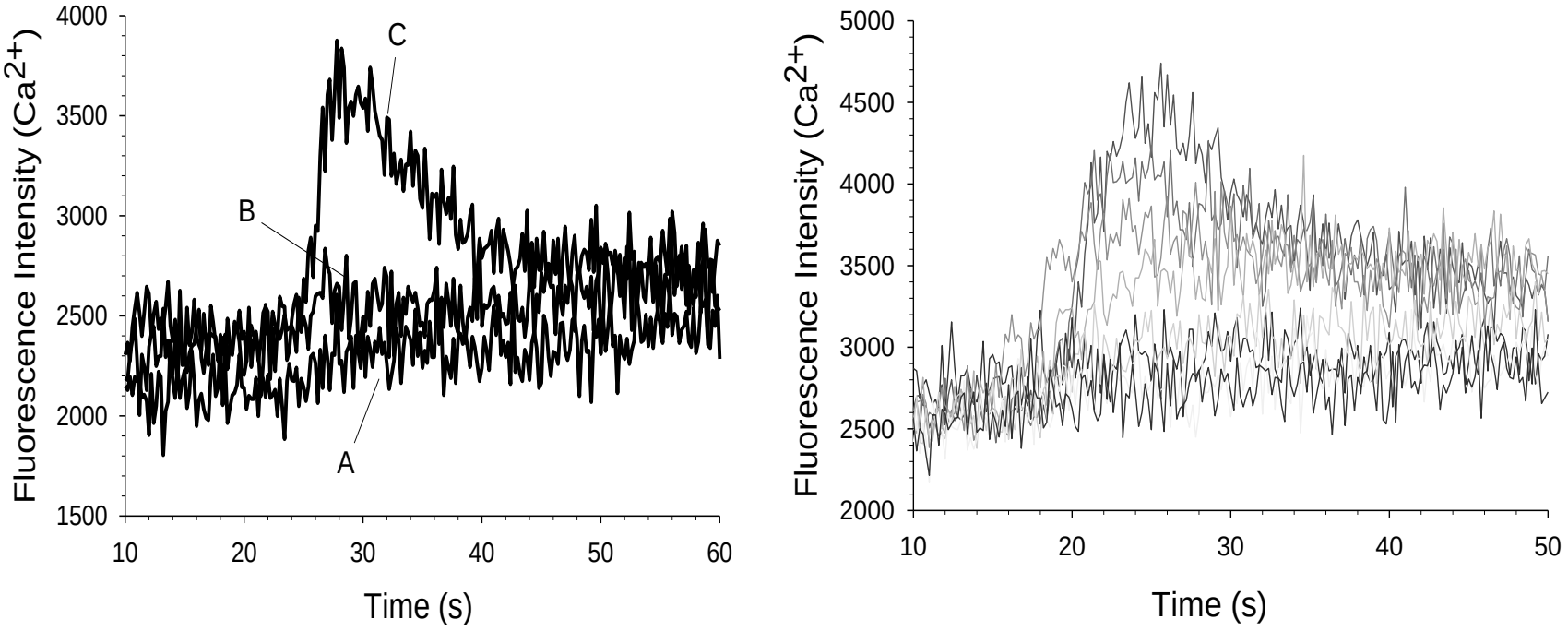

Figure 2.3: (Left) Fluorescence measurements taken over time for platelets in the presence and absence of NF449. No significant increase in Ca^{2+} is measured when CaMTB (trace C) or 2.5 uM ATP (trace B) is added to platelets alone. However, an increase in Ca^{2+} was measured when 2.5 uM ATP was added to platelets containing 0.5 uM NF449 (trace A). (Right) The effect of ATP on platelet Ca^{2+} influx with a constant concentration of 2.5 uM NF449. As the concentration of ATP was increased from 73 nM up to 5 µM, the intracellular platelet Ca^{2+} also increased.

2.4.2 Effect of Ca^{2+} free buffer on Ca^{2+} entry into the platelet via ATP and ADP agonists

A possible explanation for the increase in fluorescence emission shown in figure 2.3 is that the ATP contained ADP impurities that were stimulating P2Y-type receptors, resulting in the release of Ca^{2+} stores in the platelet granules. Therefore, studies were also performed in a Ca^{2+}-free buffer. In this construct, activation of the P2X1 receptor with ATP should not result in an increase of fluorescence emission due to Ca^{2+} entry into the platelet because there is no Ca^{2+} in the buffer to cross the platelet membrane. The data in figure 2.4 (left) show that ATP additions to platelets containing NF449 in a Ca^{2+} free environment result in no increase in fluorescence signal. The top trace in figure 2.4 (left) is another aliquot of platelets from the same sample. However, this trace was obtained using a Ca^{2+}-containing buffer and, as shown, Ca^{2+} entry into the platelet was detected. Finally, when ADP was added to NF449-containing platelets, there was an increase in fluorescence signal even in the absence of Ca^{2+}, which is due to Ca^{2+} release from granular stores in the platelets. The summarized data in figure 2.4 (right) suggests that the ATP induced Ca^{2+} entry into NF449-containing platelets is through P2X1 activation and not solely a result of an ADP impurity contained in the ATP agonist.

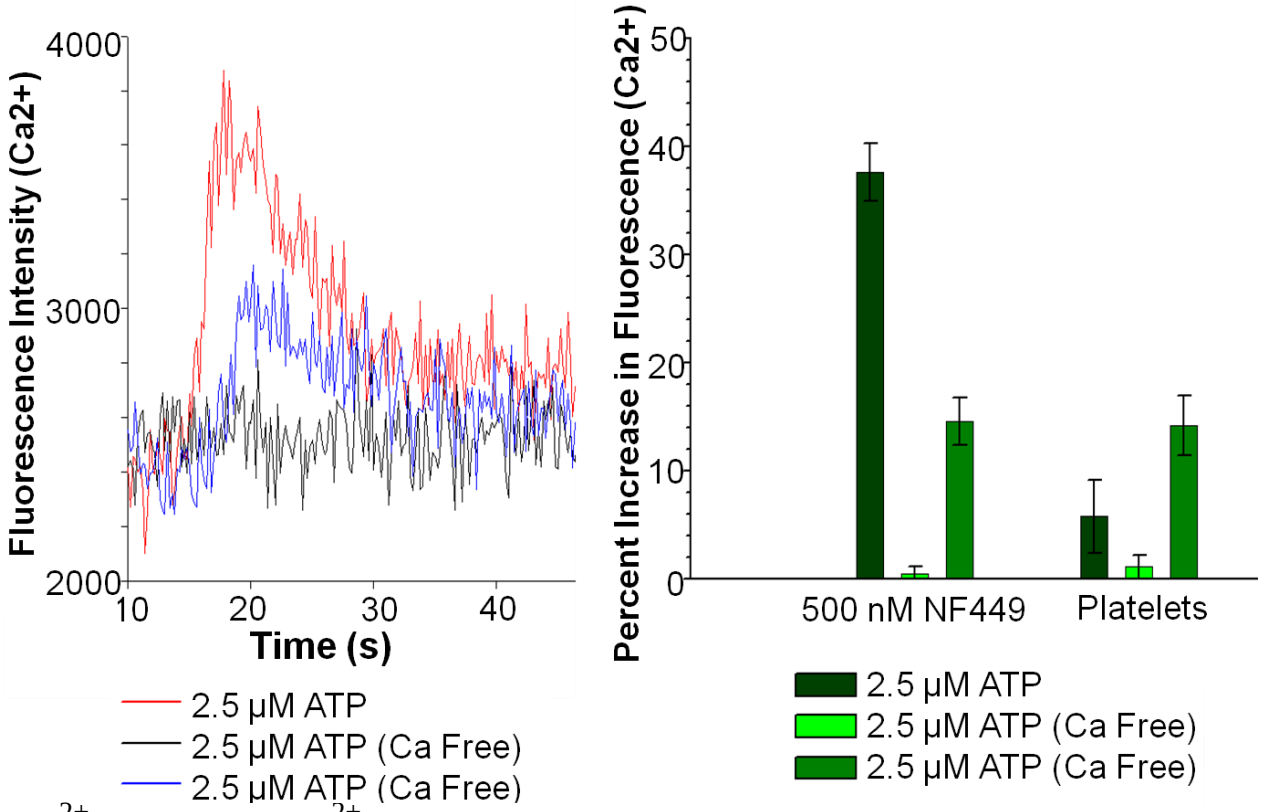

Figure 2.4: Effect of Ca^{2+} free buffer on Ca^{2+} influx in platelet containing 0.5 µM NF449. (Left) 2.5 µM ATP was added as an agonist in the presence of Ca^{2+} as represented in trace A. The typical increase in Ca^{2+} influx is seen. However, in a Ca^{2+} free environment (trace B), the addition of 2.5 µM ATP resulted in no significant increase in Ca^{2+}. Additionally, in the Ca^{2+} free environment, ADP is still able to elicit a Ca^{2+} increase (trace C). (Right) The summarized data indicates that when Ca^{2+} is not present, there is no Ca^{2+} influx due to 2.5 µM ATP in platelets containing 0.5 µM NF449 or platelets alone. However, signal due to ADP stimulation is still present. Error is standard error of the mean. N=9 (2.5 µM ATP, platelets), N=7 (2.5 µM ATP, NF449), N=4 (2.5 µM ATP, Ca^{2+} free), and N=5 (2.5 µM ADP, Ca^{2+} free).

2.4.3 Effect of α,β-me-ATP concentrations on Ca^{2+} entry into the platelet

The P2X1 receptor is most commonly studied using a form of ATP that is stable, such as α,β-me-ATP. This form of ATP ensures that breakdown to ADP does not occur, thus minimizing effects from P2Y-type events. Figure 2.5 shows a Ca^{2+} influx due to the addition of α,β-me-ATP to NF449 containing platelets (18.7 ± 0.9%), a significantly weaker signal ($P < 0.001$) in comparison to authentic ATP stimulation (39.3 ± 0.8%). No calcium influx was seen when ATP or α,β-me-ATP were added to platelets alone. Unlike ATP, higher concentrations of α,β-me-ATP did not elicit Ca^{2+} influx (data not shown), suggesting the potential for α,β-me-ATP to desensitize the P2X1 receptor more readily than ATP itself.

2.4.4 Effect of NF449 concentrations on Ca^{2+} entry into the platelet

NF449 is generally regarded as a competitive inhibitor of the P2X1 receptor and at concentrations greater than 1 μM has been shown to have non-specific inhibitory effects on P2Y receptors. However, data in figures 2.2-2.4 suggest receptor sensitization at a concentration of 0.5 and 2.5 μM NF449. Therefore, it was anticipated that concentrations of NF449 less than 1 μM would also have the same sensitizing effects. Figure 2.6 summarizes the effect of varying NF449 concentrations from 62.5 nM up to 40 μM in the presence of 2.5 μM ATP as the agonist for P2X1 stimulation and subsequent Ca^{2+} entry into the platelet. As shown, the signal resulting from the fluorescence emission due to Ca^{2+} entry into the platelet begins to increase with increments of NF449. However, as

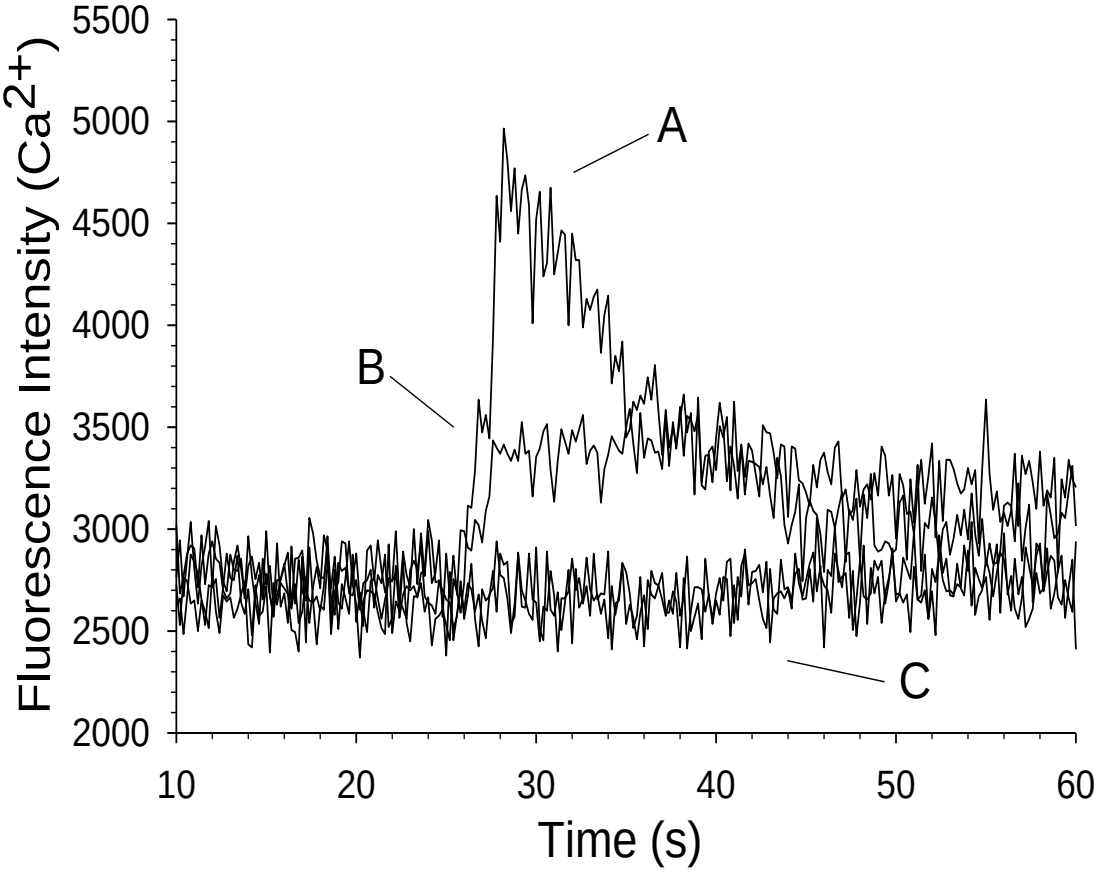

Figure 2.5: Effect of α,β-me-ATP on platelet Ca^{2+} influx. Both A and B traces indicate the presence of platelets containing 0.5 μM NF449, but the agonist for trace A is 2.5 μM ATP and the agonist for trace B is 2.5 μM α,β-me-ATP. Increases in Ca^{2+} influx were measured in the case of both agonists, but the increase due to ATP was larger than the increase due to α,β-me-ATP. The two controls in this figure, represented as C, are platelets alone that were treated with both agonists, neither showed an increase in Ca^{2+} influx.

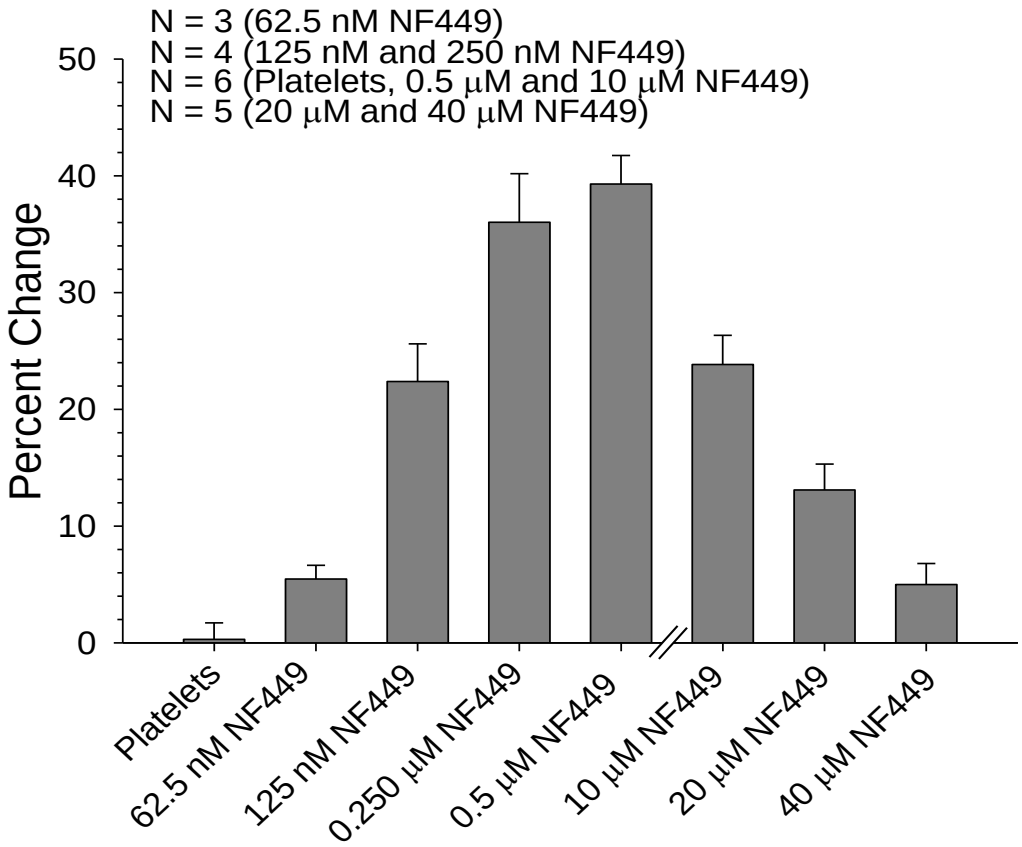

Figure 2.6: Effect of NF449 concentration on platelet Ca^{2+} influx due to 2.5 μM ATP. As NF449 concentration is increased from 0 to 0.5 μM, the Ca^{2+} influx increases, but as the concentration of NF449 is further increased from 0.5 μM to 40 μM the Ca^{2+} influx decreases from the measured maximum. Error is standard error of the mean.

the concentration of NF449 continues to increase, an inhibitory effect emerges (for an ATP concentration of 2.5 μM), resulting in reduced Ca^{2+} entry into the platelet.

Importantly, when the NF449 concentrations reached inhibitory levels (of the 2.5 μM ATP), the addition of higher concentrations of ATP were able to restore the Ca^{2+} entry into the platelets. For example, at an NF449 concentration of 0.5 μM, the percent change in fluorescence emission upon the addition of 2.5 μM ATP was 39.3 ± 2.4%. This value dropped to 13.1 ± 2.2% when the NF449 concentration was increased to 20 μM. However, when the ATP concentration was raised to 10 μM, the percent change in fluorescence emission recovered to a value of 34.1 ± 2.8%. Sample spectra are shown in figure 2.7. These results suggest that the ratio between ATP and NF449 is key in stimulating or inhibiting Ca^{2+} increase through the P2X1 receptor. Therefore, if the ATP concentration in a particular study is 2.5 μM, the optimum sensitizing concentration of NF449 is ~ 0.5 μM, while inhibitory concentrations of NF449 would be obtained at concentrations > 10 μM. Of course, these values of NF449 would change if the ATP concentrations were changed.

2.4.5 Time Dependence of NF449 Sensitization of P2X1

Previously, NF449 has been shown to sensitize P2X1, although the effect was measured at picomolar concentrations on single oocytes and only lasted for a few seconds. In studies reported here, nanomolar to low micromolar concentrations exhibited this same sensitization feature even though the NF449 was allowed to incubate with the

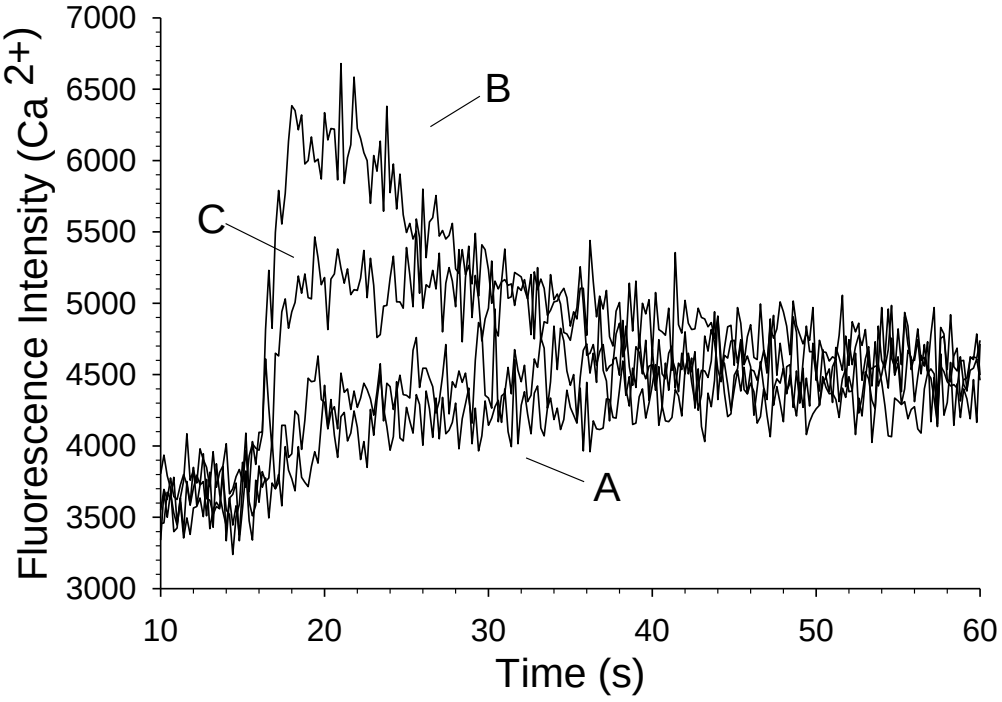

Figure 2.7: Overcoming NF449 inhibition using 10 µM ATP. As the concentration of NF449 exceeds 0.5 µM, inhibition of Ca^{2+} influx occurs when 2.5 µM ATP is added to 20 and 40 µM NF449 platelet samples (traces A). When 10 µM ATP is added, the NF449 inhibition is overcome and Ca^{2+} influx occurs in 20 and 40 µM NF449 platelet samples, traces B and C, respectively.

platelets for 30 minutes prior to the addition of agonist. Therefore, a study was performed to determine if the ability of NF449 to sensitize the platelet P2X1 receptor was time dependent. The time study was executed using platelets incubated with 62.5 nM NF449 followed by the addition of 2.5 μM ATP as the agonist. The results of this study, shown in figure 2.8, indicate that the fluorescence signal from Ca^{2+} entry due to addition of the ATP agonist decreased with time. The increase at 1 min is thought to be less than that of the 5 min signal due to NF449 not having enough time to diffuse to the platelet surface. The subsequent decrease in signal suggests that the sensitizing effect of NF449 is indeed time dependent, consistent with the previous report.[27] However, it appears that increasing the NF449 concentration prolongs its sensitization abilities.

2.4.6 P2Y1 inhibition with MRS and the effect on Ca^{2+} influx

In order to investigate the P2Y1 receptor action in the presence of ADP and ATP, MRS2179 was employed. MRS2179 is a competitive antagonist of P2Y1, and is more selective towards P2Y1 than P2X1.[33-34] As shown in figure 2.9, with increasing concentration of MRS2179, the intracellular Ca^{2+} signal decreases in response to ADP. However, when NF449 is also added to the highest concentration of MRS2179, some of the ADP signal is recovered as well as Ca^{2+} influx due to ATP. Though, the Ca^{2+} signal from ATP is not as high as for samples that were only sensitized with NF449. This could suggest a relationship between the sensitization of P2X1 and the ability of P2Y1 to

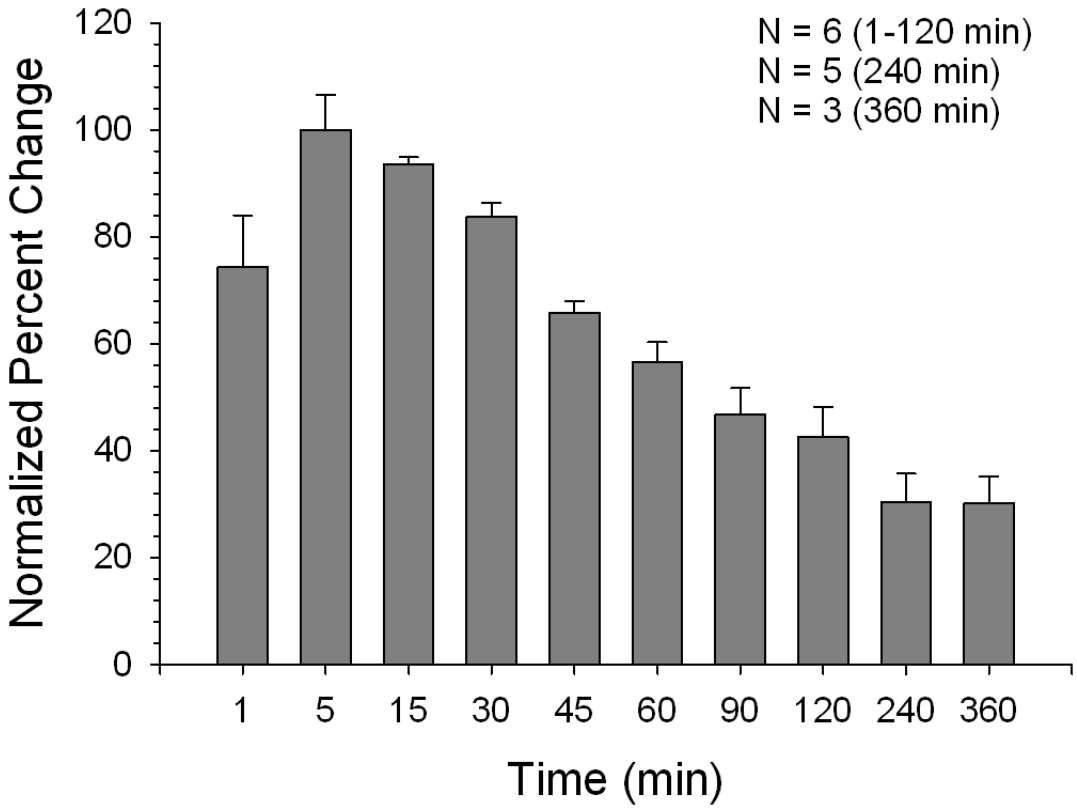

Figure 2.8: NF449 potency over time with 2.5 µM ATP agonist. Using 62.5 nM NF449, platelet Ca^{2+} influx was measured over the course of 6 hours with the data being normalized to the 5 min. percent change in signal. The Ca^{2+} influx peaked at 5 min and decreased steadily over time. Error is standard error of the mean.

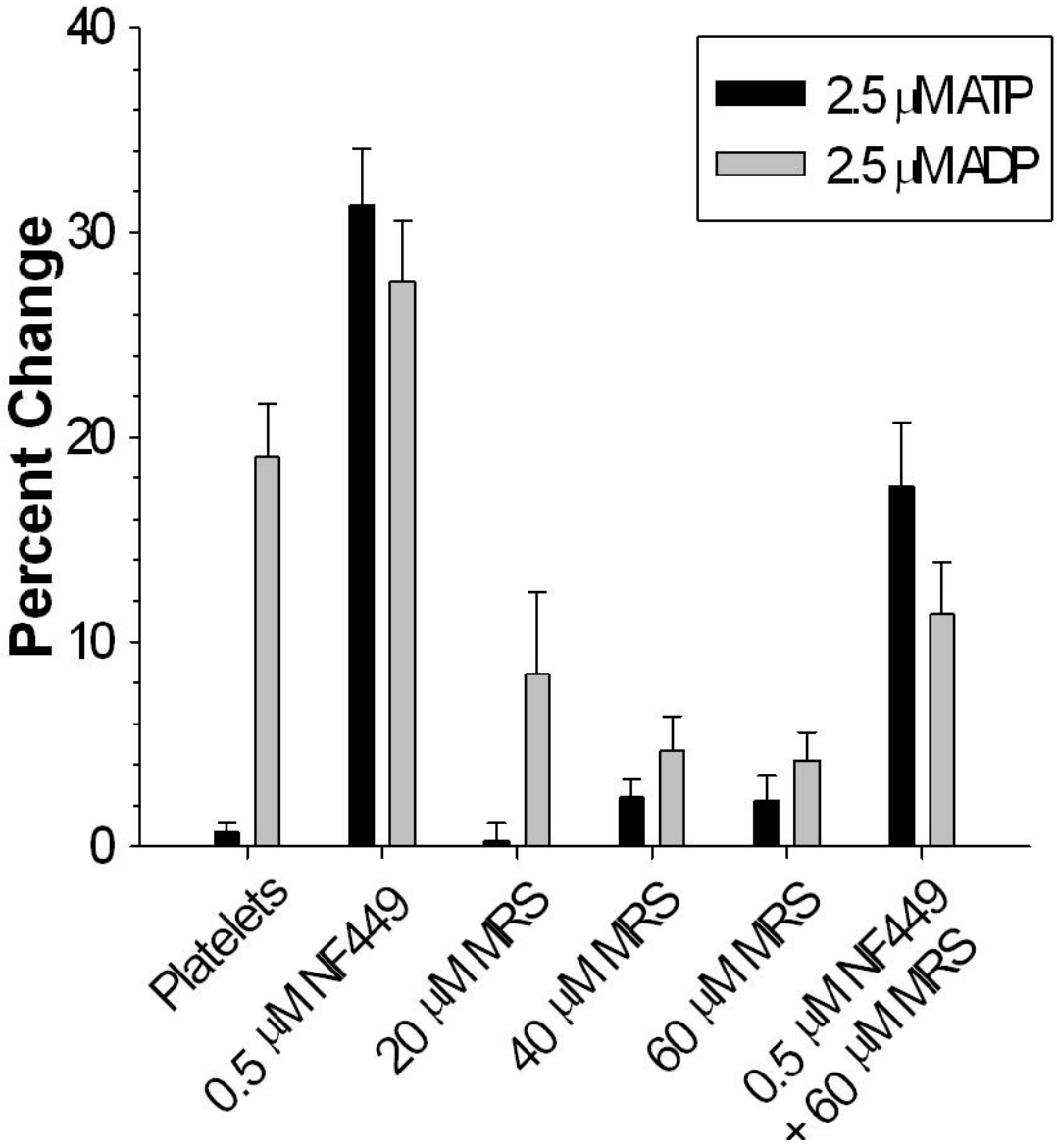

Figure 2.9: The effect of P2Y1 inhibition on platelet Ca^{2+}. As increasing concentrations of MRS are added to the platelet solution it inhibits the Ca^{2+} release due to ADP binding P2Y1. However, when NF449 is also added to the samples containing 60 μM MRS, the Ca^{2+} signal from ATP and ADP recovered. P2Y1 also has some inhibitory effect on P2X1 so; the Ca^{2+} signal from ATP is lower compared to the sample that was sensitized with NF449 alone. Error is standard error of the mean. N is 4 or higher for all bars.

mobilize Ca^{2+} in response to ADP. It should be noted that ATP could not evoke Ca^{2+} influx without the presence of NF449 to sensitize the platelets prior to study.

2.5 Conclusions

Collectively, the data in figures 2.5 and 2.7 suggest something more profound about the effect of NF449 on P2X1 and the receptor itself. Specifically, the data in figures 2.5 and 2.8 demonstrate that the effect of NF449 on P2X1 is both concentration- and time-dependent, respectively. Moreover, both of these effects can be immediately overcome by high concentrations of ATP. In addition, the data in figure 2.6 show that the overall signal from the addition of ATP is higher when both P2X1 and P2Y1 are open. This suggests that the addition of ATP to the platelet sample results in an increase in P2Y1 activity. It is possible that once ATP is bound to P2X1 and Ca^{2+} enters, the ATP is hydrolyzed to ADP, which can subsequently activate P2Y1 or P2Y12. The fate of ATP after it is bound to P2X1 is not known. If such a relationship exists, it gives more weight to the effect of ATP on platelet activity since initially ATP would bind P2X1, but then its degradation product could go on to activate the P2Y receptors, which are also involved in platelet activation.

The P2X1 receptor activity can explain why disease states with altered RBC ATP release also have hyperactive platelets. Resting platelets are constantly coming into contact with RBCs in the vasculature so, it follows that ATP released from these RBCs would be binding P2X1 and causing low levels of activation without the presence of an injured endothelium. The Spence group showed that ATP affected platelets adhering to an uninjured endothelium and that RBCs incubated with an ATP release inhibitor affected platelet adhesion.[35] It is a possibility that i*n vivo* when an injury occurs, platelets

are activated from exposed collagen and granular release from the platelets, but also the ATP released from RBCs. The ability to study the platelet without apyrase or the stable α,β-me-ATP allows for the effects of native ATP on the platelet to be studied without the risk of apyrase affecting the amount of available ATP or α,β-me-ATP derived desensitization. These sample handling tools can be used in conjunction with studies on washed platelets or platelets in the presence of RBC's in order to study P2X1 activity.

REFERENCES

REFERENCES

1. S. P. Kunapuli, Z. Ding, R. T. Dorsam, S. Kim, S. Murugappan, T. M. Quinton, ADP receptors - targets for developing antithrombotic agents. *Curr. Pharm. Des.* 2003, *9*. 2303-2316.

2. M. P. Mahaut-Smith, S. J. Ennion, M. G. Rolf, R. J. Evans, ADP is not an agonist at P2X1 receptors: evidence for separate receptors stimulated by ATP and ADP on human platelets. *Br J Pharmacol* 2000, *131*. 108-114.

3. S. Murugappan, S. P. Kunapuli, The role of ADP receptors in platelet function. *Front. Biosci.* 2006, *11*. 1977-1986.

4. C. Vial, B. Hechler, C. Leon, J. P. Cazenave, C. Gachet, Presence of P2X1 purinoceptors in human platelets and megakaryoblastic cell lines. *Thromb Haemost* 1997, *78*. 1500-1504.

5. M. G. Rolf, C. A. Brearley, M. P. Mahaut-Smith, Platelet shape change evoked by selective activation of P2X1 purinoceptors with alpha ,beta -methylene ATP. *Thromb Haemost* 2001, *85*. 303-308.

6. C. Y. E. Fung, C. A. Brearley, R. W. Farndale, M. P. Mahaut-Smith, A major role for P2X1 receptors in the early collagen-evoked intracellular Ca2+ responses of human platelets. *Thromb Haemost* 2005, *94*. 37-40.

7. B. Hechler, N. Lenain, P. Marchese, C. Vial, V. Heim, M. Freund, J.-P. Cazenave, M. Cattaneo, Z. M. Ruggeri, R. Evans, C. Gachet, A role of the fast ATP-gated P2X1 cation channel in thrombosis of small arteries in vivo. *J. Exp. Med.* 2003, *198*. 661-667.

8. M. P. Mahaut-Smith, G. Tolhurst, R. J. Evans, Emerging roles for P2X1 receptors in platelet activation. *Platelets* 2004, *15*. 131-144.

9. C. Oury, E. Toth-Zsamboki, C. Thys, J. Tytgat, J. Vermylen, M. F. Hoylaerts, The ATP-gated P2X1 ion channel acts as a positive regulator of platelet responses to collagen. *Thromb Haemost* 2001, *86*. 1264-1271.

10. C. Y. E. Fung, C. Cendana, R. W. Farndale, M. P. Mahaut-Smith, Primary and secondary agonists can use P2X1 receptors as a major pathway to increase intracellular Ca2+ in the human platelet. *J. Thromb. Haemostasis* 2007, *5*. 910-917.

11. S. Takano, J. Kimura, I. Matsuoka, T. Ono, No requirement of P2X1 purinoceptors for platelet aggregation. *European Journal of Pharmacology* 1999, *372*. 305-309.

12. S. Jones, R. J. Evans, M. P. Mahaut-Smith, Extracellular Ca2+ modulates ADP-evoked aggregation through altered agonist degradation: implications for conditions used to study P2Y receptor activation. *Br J Haematol 153*. 83-91.

13. M. P. Mahaut-Smith, S. Jones, R. J. Evans, The P2X1 receptor and platelet function. *Purinergic Signal*. DOI: 10.1007/s11302-011-9224-0.

14. S. Valera, N. Hussy, R. J. Evans, N. Adami, R. A. North, A. Suprenant, G. Buell, A new class of ligand-gated ion channel defined by P2X receptor for extracellular ATP. *Nature (London, United Kingdom)* 1994, *371*. 516-19.

15. C. J. Lewis, R. J. Evans, Lack of run-down of smooth muscle P2X receptor currents recorded with the amphotericin permeabilized patch technique, physiological and pharmacological characterization of the properties of mesenteric artery P2X receptor ion channels. *Br J Pharmacol* 2000, *131*. 1659-1666.

16. A. Baurand, A. Eckly, N. Bari, C. Leon, B. Hechler, J.-P. Cazenave, C. Gachet, Desensitization of the platelet aggregation response to ADP: differential down-regulation of the P2Y1 and P2cyc receptors. *Thromb Haemost* 2000, *84*. 484-491.

17. C. Gachet, P2 receptors, platelet function and pharmacological implications. *Thromb Haemost* 2008, *99*. 466-472.

18. A. R. Hardy, P. B. Conley, J. Luo, J. L. Benovic, A. W. Poole, S. J. Mundell, P2Y1 and P2Y12 receptors for ADP desensitize by distinct kinase-dependent mechanisms. *Blood* 2005, *105*. 3552-3560.

19. J. Jin, S. P. Kunapuli, Coactivation of two different G protein-coupled receptors is essential for ADP-induced platelet aggregation. *Proceedings of the National Academy of Sciences of the United States of America* 1998, *95*. 8070-8074.

20. P. Savi, P. Beauverger, C. Labouret, M. Delfaud, V. Salel, M. Kaghad, J. M. Herbert, Role of P2Y1 purinoceptor in ADP-induced platelet activation. *FEBS Letters* 1998, *422*. 291-295.

21. C. Leon, B. Hechler, M. Freund, A. Eckly, C. Vial, P. Ohlmann, A. Dierich, M. LeMeur, J.-P. Cazenave, C. Gachet, Defective platelet aggregation and increased resistance to thrombosis in purinergic P2Y1 receptor-null mice. *Journal of Clinical Investigation* 1999, *104*. 1731-1737.

22. J. A. Erhardt, K. Pillarisetti, J. R. Toomey, Potentiation of platelet activation through the stimulation of P2X1 receptors. *J Thromb Haemost* 2003, *1*. 2626-35.

23. P. M. Dunn, A. G. H. Blakeley, Suramin - a Reversible P2-Purinoceptor Antagonist in the Mouse Vasdeferens. *Br J Pharmacol* 1988, *93*. 243-245.

24. K. Braun, J. Rettinger, M. Ganso, M. Kassack, C. Hildebrandt, H. Ullmann, P. Nickel, G. Schmalzing, G. Lambrecht, NF449: a subnanomolar potency antagonist at recombinant rat P2X1 receptors. *Naunyn Schmiedebergs Arch Pharmacol* 2001, *364*. 285-290.

25. M. Hulsmann, P. Nickel, M. Kassack, G. Schmalzing, G. Lambrecht, F. Markwardt, NF449, a novel picomolar potency antagonist at human P2X1 receptors. *European Journal of Pharmacology* 2003, *470*. 1-7.

26. M. U. Kassack, K. Braun, M. Ganso, H. Ullmann, P. Nickel, B. Boing, G. Muller, G. Lambrecht, Structure-activity relationships of analogues of NF449 confirm NF449 as the most potent and selective known P2X1 receptor antagonist. *Eur. J. Med. Chem.* 2004, *39*. 345-357.

27. J. Rettinger, K. Braun, H. Hochmann, M. U. Kassack, H. Ullmann, P. Nickel, G. Schmalzing, G. Lambrecht, Profiling at recombinant homomeric and heteromeric rat P2X receptors identifies the suramin analogue NF449 as a highly potent P2X1 receptor antagonist. *Neuropharmacology* 2005, *48*. 461-468.

28. T. Kawate, J. C. Michel, W. T. Birdsong, E. Gouaux, Crystal structure of the ATP-gated P2X4 ion channel in the closed state. *Nature (London, United Kingdom)* 2009, *460*. 592-598.

29. M. Hattori, E. Gouaux, Molecular mechanism of ATP binding and ion channel activation in P2X receptors. *Nature (London, United Kingdom) 485*. 207-212.

30. S. El-Ajouz, D. Ray, R. C. Allsopp, R. J. Evans, Molecular basis of selective antagonism of the P2X1 receptor for ATP by NF449 and suramin: contribution of basic amino acids in the cysteine-rich loop. *Br J Pharmacol* 2012, *165*. 390-400, DOI: 10.1111/j.1476-5381.2011.01534.x.

31. B. Hechler, S. Magnenat, M. L. Zighetti, M. U. Kassack, H. Ullmann, J.-P. Cazenave, R. Evans, M. Cattaneo, C. Gachet, Inhibition of platelet functions and thrombosis through selective or nonselective inhibition of the platelet P2 receptors with increasing doses of NF449 [4,4',4",4"'-(carbonylbis(imino-5,1,3-benzenetriylbis(carbonylimino)))tetrakis-benzene-1,3-disulfonic acid octasodium salt]. *J. Pharmacol. Exp. Ther.* 2005, *314*. 232-243.

32. M. Hohenegger, M. Waldhoer, W. Beindl, B. Boing, A. Kreimeyer, P. Nickel, C. Nanoff, M. Freissmuth, Gsalpha -selective G protein antagonists. *Proceedings of the National Academy of Sciences of the United States of America* 1998, *95*. 346-351.

33. J. L. Boyer, A. Mohanram, E. Camaioni, K. A. Jacobson, T. K. Harden, Competitive and selective antagonism of P2Y1 receptors by N6-methyl 2'-deoxyadenosine 3',5'-bisphosphate. *Br J Pharmacol* 1998, *124*. 1-3, DOI: 10.1038/sj.bjp.0701837.

34. J. L. Boyer, T. Romero-Avila, J. B. Schachter, T. K. Harden, Identification of competitive antagonists of the P2Y1 receptor. *Mol. Pharmacol.* 1996, *50*. 1323-1329.

35. W. Karunarathne, C. J. Ku, D. M. Spence, The dual nature of extracellular ATP as a concentration-dependent platelet P2X1 agonist and antagonist. *Integr Biol* 2009, *1*. 655-663, DOI: Doi 10.1039/B909873a.

CHAPTER 3: INTEGRATION OF MULTIPLE COMPONENTS IN POLYSTYRENE-BASED MICROFLUIDIC DEVICES

3.1 Introduction to Microfluidic Device Fabrication

As discussed in Chapter 1, soft lithography is a fast and easy method for rapid fabrication of microfluidic devices.[1-2] Furthermore, microfluidic devices are popular for use in studying biological systems due to their ability to perform fast/high-throughput analysis,[3-4] utilize small sample volumes,[5] and integrate such processes.[6-9] The incorporation of cells onto microfluidic devices has become popular because dimensions mimicking *in vivo* environments can be fabricated and that both adherent and non-adherent cells can be investigated separately or simultaneously.[10-13]

3.1.1 PDMS Microfluidic Devices

One of the most commonly used elastomeric polymers, polydimethyl siloxane (PDMS), is optically transparent, gas permeable, pliable and has been useful for various cell based applications. PDMS based microfluidic devices have been used to study interactions between multiple vascular cell types,[14-16] interactions between cells and underlying adhesion proteins,[17] cell migration,[18] automated cell culture,[19] cell permeability,[20] transendothelial electrical resistance,[21] and electrochemical detection of analytes released by cells.[6, 22]

While PDMS has been a successful material for creating cell based experiments and platforms, it has some disadvantages. PDMS, a crosslinked polymer composed of

hydrophobic dimethyl-siloxane oligomers, has been shown to absorb small hydrophobic molecules[23], leach un-crosslinked oligomers into solution,[24] and allow evaporation through bulk material.[25] Furthermore, efforts have been made to make microfluidic devices amenable for use with standard lab equipment and easier to use in general. This includes integration with passive pumping and automated liquid handlers,[26-27] and the ability to make microfluidic arrays capable of plate reader detection,[3, 28] but these devices are still academic prototypes and they do not fit with all standard lab equipment. Though this is a good start to making microfluidic devices integrated with standard equipment more work in this area is needed.

3.1.2 Polystyrene Microfluidic Devices

Devices made from materials more established for cell culture, such as polystyrene (PS), have the potential to be more compatible for cell culture on microfluidic devices than PDMS.[11] Multiple groups have focused on the fabrication of polystyrene devices for microarrays or cell-based assays.[29-34] Takayama *et al.* tested several "hard top, soft bottom" microfluidic devices using a combination of the following rigid and elastomeric polymers: PS, glycol-modified polyethylene terephthalate (PETG), or cyclic olefin copolymer (COC) and polyurethane (PU) or PDMS coated with parylene C. To fabricate the rigid layer of the devices, a PDMS master mold was made using conventional soft lithography techniques[1] and high temperature epoxy was poured onto the mold and allowed to cure. The result is an epoxy mold with positive features. Then, via hot

embossing, the epoxy mold was pressed into PS, PETG or COC. Finally, the soft bottom of the device was bonded to the rigid plastic via plasma bonding. These devices had lower evaporation and lower oxygen permeability when compared to devices made solely out of PDMS.[35]

Beebe *et al.* took this approach one step further and fabricated a device whose top and bottom are made out of polystyrene. Using a similar technique based on soft lithography to make epoxy molds and hot embossing to create channel structures on PS, arrayed devices were fabricated. Though a device made completely of PS was fabricated, a limitation of the method still exists. This limitation includes the potential for channels to collapse during the thermal bonding of PS to PS when aspect ratios are too high.[30] A feature common to both of these previous methods is the use of a heated hydraulic press and multiple molding steps.

Allbritton *et al.* developed a method that only involves the production of a PDMS mold via soft lithography, without the need for a heated press to produce channel structure, as gamma-butyrolactone (GBL) was utilized to dissolve PS onto the mold. Importantly, GBL dissolved PS without swelling the PDMS mold. Using this dissolving process, devices with microwell and micropost arrays were fabricated and used to study adherent and non-adherent cells. However, to seal the devices, a blank PS sheet was made (using the same GBL process) and then sealed to the other PS piece via hot plate heating and manual pressure.[36]

Another study investigated the biocompatibility of cells on different substrates, where a hot embosser was used to create a chamber that cells were cultured in and studied.[29]

While these previous fabrication strategies were useful in demonstrating the advantages of using polystyrene as a biocompatible microfluidic device material, there has been a lack of integration with standard lab equipment such as pipets or instrumentation. This chapter will focus on a method to fabricate a polystyrene microfluidic device that is easy, capable of cell culture and integration with standard lab equipment.

3.2 Methods

3.2.1 Fabrication of a polystyrene device with integrated channels

The general strategy for fabricating polystyrene devices with integrated channels is shown in figure 3.1. A PDMS mold with raised features was fabricated based on previously established soft lithography techniques,[37-38] except a positive mask was used to produce recessed features in the master. Masters were fabricated on clean silicon wafers with SU-8 50 photoresist (Microchem Corporation, Newton, MA, USA) spun at 500 rpm for 15 s and then 1000 rpm for 30 s, eventually leading to features that were 100 μm tall. The coated wafer was then exposed to ultraviolet light through a transparency positive mask containing 250 μm wide channels in a serpentine pattern. After development, this resulted in a master with recessed features. A 10:1 ratio of elastomer:curing agent (Sylgard 184, Ellsworth Adhesives, Germantown, WI, USA) was then poured over the completed master, cured at 75 ˚C, and subsequently removed from the master and sealed to a glass slide using a thin layer of uncured PDMS. A retaining ring, made from PDMS, was then sealed to the mold to eventually hold melted PS. A surface modification on the PDMS was then performed by preparing a 0.1 M solution of (3-mercaptopropyl)-trimethylsiloxane (Sigma-Aldrich, St. Louis, MO, USA) in

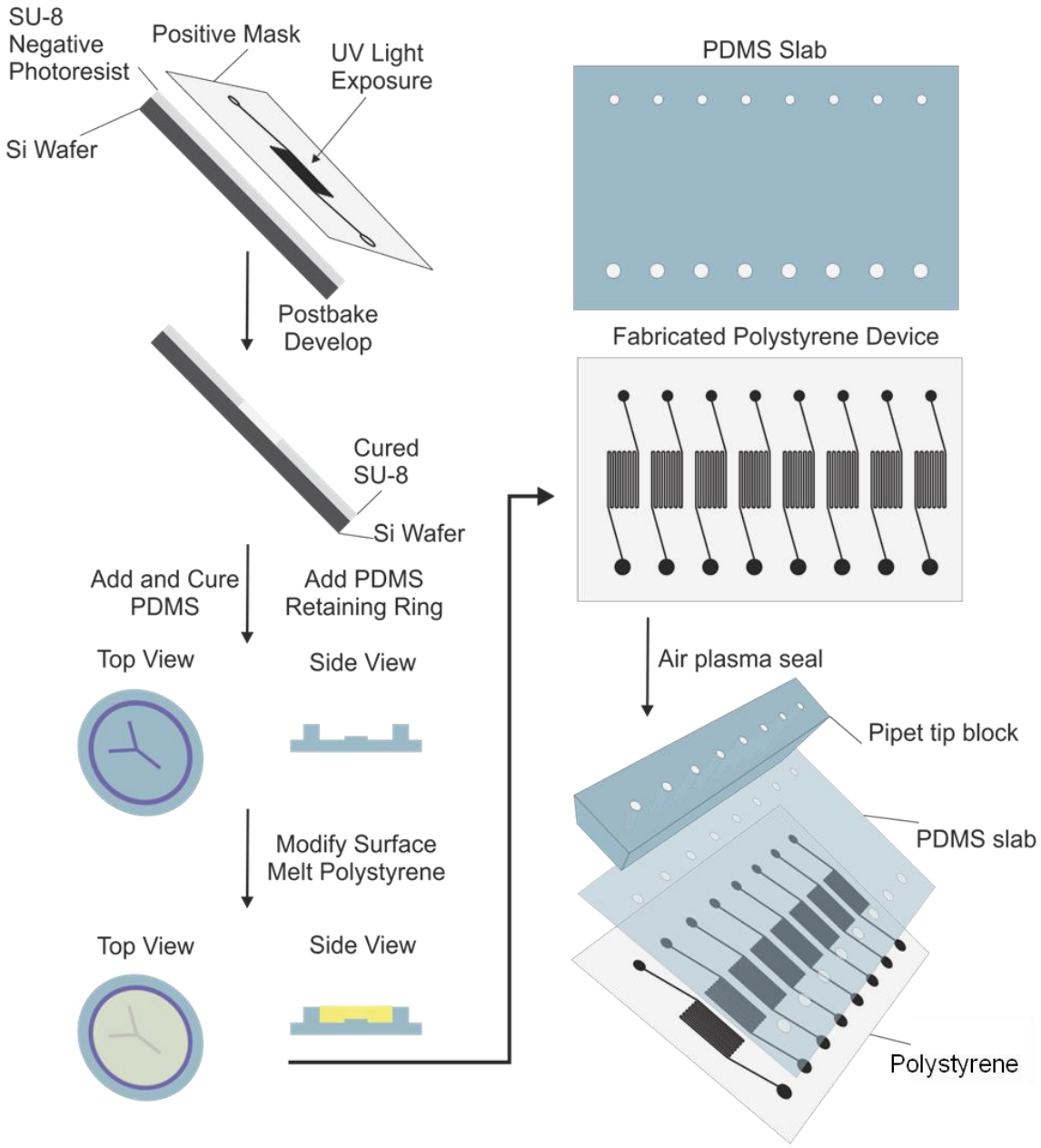

Figure 3.1: Fabrication of polystyrene devices with integrated channels. A silicon master is coated with SU-8 50 photoresist, and exposed to UV light through a positive photomask containing the serpentine features. The master is then developed and a PDMS replicate of the master is made. This PDMS mold is then sealed to a piece of glass, and a retaining ring of PDMS sealed along the outside. The PDMS is modified with 0.1 M (3-mercaptopropyl)-trimethylsiloxane, and polystyrene melted into the mold at 185 °C for 9 hours. The completed device is then removed and a PDMS cover slab with punched access holes is sealed to the polystyrene device through exposure to air plasma.

The acetonitrile was allowed to evaporate, and then approximately 5 g of polystyrene from Petri dishes were melted in the PDMS mold *via* contact heating for 9 hours on a hotplate set to 185 ˚C. The hotplate was then turned off and the PS device cooled to room temperature before it was removed from the mold. Once the PS device was removed from the mold, the channels were air plasma sealed to a 10:1 PDMS layer with an inlet (1/8 in) at each channel. This PDMS layer was made by pouring the elastomer and curing agent mixture onto a blank silicon wafer and after curing, inlets were punched. In order to achieve air plasma sealing, the PDMS and PS layers were cleaned with isopropyl alcohol and doubly deionized water before being dried under vacuum for 5 min and then exposed to air plasma for 1 min.[37] Immediately following exposure to plasma, the two layers were aligned by hand and sealed. To ensure permanent sealing, the device was placed in a 75 ˚C oven for 30 min.

A PDMS injection block was also fabricated for sample delivery. Pipet tips were suspended in a 10:1 ratio of elastomer:curing agent and cured for 30 min at 75 ˚C. The pipet tips were then removed and inlets were punched with a 20 gauge luer stub adapter. The PDMS injection block was then cut to the size of the polystyrene chip and air plasma sealed to the device in the same manner as described above.

3.2.2 Integration of the Polystyrene Device with a Plate Reader

In order to make the device amenable for measurement in a plate reader (Spectramax M4, Molecular Devices, Sunnyvale, CA, USA) a conventional, black, 96-well plate (Greiner Bio-One, Monroe, NC, USA) was modified by removing the bottom of wells with a rotary tool. This plate was then aligned over the serpentine channels in the

fabricated polystyrene microfluidic device, and the assembly was inserted into the plate reader for analysis.[3] Fluorescein standards were then pipeted into the device using the pipet interface block described in the methods section above. Fluorescence measurements were obtained using an excitation wavelength of 494 nm and an emission wavelength of 521 nm. Fluorescein standards were prepared in phosphate buffered saline at concentrations of 0, 18, 37, 75, and 150 μM. Standards were pumped through individual channels on the polystyrene device using a 100 μL pipet set to 40 μL.

3.3 Results

Although PDMS has been widely used as a substrate material for microfluidic devices, limitations of its use for biological assays include poor cell adhesion, absorption of hydrophobic molecules, and swelling in organic solvents.[11] There have been several reports of fabricating polystyrene-based microfluidic devices with hot embossing methods.[29-30, 34] However, many groups that routinely fabricate microfluidic devices do not necessarily have access to all the tools needed for hot embossing so, being able to utilize the common soft lithography equipment already in place would be beneficial. Additionally, hot embossing techniques do not allow for any integration of analytical tools during the fabrication process, such as electrodes or pumping mechanisms. In the approach described by Allbritton's group, where GBL was used to dissolve PS and then poured onto a PDM mold, resulted in devices that are thin (0.3 mm) and requires full evaporation of the solvent used to dissolve the PS.[36] Thicker PS layers are needed (3

mm) to allow for integrated channels as well as be a robust foundation for integrating the PDMS injection block.

This led to the development of a different strategy based upon melting of polystyrene from Petri dishes on a conventional hotplate against a PDMS mold. The goal of this method is to produce thicker, robust devices that can be fabricated in a day with no special equipment, bubble formation or solvent evaporation. Furthermore, these devices were further integrated with pipets for pumping and plate reader detection schemes. Additionally, the Martin group has shown that these devices can be similarly fabricated with electrodes and suitable for electrochemical detection schemes.[39]

3.3.1 Fabrication of Polystyrene-based Devices

Figure 3.1 outlines the process by which PDMS molds were created for subsequent channel formation in polystyrene devices. The process of fabricating a master, where a lithographically-derived master with recessed features was used to create the PDMS mold with raised features. A retaining wall fabricated from PDMS was then sealed to this mold. It was determined that the mold and retaining ring should be of the same material to ensure equal thermal expansion. Thus, when pieces of a polystyrene-based Petri dish were melted onto the PDMS with retaining walls, serpentine channels were formed in the polystyrene. While upper and lower channel width limits were not determined here, in this study we routinely utilized channel widths ranging from 200 to 300 μm. In order to seal the channels on the polystyrene device, a 10:1 PDMS layer with an inlet and waste well for each serpentine channel was subjected to air plasma and irreversibly sealed to the PS.

Images of the master, PDMS mold and corresponding PS device were taken using scanning electron microscopy (SEM). The PDMS mold and PS device were sputter coated with gold prior to imaging. The master contains recessed channels, which correspond to raised channels on the PDMS mold. The PS device, which is made from the PDMS mold, also has recessed channels. As shown in figure 3.2**,** the SEM images illustrate the successful transfer of features from the PDMS mold to the PS device as the feature on the mold is replicated onto the PS.

The last step in device construction involved the creation of an injection block that was molded out of PDMS using suspended pipet tips. The PDMS block was cut to size and aligned over the inlets that were punched in the PDMS layer sealed to the polystyrene. The block was then air plasma sealed in a similar manner to the PDMS layer and the final device is shown in figure 3.3**.** A unique feature of the injection block is that it is molded to support the use of pipets, thus enabling a standard micropipet or fluidic injection system to serve as the device pump. Pipet tips, suitable for a 100 or 200 µL pipet, were used to create the mold and thus, deliver solutions to the serpentine channels and out the waste well (figure 3.3). This allows for the use of pipets to induce flow rather than syringe-based pumps that involve multiple syringes and intensive rinsing procedures. A multi-channel pipet can be used to pump solution through 8 channels simultaneously and as shown in a side view of a device (figure 3.3), each pipet tip directly introduces fluid to the channel. It has also been shown that this device is capable of enabling blood flow,[39] which is a complex biological fluid often studied in clinical laboratories. The ability to propel small volumes of biological samples through a

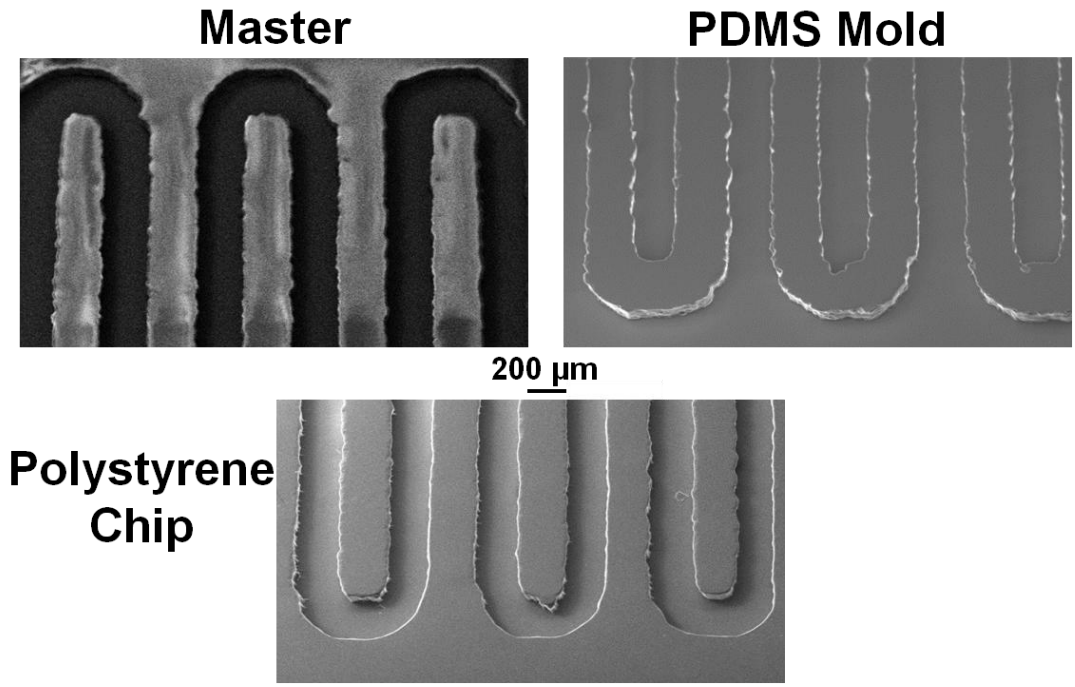

Figure 3.2: SEM Images of master, PDMS mold and PS device. Top left: image of sample master with recessed channels. Top right: image of PDMS mold with raised channels. Bottom: image of corresponding PS device made from PDMS mold. PS device has recessed channels.

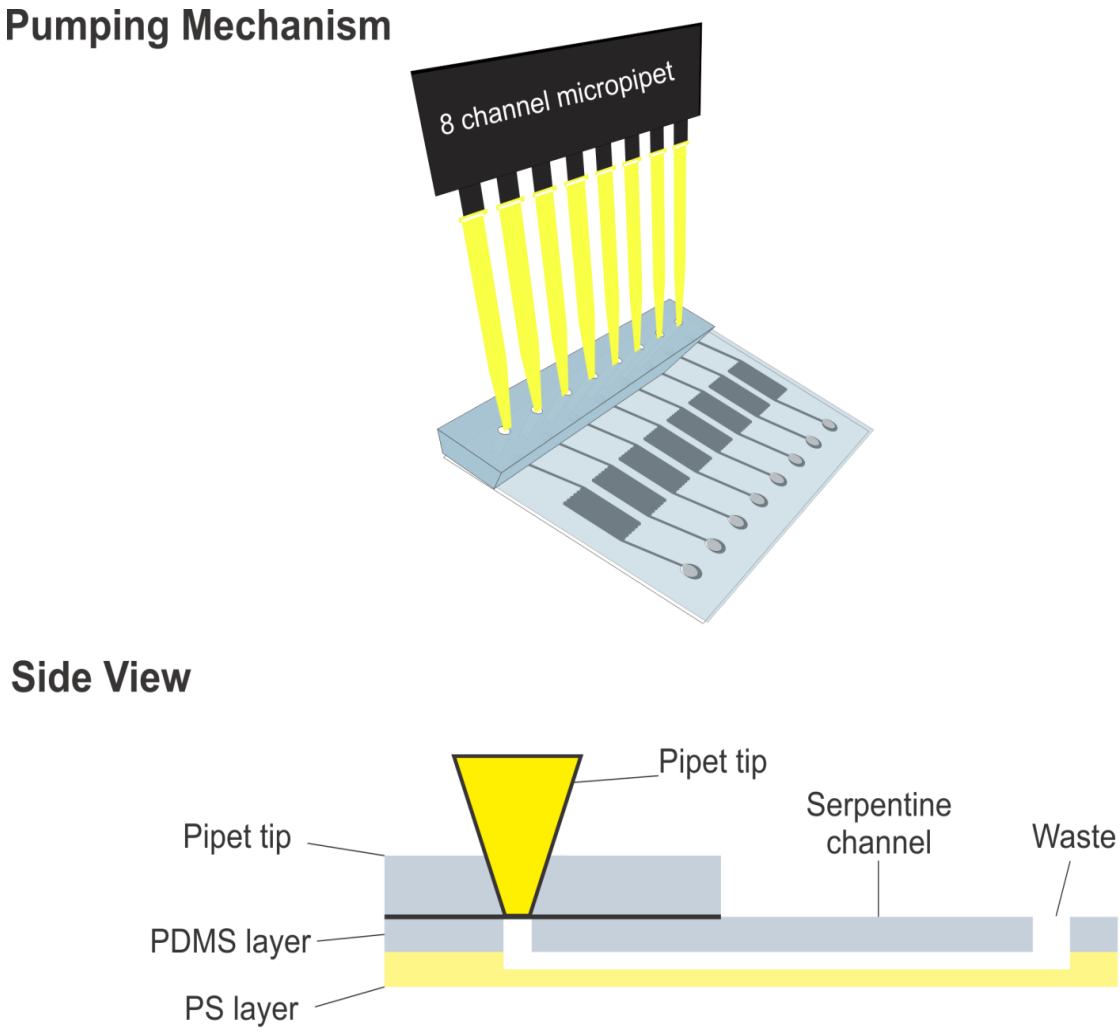

Figure 3.3: High-throughput micropipet pumping in polystyrene based microfluidic device. Top-view of the device, where an 8-channel pipet can individually and simultaneously address each channel. A pipet block is molded from immobilized 200 µL pipet tips in PDMS. This is sealed to the cover slab of PDMS over an access hole. The polystyrene device containing the serpentine channels is then sealed to the PDMS components. The side view of the device shows how the pipet tips address each serpentine channel.

microfluidic device in a high throughput manner could be useful in laboratories where such fluids are investigated on a routine basis.

3.3.2 Alignment in Plate Reader

An optical plate reader is standard equipment in most high throughput screening laboratories. The serpentine channels on the polystyrene device were fabricated to have the same width and distance apart as wells on a standard 96-well plate so that they could be analyzed on a standard plate reader. Fluorescein standards were prepared in phosphate buffered saline at concentrations of 0, 18, 37, 75, and 150 μM and then used to optimize alignment of the polystyrene device in the plate reader. Standards were pumped through individual channels on the polystyrene device using a 100 μL pipet set to 40 μL (figure 3.4A). In order to make the device amenable for measurement in the plate reader, a 96-well plate was aligned on top of the device so that drilled-out wells corresponded to each channel's serpentine (figure 3.4B). Fluorescence measurements were then taken using an excitation wavelength of 494 nm and an emission wavelength of 521 nm. It was important to determine whether or not the device was aligned properly in the plate reader by testing the linearity of the fluorescein standard curve. The alignment in the plate reader proved successful as fluorescence intensity was linear (R^2=0.99) with concentration (figure 3.4C). To ensure that the top PDMS layer had sufficiently sealed to the channel containing PS layer, fluorescence microscopy was used to show that the channels were not leaking. As shown in figure 3.5, when fluorescein is pumped through the device using a pipet and imaged using a fluorescein isothiocyanate (FITC) filter on a fluorescence microscope, the edges of the channel are clearly visible, indicating the channel is sealed.

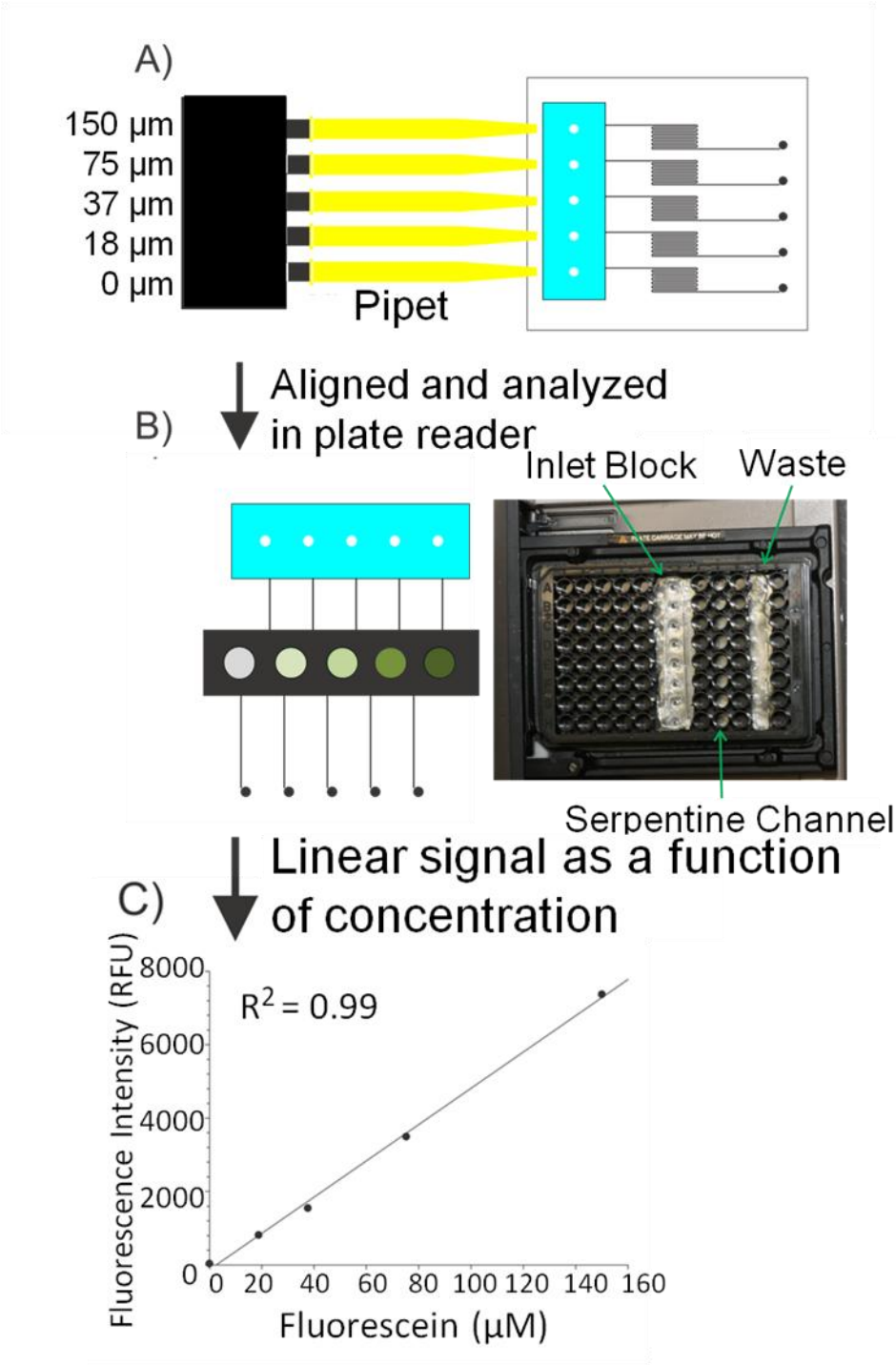

Figure 3.4: Pumping, alignment and fluorescence analysis from a polystyrene device. A) Fluorescein standards are pumped with a pipet into the device. B) The device is then placed in a plate reader and fitted with a microplate as a guide. Fluorescence analysis is performed with ex. 494 nm and em. 521 nm.

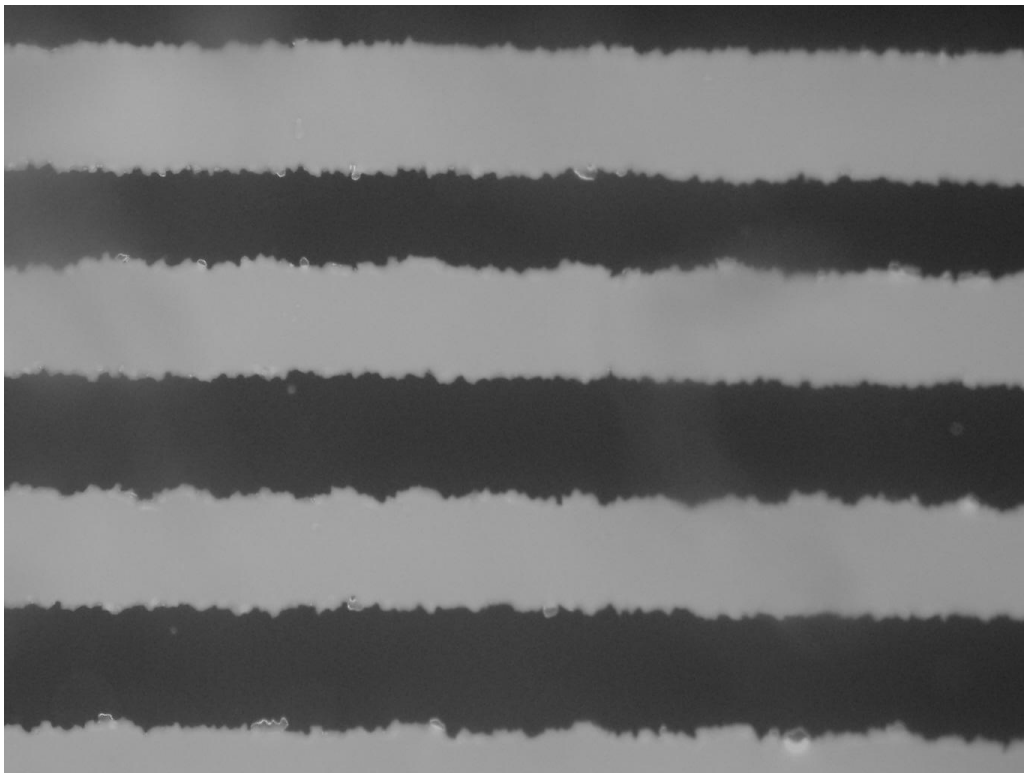

Figure 3.5: Image of fluorescein in serpentine channels. After fluorescein (ex. 494 nm, em. 521 nm) was pumped through the serpentine channel, fluorescence microscopy was used take an image of the channel. The "bright" portion is the fluorescein in the channel, whereas the "dark" portion is the space between bends in the serpentine, thus, the channel was successfully sealed and is not leaking.

One of the other concerns about these devices was the potential for analyte absorption into the material. Absorption was investigated in PDMS and native polystyrene devices using the anti-platelet drug, clopidogrel. It was found that clopidogrel absorbs significantly in a PDMS device after 30 minutes, when compared to standards. However, for the PS device, clopidogrel was recovered at statistically equivalent concentrations to the standards. These studies were performed using mass spectrometry for analysis.[39]

3.4 Conclusions

Microfluidic devices can be fabricated from polystyrene using standard soft-lithographic procedures and equipment without the need for embossing procedures or solvent evaporation wait time. This new fabrication strategy allows for any lab already set up to do standard lithography to create a polystyrene device. In addition, the rigidity of polystyrene makes it more amenable to integration with equipment associated with high- throughput screening, such as plate readers and pipets for fluid delivery.

The ultimate goal for these microfluidic devices would be to incorporate multiple cells types on one device and integrate multiple detection schemes. In the Spence group, this would involve integrating more blood components, such as red blood cells, platelets and endothelial cells, to study these cells together as a system, rather than individually, in order to better imitate the *in vivo* environment. Furthermore, when multiple cell types are used there is often the desire to measure multiple analytes related to the cell system being studied. In the example of blood components, such analytes as ATP, NO, Ca^{2+} would be relevant to study, but would employ detections techniques of chemiluminescence, electrochemistry, and fluorescence. However, the ability to integrate multiple detection

schemes is often limited by the reliability of the microfluidic device being used. When multiple cell types, detection schemes, and pumping mechanism are used on one device the need for exact timing and proper function is important. If one detection scheme should fail, or one cell type fails to culture, then a whole experiment may be deemed a failure. Thus, reliability of the devices being used has to be examined.

PDMS is a suitable material for device prototyping, but its flexibility does not make it suitable for robust device designs. PS has a low glass transition temperature, which allows it to be molded at lower temperatures and it is the material commonly used for cell culture. PS is also a rigid material, which lends itself to integration with pumping mechanism and detection schemes as PS can be molded into a 96-well plate format suitable for plate reader detection. For these reasons, the PS device describe herein has the potential to be used to study biological process occurring in cells as polystyrene is a common material used in cell culture and can be integrated with pumping mechanism and detection schemes. Chapter 4 will investigate the use of these devices in studying cellular behavior.

REFERENCES

REFERENCES

1. D. C. Duffy, J. C. McDonald, O. J. A. Schueller, G. M. Whitesides, Rapid Prototyping of Microfluidic Systems in Poly(dimethylsiloxane). *Analytical Chemistry* 1998, *70*. 4974-4984.

2. G. M. Whitesides, E. Ostuni, S. Takayama, X. Jiang, D. E. Ingber, Soft lithography in biology and biochemistry. *Annu. Rev. Biomed. Eng.* 2001, *3*. 335-373.

3. S. T. Halpin, D. M. Spence, Direct Plate-Reader Measurement of Nitric Oxide Released from Hypoxic Erythrocytes Flowing through a Microfluidic Device. *Anal. Chem.* 2010, *82*. 7492-7497, DOI: 10.1021/ac101130s.

4. S. C. Jacobson, C. T. Culbertson, J. E. Daler, J. M. Ramsey, Microchip Structures for Submillisecond Electrophoresis. *Anal. Chem.* 1998, *70*. 3476-3480, DOI: 10.1021/ac980349t.

5. M. W. Li, A. L. Bowen, N. G. Batz, R. S. Martin, in *Lab on a Chip Technology, Part II: Fluid Control and Manipulation*, ed. K. E. Herold, A. Rasooly. Caister Academic Press: Nofolk, UK, 2009, pp 385-403.

6. A. L. Bowen, R. S. Martin, Integration of On-Chip Peristaltic Pumps and Injection Valves with Microchip Electrophoresis and Electrochemical Detection. *Electrophoresis* 2010, *31*. 2534–2540.

7. L. I. Genes, N. V. Tolan, M. K. Hulvey, R. S. Martin, D. M. Spence, Addressing a vascular endothelium array with blood components using underlying microfluidic channels. *Lab Chip* 2007, *7*. 1256-1259.

8. L. C. Mecker, R. S. Martin, Integration of Microdialysis Sampling and Microchip Electrophoresis with Electrochemical Detection. *Anal. Chem* 2008, *80*. 9257-9264.

9. S. D. Noblitt, G. S. Lewis, Y. Liu, S. V. Hering, J. L. Collett, C. S. Henry, Interfacing Microchip Electrophoresis to a Growth Tube Particle Collector for Semicontinuous Monitoring of Aerosol Composition. *Anal. Chem.* 2009, *81*. 10029-10037, DOI: 10.1021/ac901903m.

10. J. El-Ali, P. K. Sorger, K. F. Jensen, Cells on chips. *Nature* 2006, *442*. 403-411.

11. M. L. Kovarik, P. C. Gach, D. M. Ornoff, Y. Wang, J. Balowski, L. Farrag, N. L. Allbritton, Micro Total Analysis Systems for Cell Biology and Biochemical Assays. *Anal Chem* 2012, *84*. 516-540.

12. R. S. Martin, P. D. Root, D. M. Spence, Microfluidic technologies as platforms for performing quantitative cellular analyses in an *in vitro* environment. *Analyst* 2006, *131*. 1197-1206.
13. D. M. Spence, N. J. Torrence, M. L. Kovarik, R. S. Martin, Amperometric Determination of Nitric Oxide in An Endothelial Cell-coated Microchip Channel. *Analyst* 2004, *129*. 995-1000.

14. L. I. Genes, N. V. Tolan, M. K. Hulvey, R. S. Martin, D. M. Spence, Addressing a vascular endothelium array with blood components using underlying microfluidic channels. *Lab Chip* 2007, *7*. 1256-1259.

15. T. D. A. Oblak, P. Root, D. M. Spence, Fluorescence Monitoring of ATP-Stimulated, Endothelium-Derived Nitric Oxide Production in Channels of a Poly(dimethylsiloxane)-Based Microfluidic Device. *Analytical Chemistry* 2006, *78*. 3193-3197.

16. C.-J. Ku, T. D'Amico Oblak, D. M. Spence, Interactions between Multiple Cell Types in Parallel Microfluidic Channels: Monitoring Platelet Adhesion to an Endothelium in the Presence of an Anti-Adhesion Drug. *Anal. Chem. (Washington, DC, U. S.)* 2008, *80*. 7543-7548.

17. E. W. K. Young, A. R. Wheeler, C. A. Simmons, Matrix-dependent adhesion of vascular and valvular endothelial cells in microfluidic channels. *Lab Chip* 2007, *7*. 1759-1766.

18. S. Chung, R. Sudo, P. J. Mack, C.-R. Wan, V. Vickerman, R. D. Kamm, Cell migration into scaffolds under co-culture conditions in a microfluidic platform. *Lab Chip* 2009, *9*. 269-275.

19. R. Gomez-Sjoberg, A. A. Leyrat, D. M. Pirone, C. S. Chen, S. R. Quake, Versatile, fully automated, microfluidic cell culture system. *Analytical Chemistry* 2007, *79*. 8557-63, DOI: 10.1021/ac071311w.

20. E. W. K. Young, M. W. L. Watson, S. Srigunapalan, A. R. Wheeler, C. A. Simmons, Technique for Real-Time Measurements of Endothelial Permeability in a Microfluidic Membrane Chip Using Laser-Induced Fluorescence Detection. *Anal. Chem. (Washington, DC, U. S.) 82*. 808-816.

21. P. A. Vogel, S. T. Halpin, R. S. Martin, D. M. Spence, Microfluidic Transendothelial Electrical Resistance Measurement Device that Enables Blood Flow and Postgrowth Experiments. *Anal Chem* 2011, *83*. 4296–4301.

22. M. W. Li, R. S. Martin, Microchip-based integration of cell immobilization, electrophoresis, post-column derivatization, and fluorescence detection for monitoring the release of dopamine from PC 12 cells. *Analyst (Cambridge, United Kingdom)* 2008, *133*. 1358-1366.

23. M. W. Toepke, D. J. Beebe, PDMS absorption of small molecules and consequences in microfluidic applications. *Lab Chip* 2006, *6*. 1484-1486.
24. K. J. Regehr, M. Domenech, J. T. Koepsel, K. C. Carver, S. E. Ellison-Zelski, W. L. Murphy, L. A. Schuler, E. T. Alarid, D. J. Beebe, Biological implications of polydimethylsiloxane-based microfluidic cell culture. *Lab Chip* 2009, *9*. 2132–2139.

25. E. Verneuil, A. Buguin, P. Silberzan, Permeation-induced flows: Consequences for silicone-based microfluidics. *Europhys. Lett.* 2004, *68*. 412-418.

26. I. Meyvantsson, J. W. Warrick, S. Hayes, A. Skoien, D. J. Beebe, Automated cell culture in high density tubeless microfluidic device arrays. *Lab Chip* 2008, *8*. 717-724.

27. J. P. Puccinelli, X. Su, D. J. Beebe, Automated high-throughput microchannel assays for cell biology: operational optimization and characterization. *Jala 15*. 25-32.

28. I. Barbulovic-Nad, H. Yang, P. S. Park, A. R. Wheeler, Digital microfluidics for cell-based assays. *Lab Chip* 2008, *8*. 519-526.

29. P. M. van Midwoud, A. Janse, M. T. Merema, G. M. M. Groothuis, E. Verpoorte, Comparison of Biocompatibility and Adsorption Properties of Different Plastics for Advanced Microfluidic Cell and Tissue Culture Models. *Anal Chem* 2012, *84*. 3938–3944.

30. E. W. Young, E. Berthier, D. J. Guckenberger, E. Sackmann, C. Lamers, I. eyvantsson, A. Huttenlocher, D. J. Beebe, Rapid prototyping of arrayed microfluidic systems in polystyrene for cell-based assays. *Anal Chem* 2011, *83*. 1408-1417.

31. D. A. Detwiler, N. C. Dobes, C. E. Sims, J. N. Kornegay, N. L. Allbritton, Polystyrene-coated micropallets for culture and separation of primary muscle cells. *Anal Bioanal Chem* 2012, *402*. 1083-1091.

32. G. Mehta, J. Lee, W. Cha, Y.-C. Tung, J. J. Linderman, S. Takayama, Hard Top Soft Bottom Microfluidic Devices for Cell Culture and Chemical Analysis. *Anal. Chem.* 2009, *81*. 3714-3722, DOI: 10.1021/ac802178u.

33. A. Chen, D. K. Lieu, L. Freschauf, V. Lew, H. Sharma, J. Wang, D. Nguyen, I. Karakikes, R. J. Hajjar, A. Gopinathan, E. Botvinick, C. C. Fowlkes, R. A. Li, M. Khine, Shrink-Film Configurable Multiscale Wrinkles for Functional Alignment of Human Embryonic Stem Cells and their Cardiac Derivatives. *Advanced Materials* 2011, *23*. 5785-5791, DOI: 10.1002/adma.201103463.

34. V. N. Goral, Y. C. Hsiesh, O. N. Petzold, R. A. Faris, P. K. Yuen, Hot embossing of plastic microfluidic devices using poly(dimethylsiloxane) molds. *J Micromech Microen* 2011, *21*. 017002.

35. G. Mehta, J. Lee, W. Cha, Y.-C. Tung, J. J. Linderman, S. Takayama, Hard Top Soft Bottom Microfluidic Devices for Cell Culture and Chemical Analysis. *Anal. Chem. (Washington, DC, U. S.)* 2009, *81*. 3714-3722.

36. Y. Wang, J. Balowski, C. Phillips, R. Phillips, C. E. Sims, N. L. Allbritton, Benchtop micromolding of polystyrene by soft lithography *Lab Chip* 2011, *11*.

37. D. C. Duffy, J. C. McDonald, O. J. A. Schueller, G. M. Whitesides, Rapid Prototyping of Microfluidic Systems in Poly(dimethylsiloxane). *Anal. Chem* 1998, *70*. 4974-4984, DOI: 10.1021/ac980656z.

38. R. S. Martin, A. J. Gawron, S. M. Lunte, C. S. Henry, Dual-electrode electrochemical detection for poly(dimethylsiloxane)-fabricated capillary electrophoresis microchips. *Anal. Chem.* 2000, *72*. 3196-3202.

39. A. S. Johnson, K. B. Anderson, S. T. Halpin, D. C. Kirkpatrick, D. M. Spence, R. S. Martin, Integration of multiple components in polystyrene-based microfluidic devices part I: fabrication and characterization. *Analyst (Cambridge, United Kingdom) 138*. 129-136.

CHAPTER 4: ANALYSIS OF ENDOTHELIAL CELLS USING A POLYSTYRENE BASED MICROFLUIDIC DEVICE AND 96 WELL PLATE READER DETECTION

4.1 Introduction

As discussed in Chapter 3, microfluidic devices have become popular for studying cells due to their ability to mimic *in vivo* dimensions (e.g. blood vessels, which can be anywhere from 10 μm to 25 mm in diameter) and integrate various detection schemes.[1-4] Polydimethylsiloxane (PDMS) is one of the most widely-used materials in microfluidic device fabrication because it is easy to work with, inexpensive, transparent and gas permeable.[5-6] Although PDMS devices have been successfully used in numerous cell applications,[1, 7-9] there are limitations with this material, including: poor cell adhesion for some cell lines, partitioning of hydrophobic molecules in the PDMS, and leaching of un-crosslinked monomers from the bulk PDMS.[10] Thus, making microfluidic devices out of more biocompatible substrates, such as polystyrene (PS), has been the focus of several studies.[11-15] Chapter 3 explained how these PS devices were fabricated, while Chapter 4 will focus on how these devices can be utilized for studying a cell based system.

4.1.1 Cell Analysis on Polystyrene Microfluidic Devices

Takayama *et al.* used a device that had a PS top with channels embedded, and sealed the device with a polyurethane (PU) soft bottom. Human dermal microvascular cells (HDMECs) were cultured on the device and oxygen tension measurements were performed via the use of an oxygen sensitive fluorescent dye. The results showed lower

evaporation and lower oxygen permeability compared to a device made completely from PDMS.[16] However, in this construct, the only cellular work that occurred was successful cell culture on the device, as no other cellular analyses were performed.

Beebe *et al.* fabricated arrayed polystyrene devices via a simple hot embossing method that involves PDMS and epoxy molds. Using these arrayed devices, human umbilical vein endothelial cells (HUVECs) were cultured in the device and after activation by interleukin 1β, the upregulation of E-selectin was monitored via fluorescence imaging. Additionally, chemotaxis of neutrophils was monitored across the length of the channel in the presence of a chemoattractant via imaging.[12] This is a good example of how microscopy can be employed to study cell upregulation and migration on a polystyrene device.

Another example of a PS device used to study cell behavior is from Allbritton *et al.* where PS was molded into arrays of either microwells or microposts for segregation and tracking of non-adherent and adherent cells. The microwells were used to capture nonadherent cells and the adherent cells would attach to the microposts and proliferate. Scanning electron microscopy (SEM) was used to track this cell activity.[17] Allbritton *et al.* also created PS coated micropallets for improving cell adhesion and proliferation of primary muscle cells.[13]

Lastly, Midwoud *et al.* recently compared the use of different thermoplastics, including polystyrene, for the adherence of human hepatoma cells in a patterned structure, with the substrates being characterized in terms of surface treatment, adsorption of hydrophobic compounds, and biocompatibility.[11]

All of the previously mentioned studies demonstrated that polystyrene is a suitable substrate for cell studies performed on microfluidic devices. However, there have not been any examples of using these devices to monitor intra- or extra-cellular function by integrating the devices with current laboratory equipment. The device presented in Chapter 3 has the ability to use a pipet as a pumping mechanism as well as a 96 well plate reader for detection of cellular events. Furthermore, cell culture is successful on the device and in this construct, cell uptake, production and release can be monitored for several analytes.

4.2 Methods

4.2.1 Endothelial Cell Culture in Polystyrene-based Microchannels

In order to facilitate cell adhesion in the channels of the polystyrene device, a 100 μg/mL solution of bovine plasma fibronectin (Invitrogen, Carlsbad, CA, USA) cell adhesion protein was introduced to the channels via the injection block (described in Chapter 3) and allowed to adsorb for 1 hr in a 37 °C and 5% CO_2 incubator. The channels were then dried and exposed to UV light for 15 minutes. Bovine pulmonary artery endothelial cells (bPAECs) were purchased in frozen cryovials (Lonza, Walkersville, MD, USA). The vials were thawed to room temperature and added to a T-75 tissue culture flask containing 9 mL of endothelial growth media (EGM) that had been equilibrated to 37 °C. The EGM consists of a low glucose (5.5 mM) Dulbecco's Modified Eagles Medium (DMEM, MIDSCI, St. Louis, MO, USA) supplemented with 2.5% v/v adult bovine serum (Sigma-Aldrich, St. Louis, MO, USA), 7.5% fetal bovine serum (Lonza), penicillin, streptomycin, and amphotericin B (MIDSCI, St. Louis, MO USA). bPAECs were allowed to grow in a humidified incubator at 37 °C and 5% CO_2

until they were determined as confluent by optical microscopy. Media was changed the day after plating and then every 2 days thereafter. The bPAECs were subcultured when the cells reached >80% confluence as visualized by optical microscopy.

In order to seed bPAECs into the channels of the microfluidic device, bPAECs were washed with 10 mL of HEPES and then treated with 5 mL of 0.25% trypsin/EDTA. This solution was then removed and the cells suspended in 10 mL of EGM. The cell suspension was removed from the flask and centrifuged at 1500 *g* for 5 min. The supernatant was removed and the pellet was resuspended in 450 µL of equilibrated media. This concentrated cell solution was introduced to the channels in the same manner as the fibronectin and incubated for 1 hr at 37 °C and 5% CO_2. After an hour of growth, the ECs were re-seeded in the channel and media was subsequently changed every 2 hrs. The ECs were allowed to grow to confluence overnight and used the day after seeding.

To verify cell confluence in the channels, 1 µM 5-chloromethylfluorescein diacetate (CMFDA) cell tracker (Molecular Probes, Carlsbad, CA, USA) was pumped through the channels to fluorescently label the bPAECs for monitoring with an optical microscope (Olympus IX71 Microscope, Olympus America, Melville, NY, USA) fitted with a FITC filter cube (Chroma Technology Corp, Bellows Falls, VT, USA) containing the excitation (460-500 nm) and emission (505-560 nm) filters.

4.2.2 Fluorescence Detection of Intracellular Endothelial Nitric Oxide

A 5 mM stock solution of the intracellular nitric oxide (NO) probe DAF-FM-DA (4-amino-5-methylamino-2',7'-difluorofluorescein diacetate, Molecular Probes) was made

by dissolving 50 μg in 20 μL anhydrous dimethyl sulfoxide (DMSO). A 10 μM solution of DAF-FM-DA was prepared by diluting 2 μL of stock to 1 mL with physiological salt solution (PSS). The concentrations of salts (in mM) in the PSS were as follows: 4.7 KCl, 2.0 $CaCl_2$, 1.2 $MgSO_4$, 140.5 NaCl, 21.0 Tris, and 5.5 glucose (pH 7.4). The 10 μM DAF-FM-DA solution was then pumped (via the PDMS injection block) over the bPAECs using a 100 μL pipet set to 40 μL, and then repeated to ensure adequate cell exposure to probe. The device was then incubated for 1 hr at 37 °C and 5% CO_2. After incubation, the channels were rinsed twice with PSS to remove excess probe, followed by a waiting period of 10 min at 37 °C and 5% CO_2 to allow for probe de-esterification by intracellular mechanisms.

Initial fluorescence measurements of the bPAECs were taken by aligning a 96 well plate, with drilled out wells corresponding to each channel's serpentine, on top of the PS device. Fluorescence measurements were performed using a plate reader (Spectramax M4, Molecular Devices, Sunnyvale, CA, USA) set to an excitation wavelength of 495 nm and an emission wavelength of 521 nm. These measurements served to represent the baseline levels of NO in the cells. After measurement, adenosine triphosphate (ATP, Sigma-Aldrich) was pumped over the bPAECs in the same manner as the probe. ATP standards were prepared by dissolving ATP in 25 mL PSS to make a 1 mM stock solution. Next, a 100 μM solution was prepared by diluting 100 uL of the ATP stock solution to 1 mL; this 100 μM solution was then diluted further to prepare a 0.5 μM ATP solution that was subsequently pumped over the bPAECs in the device. Following a 30 minute incubation period at 37 °C and 5% CO_2, the final fluorescence measurements

were taken on the plate reader in the same manner as before. The differences in fluorescence were obtained and normalized to the channels that had been addressed with 0 μM ATP (PSS alone).

4.2.2 Fluorescence Detection of Endothelial Calcium Uptake

A 2.3 mM stock solution of the intracellular calcium (Ca^{2+}) specific fluorescence probe Fluo-4 AM (Invitrogen, Grand Island, NY, USA) was made by dissolving a 50 μg vial in 20 μL of anhydrous DMSO. Next, a 5 μL aliquot of the stock solution, along with 5 μL of 200 mg/mL pluronic F-127 surfactant (Invitrogen, Grand Island, NY, USA), were combined in order to enhance the probe's penetration capacity. Finally, the probe solution was diluted to 2 mL in Ca^{2+} free PSS to create a 5.7 μM solution. The 5.7 μM Fluo-4 AM was then pumped over the bPAECs using a 100 μL pipet set to 40 μL (via the PDMS injection block), then repeated to ensure adequate cell exposure to probe. The device was then incubated for 30 min at 37 °C and 5% CO_2. After incubation, the channels were rinsed twice with Ca^{2+} free PSS to remove excess probe and incubated for an additional 10 min at 37 °C and 5% CO_2 to allow for probe de-esterification by intracellular mechanisms. Initial fluorescence measurements of the bPAECs were obtained using the plate reader as described above for the NO, although the excitation and emission wavelength settings were modified to 496 nm and 516 nm, respectively. These measurements served to represent the baseline levels of Ca^{2+} in the cells.

After measurement, PSS (with Ca^{2+}) or 10 µM Ca^{2+} ionophore A23187 (Sigma-Aldrich, St. Louis, MO USA) in PSS were pumped over the bPAECs in the same manner as the probe. The Ca^{2+} ionophore was prepared by dissolving 5 mg in 1.9 mL of anhydrous DMSO to create a 5 mM stock solution. Next, a 100 µM working solution was prepared by diluting 20 µL of stock to 1 mL in PSS and finally, a 1:10 dilution in PSS was performed, resulting in a final concentration of 10 µM Ca^{2+} ionophore. Once PSS or ionophore was flowed over the bPAECs, the device was allowed to incubate for 10 min at 37 °C and 5% CO_2. Final fluorescence measurements were taken on the plate reader as described above.

4.2.3 Cell Viability Study

Saponin (Sigma Aldrich, St. Louis, MO, USA) was used to permeabilize bPAEC membranes in order to induce cell death. A 0.25% solution of Saponin was made by dissolving 13.2 mg into 5.28 mL of water. A 1 mL aliquot of the 0.25% solution was then diluted to 10 mL with PSS resulting in a 0.025% solution. This solution, or PSS, was then flowed over bPAECs cultured in the polystyrene device.

The nucleic acid stain, Sytox Green (Invitrogen), which only labels cell with compromised membranes, was used to determine whether or not saponin had killed the immobilized bPAECs. Its excitation and emission maxima are 504 and 523 nm, respectively when bound to DNA. After Saponin or PSS was flowed over the cells, 1 µM Sytox Green was flowed over the bPAECs. The probe was allowed to incubate at 37 ˚C

for 15 min. and then imaged using fluorescence microscopy and fluorescence intensity recorded using a plate reader.

4.3 Results

A limitation of PDMS devices is poor cell adhesion of some cell lines for example, PC 12 cells. Adherent proteins, such as collagen, or fibronectin, are commonly used to facilitate cell adherence can be coated onto PDMS surfaces. However, despite the use of adhesion proteins, cells are still not as adherent on PDMS as they are in conventional cell culture substrates such as polystyrene. Previous studies have investigated the biocompatibility of cells on various thermoplastics including polystyrene, with the surfaces being rendered hydrophilic by means of UV-ozone or plasma treatment.[11, 17] In the case of PC 12 cells, it was found that they were more adherent on a polystyrene surface than a PDMS device with 8% and 75% of the cells lost after rinsing, respectively.[18]

4.3.1 Monitoring Nitric Oxide Production, Calcium Uptake and Viability in Endothelial Cells

The pumping mechanism using the PDMS injection block to interface with a pipet (as described in Chapter 3) was used to introduce bPAECs into to the polystyrene-based microchannels. A side view of one channel is shown in Figure 4.1, where a layer of fibronectin (cell adhesion protein) was first introduced to the channel (via the injection block). After allowing the fibronectin to absorb for 1 hr, a concentrated solution of

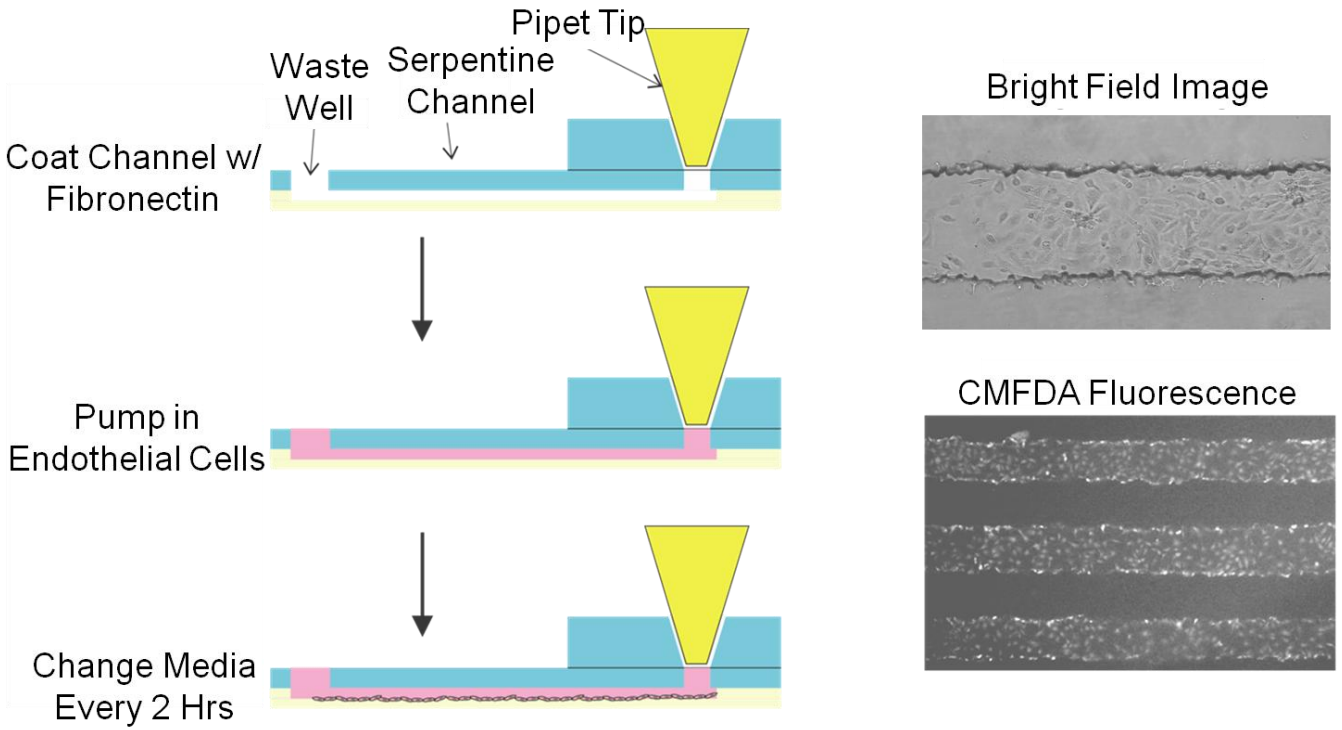

Figure 4.1: Endothelial cell culture on a polystyrene device**.** To culture endothelial cells, the device was first coated with fibronectin. Next, a suspension of endothelial cells was pumped into the device. The device was then incubated at 37 °C, 5% CO_2 for 2 hours. Media was changed every two hours until cell confluence was observed. A bright field image is shown on the top right, while the image on the bottom right was obtained by incubating the cells with CellTracker CMFDA fluorescenct probe.

bPAECs was introduced into the device and allowed to adhere and grow in the microchannel (in an incubator), with frequent media changes (every 2 hrs). The bPAECs on the polystyrene grew to confluence overnight and were visualized by optical microscopy as shown in the bright field image in Figure 4.1. To further ensure that the cells in the serpentine channels were confluent, they were also labeled with the cell tracker CMFDA and visualized under the FITC filter of the microscope (as pictured in the fluorescent image, Figure 4.1). Before any biological studies were performed on the bPAECs cultured in the polystyrene device, they were first visualized with optical microscopy to confirm the presence of healthy, confluent cells.

The in-channel cultured bPAECs were incubated with the intracellular NO probe DAF-FM DA and then exposed to ATP, a known stimulus of NO production in endothelial cells;[7, 19] therefore, it was anticipated that ATP would result in increased intracellular bPAEC NO production. Upon application of 0.5 μM ATP to the cells in the serpentine channel, a significant increase in NO production was observed when compared to applying PSS alone (Figure 4.2). This increase was measured by aligning the device in the plate reader and performing top-read fluorescence measurements in a high-throughput manner. The device was also utilized to measure cellular uptake by monitoring Ca^{2+} influx into the bPAECs after stimulation by a Ca^{2+} ionophore. Cells in the device treated with Ca^{2+} ionophore exhibited a 42 ± 13% increase in fluorescence compared to cells treated with PSS alone, which only exhibited a 17 ± 2% increase in fluorescence (N=3, error: SEM, p-value < 0.05) as shown in Figure 4.3. These studies suggest that the polystyrene devices with imprinted channels can be integrated with existing infrastructure

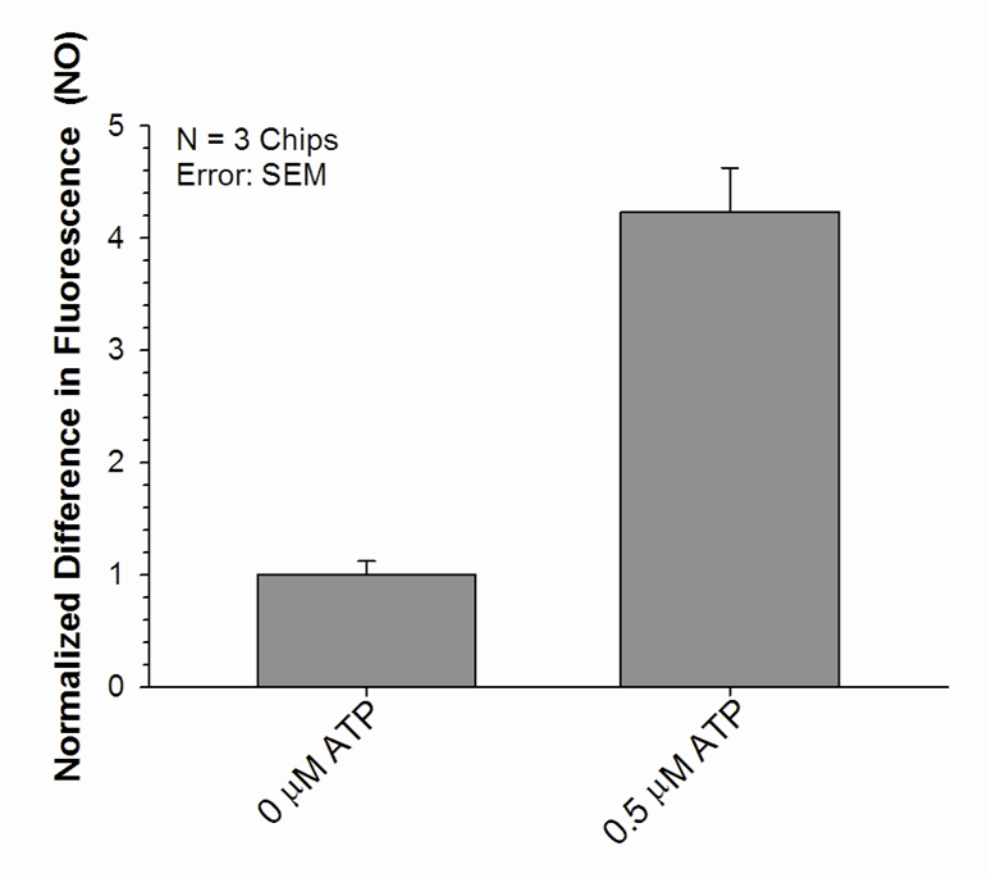

Figure 4.2: Intracellular measurement of NO. These cells were incubated with 10 μM DAF-FM-DA, an intracellular NO probe, at 37 °C for 30 min; excess probe was rinsed off the cells by pumping buffer without probe through the channels. After the incubation period, a basal fluorescence measurement was taken using a standard plate reader. Next, 0.5 μM ATP was pumped over the cells and allowed to incubate for an additional 30 min in order to stimulate NO production in the endothelial cells. A final fluorescence measurement was taken using the plate reader and the difference in fluorescence calculated. This value was normalized to the difference in fluorescence for a 0 μM ATP standard. The average changes in fluorescence for n=3 separate devices is shown in, along with error bars representing the standard error of the mean. The changes are significant for $p<0.001$.

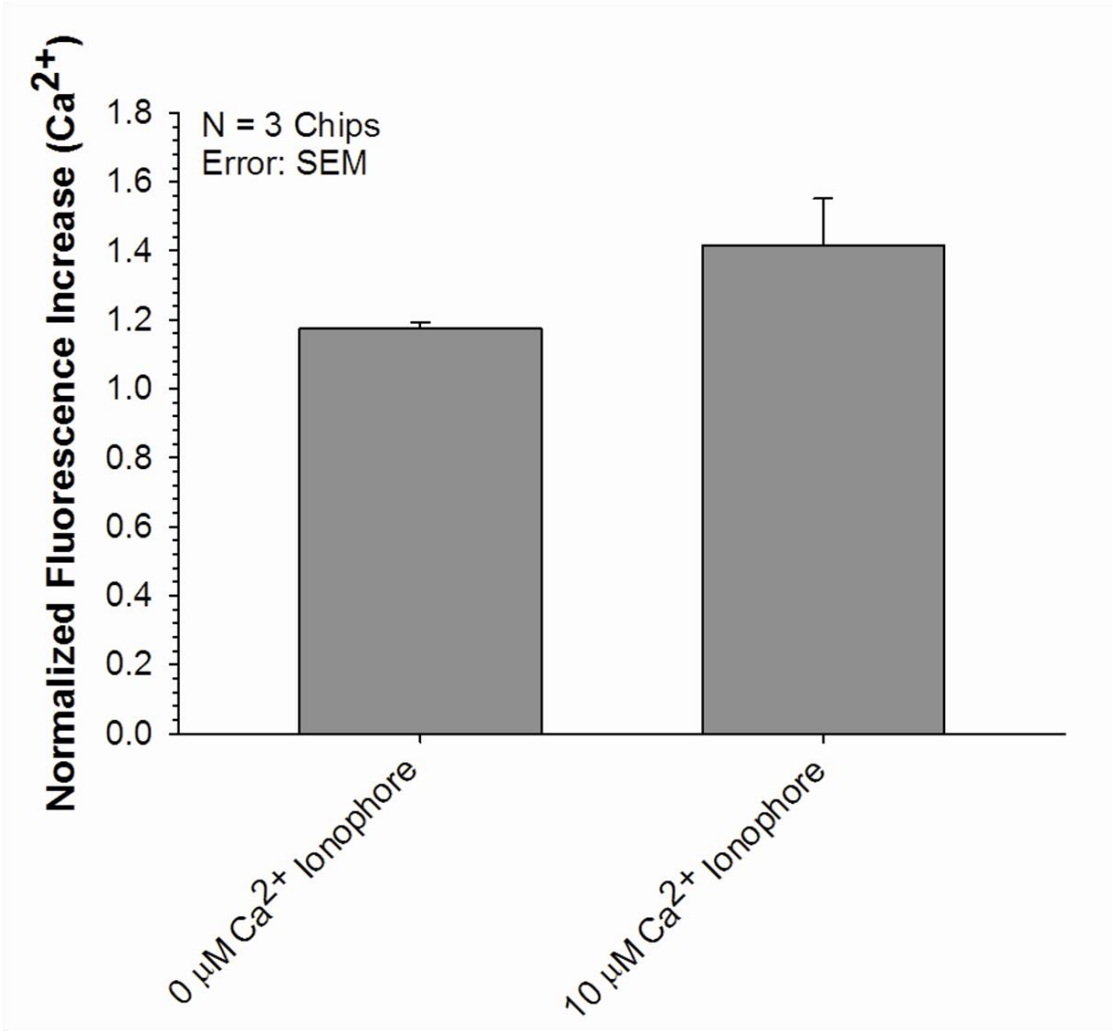

Figure 4.3 Intracellular Measurement of Ca^{2+} Uptake: These cells were incubated with 5.7 µM Fluo 4AM**,** an intracellular Ca^{2+} probe, at 37 °C for 30 min; excess probe was rinsed off the cells by pumping buffer without probe through the channels. After the incubation period, a basal fluorescence measurement was taken using a standard plate reader. Next, 10 µM Ca^{2+} ionophore was pumped over the cells and allowed to incubate for an additional 10 min in order to stimulate Ca^{2+} uptake in the endothelial cells. A final fluorescence measurement was taken using the plate reader and the difference in fluorescence calculated. This value was normalized to the difference in fluorescence for a 0 µM ionophore. The average changes in fluorescence for n=3 separate devices is shown, along with error bars representing the standard error of the mean. The changes are significant for $p<0.05$.

(pipets for pumping and plate readers for detection) and can be utilized to study both an intracellular process (NO production) and cellular uptake (Ca^{2+} influx).

Another study was performed to see if this device could be used to monitor cell viability. Saponin was flowed over cells cultured in the PS device in order to induce cell death. The bPAECs were then incubated with Sytox Green, which is a fluorescent nucleic acid stain that does not cross the membrane of live cells. The increase in fluorescence for cells treated with saponin, versus the control treated with PSS, is shown in Figure 4.4 and is statistically different ($p<0.001$).

4.4 Conclusions

The polystyrene device whose fabrication was described in Chapter 3 was used to study endothelial cells. Endothelial cells, those that comprise the inner wall of blood vessels, were immobilized into a polystyrene device. These cells were stimulated to produce nitric oxide, which was determined intracellularly with a fluorescence probe. Furthermore, these cells' uptake of Ca^{2+} was also determined with an intracellular fluorescence probe. In a separate set of experiments done by the Martin group, though using a similar polystyrene device integrated with electrodes the stimulated (K^{+}) release of catecholamines from a layer of immobilized PC 12 cells was also measured.[18] Finally, the ability to induce and study cell death was also accomplished through the use of this device. These results demonstrate that devices fabricated in polystyrene are capable of being used in many of the same types of assays as those devices made from other materials, such as PDMS. The use of polystyrene is advantageous in fabrication

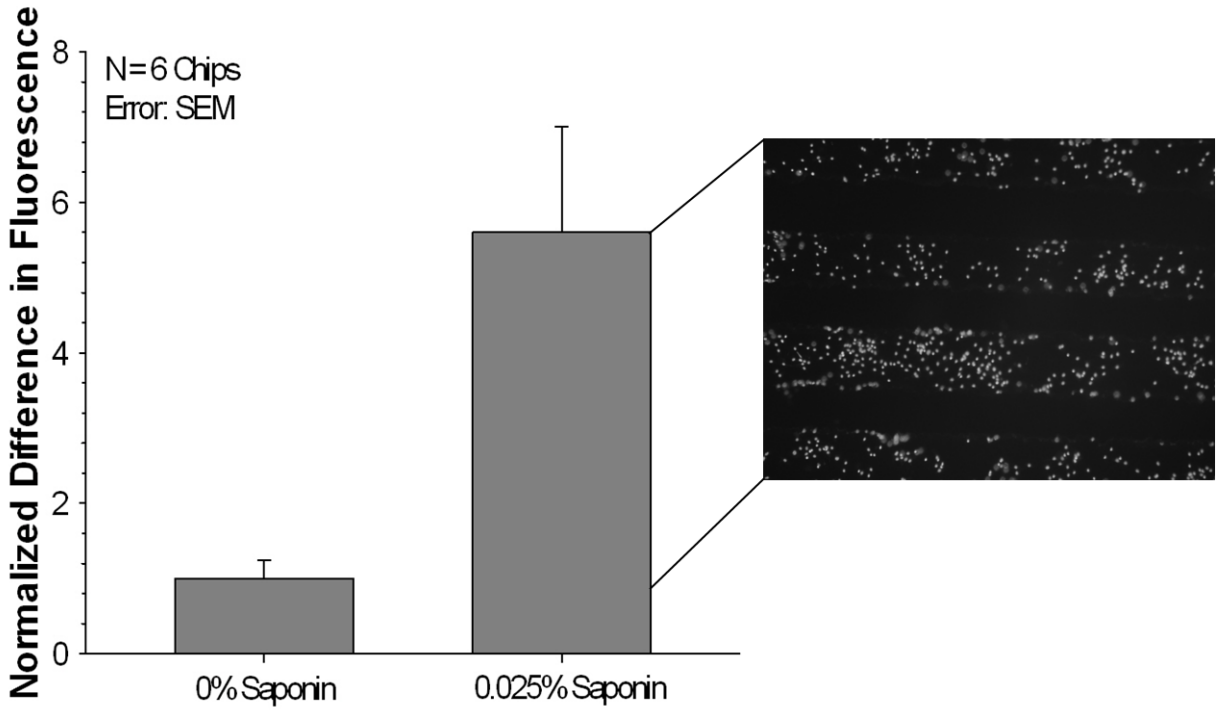

Figure 4.4: Cell Viability. Saponin, a detergent that permeabilizes cell membranes, was used to induce endothelial cell death as visualized by the nucleic acid stain Sytox Green. Sytox Green does not label live cells thus, the image on the right indicates the presence of dead cells after saponin administration. The bar graph shows an increase in fluorescence, indicative of cell death, for cells treated with saponin as compared to cells treated with PSS. The average changes in fluorescence for n=5 separate devices is shown, along with error bars representing the standard error of the mean. The changes are significant for $p<0.001$.

strategies that seek to employ integration with electrodes, injection blocks for pipet pumping, and plate reader detection schemes. This allows for endothelial cell behaviour (NO production, Ca^{2+} uptake, viability) to be studied in a high throughput manner. Furthermore, the rigidity of polystyrene and its ability to be integrated with a 96 well reader show promise in its ability to be further utilized with established, automated lab equipment.

Though in this construct the PS device was only used to study endothelial cell behaviour, it has the potential to be a powerful tool used to study multiple cell types. In Chapter 2, I discussed an aspect of platelet biology that could play a larger role in the vasculature. The Spence group hypothesizes that the ATP activated P2X1 receptor on the platelet surface is influenced by RBC and endothelial cell behaviour, specifically by their release of ATP, NO, and other platelet inhibitors or activators. The PS device can be used to study interaction between these three cell types. Whole blood, or RBCs combined with platelets, could be flowed over a layer of immobilized endothelial cells and multiple detection schemes can be incorporated in the device. The 96 well plate format would lend itself to fluorescence measurements or chemiluminescence, furthermore, cells can be collected at the end of the channel for off chip analysis such as flow cytometry for platelet activation. In this manner, P2X1 receptor function would be probed at the RBC and endothelial cell level.

As discussed previously, RBCs release ATP and these levels of ATP may influence platelet activation. To investigate this relationship, studies previously done in the Spence lab where platelets incubated with RBCs and various ATP release activators/inhibitors adhering to an uninjured endothelium[20] can be repeated on the PS

platform. In this manner, it would be possible to measure ATP release from RBCs, endothelial cell NO production and platelet activation. To measure ATP release a membrane could be incorporated into the device so that ATP released from RBCs or platelets could diffuse above the membrane to be measured via the luciferin/luciferase chemiluminescence reaction, these analytical wells would be fabricated in a 96-well format. The endothelial cell NO (platelet inhibitor) could be measured as discussed in this chapter, but the RBCs, due to their red color, would have to be washed out of the channel before a fluorescence measurement was taken. Finally, samples can be collected for off chip analysis via flow cytometry to investigate the levels of platelet activation. Flow cytometry would separate the different cell types and allow for the detection of fluorescently labelled antibodies indicative of platelet activation. The integration possibilities for this PS device would be useful for studying the interactions between different cell types though more work still needs to be done on integrating detection schemes for analytes besides NO or Ca^{2+}.

REFERENCES

REFERENCES

1. A. L. Bowen, R. S. Martin, Integration of On-Chip Peristaltic Pumps and Injection Valves with Microchip Electrophoresis and Electrochemical Detection. *Electrophoresis* 2010, *31*. 2534–2540.

2. J. El-Ali, P. K. Sorger, K. F. Jensen, Cells on chips. *Nature* 2006, *442*. 403-411.

3. R. S. Martin, P. D. Root, D. M. Spence, Microfluidic technologies as platforms for performing quantitative cellular analyses in an *in vitro* environment. *Analyst* 2006, *131*. 1197-1206.

4. D. M. Spence, N. J. Torrence, M. L. Kovarik, R. S. Martin, Amperometric Determination of Nitric Oxide in An Endothelial Cell-coated Microchip Channel. *Analyst* 2004, *129*. 995-1000.

5. D. C. Duffy, J. C. McDonald, O. J. A. Schueller, G. M. Whitesides, Rapid Prototyping of Microfluidic Systems in Poly(dimethylsiloxane). *Anal. Chem* 1998, *70*. 4974-4984, DOI: 10.1021/ac980656z.

6. M. L. Kovarik, P. C. Gach, D. M. Ornoff, Y. Wang, J. Balowski, L. Farrag, N. L. Allbritton, Micro Total Analysis Systems for Cell Biology and Biochemical Assays. *Anal Chem* 2012, *84*. 516-540.

7. L. I. Genes, N. V. Tolan, M. K. Hulvey, R. S. Martin, D. M. Spence, Addressing a vascular endothelium array with blood components using underlying microfluidic channels. *Lab Chip* 2007, *7*. 1256-1259.

8. S. T. Halpin, D. M. Spence, Direct Plate-Reader Measurement of Nitric Oxide Released from Hypoxic Erythrocytes Flowing through a Microfluidic Device. *Anal. Chem.* 2010, *82*. 7492-7497, DOI: 10.1021/ac101130s.

9. M. W. Li, R. S. Martin, Microchip-based integration of cell immobilization, electrophoresis, post-column derivatization, and fluorescence detection for monitoring the release of dopamine from PC 12 cells. *Analyst* 2008, *133*. 1358-1366.

10. K. J. Regehr, M. Domenech, J. T. Koepsel, K. C. Carver, S. E. Ellison-Zelski, W. L. Murphy, L. A. Schuler, E. T. Alarid, D. J. Beebe, Biological implications of polydimethylsiloxane-based microfluidic cell culture. *Lab Chip* 2009, *9*. 2132–2139.

11. P. M. van Midwoud, A. Janse, M. T. Merema, G. M. M. Groothuis, E. Verpoorte, Comparison of Biocompatibility and Adsorption Properties of Different Plastics for Advanced Microfluidic Cell and Tissue Culture Models. *Anal Chem* 2012, *84*. 3938–3944.

12. E. W. Young, E. Berthier, D. J. Guckenberger, E. Sackmann, C. Lamers, I. eyvantsson, A. Huttenlocher, D. J. Beebe, Rapid prototyping of arrayed microfluidic systems in polystyrene for cell-based assays. *Anal Chem* 2011, *83*. 1408-1417.

13. D. A. Detwiler, N. C. Dobes, C. E. Sims, J. N. Kornegay, N. L. Allbritton, Polystyrene-coated micropallets for culture and separation of primary muscle cells. *Anal Bioanal Chem* 2012, *402*. 1083-1091.

14. G. Mehta, J. Lee, W. Cha, Y.-C. Tung, J. J. Linderman, S. Takayama, Hard Top Soft Bottom Microfluidic Devices for Cell Culture and Chemical Analysis. *Anal. Chem.* 2009, *81*. 3714-3722, DOI: 10.1021/ac802178u.

15. A. Chen, D. K. Lieu, L. Freschauf, V. Lew, H. Sharma, J. Wang, D. Nguyen, I. Karakikes, R. J. Hajjar, A. Gopinathan, E. Botvinick, C. C. Fowlkes, R. A. Li, M. Khine, Shrink-Film Configurable Multiscale Wrinkles for Functional Alignment of Human Embryonic Stem Cells and their Cardiac Derivatives. *Advanced Materials* 2011, *23*. 5785-5791, DOI: 10.1002/adma.201103463.

16. G. Mehta, J. Lee, W. Cha, Y.-C. Tung, J. J. Linderman, S. Takayama, Hard Top Soft Bottom Microfluidic Devices for Cell Culture and Chemical Analysis. *Anal. Chem. (Washington, DC, U. S.)* 2009, *81*. 3714-3722.

17. Y. Wang, J. Balowski, C. Phillips, R. Phillips, C. E. Sims, N. L. Allbritton, Benchtop micromolding of polystyrene by soft lithography *Lab Chip* 2011, *11*. 3089-3097.

18. K. B. Anderson, S. T. Halpin, A. S. Johnson, R. S. Martin, D. M. Spence, Integration of multiple components in polystyrene-based microfluidic devices part II: cellular analysis. *Analyst (Cambridge, United Kingdom) 138*. 137-143.

19. R. S. Sprague, M. L. Ellsworth, A. H. Stephenson, A. J. Lonigro, ATP: the red blood cell link to NO and local control of the pulmonary circulation. *Am J Physiol* 1996, *271*. H2717-22.

20. W. Karunarathne, C. J. Ku, D. M. Spence, The dual nature of extracellular ATP as a concentration-dependent platelet P2X1 agonist and antagonist. *Integr Biol* 2009, *1*. 655-663, DOI: Doi 10.1039/B909873a.

CHAPTER 5: CONCLUSIONS AND FUTURE DIRECTIONS

5.1 Platelet P2X1 Receptor Function

Circulating platelets are in an inactive state, but upon blood vessel injury, platelets become activated and aggregate at the injury site forming a plug, or clot, that prevents further blood loss. Purinergic receptors on the platelet surface play a role in this clotting process and include the adenosine diphosphate (ADP) activated P2Y1 and P2Y12, and the adenosine triphosphate (ATP) activated receptor P2X1. The P2X1 receptor is an ATP-gated calcium (Ca^{2+}) channel. The platelet P2X1 receptor's role in platelet activation and aggregation is not well understood, but there is evidence in the literature that it contributes to platelet activation.[1-3] The Spence group believes that RBC-derived ATP release has an effect on platelet activation via this P2X1 receptor. Disease states with increased (multiple sclerosis[4-5], sickle cell anemia[6-7]) or decreased (cystic fibrosis[8-9], diabetes[10-11], pulmonary hypertension[12-13]) RBC ATP release all exhibit platelet hyperactivity.

NF449, commonly used as a P2X1 inhibitor, was found to be a platelet sensitizer that can be used to study platelet Ca^{2+} influx induced by ATP or ADP without the presence of added apyrase.[14] This allows for a new way of studying ATP's effect on the platelet without the use of apyrase (which breaks down ATP) or a non-metabolizable form of ATP. By using NF449 in this manner, the effect of native ATP on the P2X1 receptor can be investigated. Additionally, the effects of ATP can be distinguished from

those of ADP, with regard to platelet Ca^{2+}. Experiments on washed platelets are useful for isolating the platelet's response to agonists, while the platelet's interaction with other cell types in the vasculature (RBCs, endothelial cells) is more relevant to *in vivo* conditions.

In Chapter 1, various microfluidic devices used to study platelet activation were described. The microfluidic platelet adhesion device developed by the Spence group has an advantage over many other devices as it incorporates 3 blood cell types (RBCs, platelets, and endothelial cells) to study platelet activity, whereas other systems only employ collagen and platelets. However, the adhesion device still has some drawbacks. For example, in order to observe platelet adhesion, a low flow rate (0.2 μL/min) was used during experiments and, after the samples were pumped, the device was further incubated before rinsing and detecting platelets sticking to the endothelium. This does not represent well *in vivo* conditions as blood is not continuously flowing throughout the experiment. Furthermore, while this may indicate a baseline of platelet activation, there is no injury to the endothelial cells so, it does not truly represent the formation of a thrombus. Lastly, platelets adhering were counted individually, which is a time consuming process. I propose an *in vitro* microfluidic platform for studying thrombus formation by controlled cell lysis. Endothelial cells can be cultured in the device as described previously,[3] but with collagen as the adhesion protein to better represent the environment *in vivo*. An endothelial cell injury can be induced via laser[15], chemical[16], or applied potential[17] thus, exposing collagen. Next, either whole blood or platelets alone or some combination of RBCs and platelets could be flowed over the injury and thrombus formation monitored.

Ideally, the platelets would be tagged with a fluorescent probe and visualized using microscopy and the fluorescence intensity of the thrombus monitored rather than individual platelets adhering to an undisturbed endothelium.

This device would have an advantage over current *in vitro* microfluidic models as it would not only incorporate cells of the vasculature, but also a vascular injury. This would be a useful tool in probing P2X1 function in thrombus formation as each component of the blood could be manipulated, for example, RBCs separated from platelets could be treated with an ATP release inhibitor, then recombined with platelets and the effects of this inhibition observed. Additionally, whole blood samples from healthy controls versus disease states with altered ATP release/platelet activity could also be flowed and studied in this controlled environment.

5.2 Polystyrene Microfluidic Devices

The polystyrene (PS) device from chapters 3 and 4 was successfully integrated with standard lab equipment (pipet and 96 well plate reader) and used to study endothelial cells cultured in the serpentine channels.[18-19] PS is a desirable microfluidic device material because it is commonly used for cell culture and the rigidity allows for easier integration as compared to the flexible polydimethylsiloxane (PDMS) polymer. Furthermore, one of the drawbacks of PDMS devices is absorption of compounds into the PDMS. This was demonstrated in a static system where the drug, clopidogrel, absorbed significantly into PDMS, but not PS, when compared to standards made up in polyethyelene microcentrifuge tubes.[19]

The study of drug transport across a membrane is useful in creating *in vitro* pharmacokinetic profiles for new drug candidates. This is commonly performed using a hollow fiber bioreactor cartridge employing cell culture. These cartridges contain fibers that retain bacteria or cells, but allow drugs and nutrients to flow freely. Media propelled through the cartridge provides oxygen and nutrients for the cells.[20-22] However, the cartridges use large volumes of media ~ 20 mL, are low throughput, and do not allow for any post analysis of cells. Our group has developed a PDMS based microfluidic device with a polycarbonate membrane capable of performing these measurements (unpublished data), however, as previously mentioned, PDMS may not be the best material as certain drugs may absorb into the device material. Thus, using the PS technology developed herein, a membrane was incorporated during fabrication in order to study drug transport across the membrane.

A device made of PS and PDMS that incorporated a polyester membrane and fittings to integrate pumps was developed and an image of the device is shown in figure 5.1. This device was made in a similar manner to the devices in chapter 3, but before the top PDMS layer was plasma sealed to the PS, a polyester membrane dipped in 25% toluene 75% methanol was laid across the channel and immediately dried. Though drug transport was able to be measured using this device, no improvements in drug absorption were observed when compared to a PDMS device (results not shown) even though 3 sides of the channel were made of PS and one side PDMS.

The ultimate goal would be to create a device that is made solely from polystyrene, but still incorporate a membrane. A PDMS negative mold of channels was

Figure 5.1: Membrane based polystyrene device**.** The bottom layer of this device is PS containing embedded channels, while the top layer is a PDMS slab containing wells for sample introduction (adapters), sampling (above membrane) and waste. Between these two layers is a polyester membrane that allows for diffusion from the channel to above the well. The luer adapters are attached to the device with a quick dry epoxy and this allows for syringes to be used for sample pumping.

fabricated, whereby pouring and curing epoxy over this PDMS mold, an epoxy mold with positive features was made. In brief, a 10:1 ratio EC 415 epoxy to curing agent (Adtech Plastic Systems) was poured over the PDMS mold with negative features and allowed to spread over the features. Manual spreading should be avoided as it adds bubbles to the epoxy. To reduce bubble formation the PDMS mold can be desiccated prior to pouring the epoxy or the mold with the epoxy can be put under vacuum for a very short time, the epoxy will expand rapidly under vacuum. The epoxy mold was then cured for 24 hrs on a 40 ˚C hot plate and any bubbles that surface are manually popped with a Pasteur pipet. After 24 hrs, the epoxy was carefully demolded from the PDMS mold and the following post cure was carried out on a hot plate: 93 ˚C for 2 hrs, 121 ˚C for 2 hrs, 149 ˚C for 2 hrs, 177 ˚C for 2 hrs. The result was a solid gray positive-relief epoxy mold that replicates the original SU-8 master.

This epoxy can withstand higher temperatures and pressures therefore, it can be used in a heated hydraulic press to transfer channels to sheets of polystyrene. Finally, the polystyrene embedded channels can be sealed to another sheet of polystyrene with wells to address sample and waste. The initial prototypes contained channels that were approximately 200 μm wide, although these channels would become deformed or completely blocked when sealed to a PS sheet. Thus, the channels were scaled up to 1.5 mm wide in order to optimize the sealing procedure. The final hydraulic press schedule used to embed channels in the PS is described below

The press was set to 115 ˚C (~ 120 ˚C) and allowed to equilibrate at that temperature for 20 min. Then the following layers were inserted into the press in order from bottom to top: mirror finished stainless steel plate, featureless PDMS, PS blank

sheet, epoxy mold, rubber sheet, Teflon sheet, mirror finished stainless steel plate. The press was closed with 2000 lbs of pressure and after 7 min. the temperature was turned down, the water turned on, and the press allowed to cool to 65 ˚C before removing the sample. The PS was carefully demolded from the epoxy with the PS now containing embedded channels. Any thicker edges were removed before moving on to the next step.

In order to seal the PS sheet with channels to a blank PS sheet with wells, the hydraulic press was set to 75 ˚C (~ 80 ˚C) and allowed to equilibrate for 10 min. The following layers were then inserted into the press in order from bottom to top: mirror finished stainless steel plate, featureless PDMS, PS blank with wells for inlets and outlets, PS with channels, featureless PDMS, rubber sheet, Teflon sheet, mirror finished stainless steel plate. The press was closed with 3000 lbs of pressure and after 10 min. the temperature was turned down, the water turned on, and the press was allowed to cool to 65 ˚C before removing the sample. The final product is a microfluidic device made completely out of PS with channels and inlets and outlets. These channels were successfully sealed with no blockages as shown in figure 5.2 where fluorescein was flowed and visualized using fluorescence microscopy and no leaking occurred. Further development is still needed on sealing a membrane between the two PS slabs. One of the downsides to these lithographically based fabrication strategies is the time it takes to go from device idea to functional prototype. There are multiple intermediate steps before the device is finished and this is one reason why 3 dimensional (3D) printing was investigated as a new method for creating these devices.

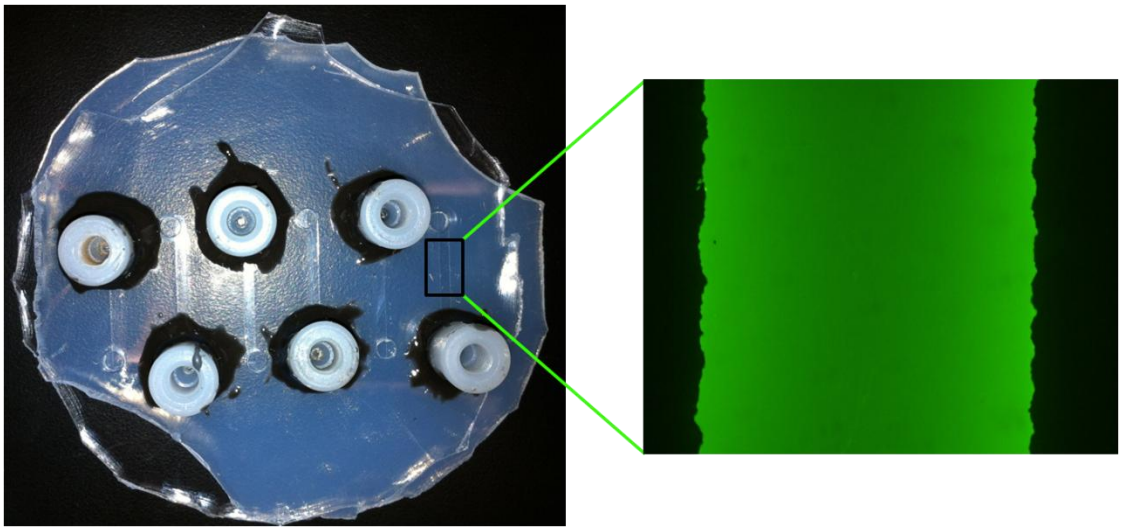

Figure 5.2: Polystyrene sealed to polystyrene device**.** The image on the left shows a two layer device where the bottom layer has channels embedded in PS and the top blank layer containing wells, also PS. These to pieces of PS was thermally sealed together using a heated hydraulic press. To ensure that no channels were obstructed, fluorescein was flowed though the channels, and the representative fluorescent image on the right shoes that the channel is sealed, not leaking.

5.3 Introduction to 3 Dimensional Printing

In this dissertation, PDMS and polystyrene have been discussed as materials for microfluidic devices and the processes by which those devices are photolithography and soft lithography. One of the downsides of conventional photolithography, soft lithography, and hot embossing is the time it takes to go from device design to a final usable device. Additionally, any modifications to the device have to be made at the master level, thereby starting the whole process anew. This, in particular, is a drawback when developing novel devices, where multiple prototypes may be necessary before a final design is decided upon. 3D printing technologies allow for fast device production, and also for designs to be modified and optimized quickly based on the ongoing data collection in the lab.

3D printing has commonly been used in manufacturing industries to produce design prototypes, but recently it has been utilized in the areas of scaffolds for tissue growth,[23-26] prototyping,[27-28] electronics[29], microfluidics[30-31], and pneumatics.[32] 3D printers build a device layer by layer based on "sliced" 3D models that are drawn using a computer program, such as Computer Aided design (CAD).[33-34] In work here, the Objet Connex 350 is used to create all 3D printed devices. The Objet 3D printer constructs the device layer by layer by inkjet deposition of photopolymerizable materials that are hardened by subsequent UV irradiation. The Objet Connex 350 is able to print polymer droplets that are 42 μm in diameter, which allows for features ranging in size from 100 – 1000 μm. Though fluidic devices that allow for mixing[30] and chambers for organic reactions[31] have been fabricated as well as scaffolds allowing for cell growth[25], to date,

no device has been directly printed that incorporates flow, drug transport and cell based techniques together on one 3D printed device. Here we fabricate a 3D printed milli-fluidic device that directly integrates with syringe pumps, allows for drug transport across a membrane, and can be used to study cell viability using commercially available cell inserts. These studies were executed with the help of my fellow graduate student, Sarah Lockwood, who performed all the mass spectrometry studies.

5.3.1 3D Printed Device Fabrication

All 3D printed devices were printed on an Objet Connex 350 printer housed in Department of Electrical and Computer Engineering at Michigan State University. All devices were printed using Objet Vero White Plus material whose composition is proprietary, but contains: isobornyl acrylate (15-30%), acrylic monomer (15-30%), urethane acrylate (15-50%), epoxy acrylate (5-10; 10-15%), acrylic monomer (5-10; 10-15%), acrylic oligomer (5-10; 10-15%) and photoinitiator (0.1-1; 1-2%). Once printed, the devices are opaque, white and rigid. Initial prototypes contained only one channel, but as many as 8 channels on one device have been printed. Using commercially available cell culture inserts (0.4 um pore diameter, Corning Incorporated, Corning, NY, USA), polycarbonate membranes were clicked into place above the channel. The channels are 3.0 mm wide and 1.5 mm deep under the membrane. To integrate the devices with syringes for pumping, the inlet was printed so that a female luer adapter (P-629, IDEX Health and Science, Oak Harbor, WA, USA) could be clicked into place and sealed with quick drying epoxy. In this manner, syringes were hooked up to the device via this adapter and a dual syringe pump was used to flow sample through the channels.

5.3.2 Sample Preparation for Drug Transport

To study drug transport in the 3D printed device, three established drugs, clopidogrel, levofloxacin (Sigma Aldrich, St. Louis, MO, USA)and linezolid (TOCRIS Bioscience, Bristol, United Kingdom), were prepared in standard solutions ranging from 100 to 2000 nM. Clopidogrel was solubilized in 0.1 M HCl, and linezolid and levofloxacin were dissolved in water to prepare 1 mg/mL stock solutions. Using a physiological salt solution (PSS) comprised of 2.0 mM $CaCl_2$, 4.7 mM KCl, 11.1 mM dextrose, 12 mM $MgSO_4$, 21.0 mM tris(hydroxymethyl)aminomethane, and 140.5 mM NaCl (final pH 7.4)(Sigma Aldrich) as a buffer, the stock solutions were diluted to the desired standard concentrations. Standards were then pumped at 1 µL/min through the channels of the 3D device for one hour. In this case, the cell culture inserts that were clicked in above the channel contained 150 µL of PSS and from that aliquots of sample (25 µL) were taken after an hour of pumping. The 25 µL samples were added to 96 µL of cold acetonitrile (Mallinckrodt Chemicals, Phillipsburg, NJ, USA) containing the internal standard, 750 nM ciprofloxacin (Sigma Aldrich). To remove any precipitate, samples were centrifuged (500 g for 10 min) and the supernatant removed. After centrifugation, the samples were added to a polycarbonate PCR plate (Denville, Metuchen, NJ, USA) and sealed using a RapidEPS seal (Bio Chromato, Fujisawa, Japan)

5.3.3 Mass Spectrometric Analysis of Drug Transport

Detection of the drugs was achieved by using a Shimadzu high performance liquid chromatograph (HPLC) coupled with multiple reaction monitoring mass spectrometry (MRM-MS/MS) with electrospray ionization (ESI) using a Waters Quattro

Micro triple quadrupole mass spectrometer. The reverse phase HPLC separation was performed through the use of a Supelco Ascentis precolumn, followed by a packed Supelco Ascentis Express C18 column (length: 3 cm, ID: 2.1 mm, particles: 2.7 µm)(Supelco, Bellefonte, PA, USA). A 10 µL sample from the PCR plate was injected onto the column where it underwent separation at 0.45 mL/min with the corresponding gradient, 95% A, 0% B for 0.25 min; 2% A, 0% B at 1.00 min; 2% A, 0% B at 1.25 min; 30% A, 15% B at 1.75 min; 30% A, 15% B at 1.90 min; 95% A, 0% B at 2.00 min. Solvent A is methanol, solvent B is acetonitrile and solvent C is 1% formic acid in water. Retention times of ciprofloxacin, clopidogrel, levofloxacin and linezolid are 1.51, 2.08, 1.48, and 1.71 minutes, respectively. Upon introduction into the Quattro Micro mass spectrometer, analytes were ionized by ESI and further analyzed using the MRM-MS/MS. The method for detection of ciprofloxacin, clopidogrel, levofloxacin and linezolid involved a cone voltage of 25 V for the internal standard and 30 V for the remaining drugs. Collisional energies for ciprofloxacin, clopidogrel, levofloxacin, and linezolid were 40, 35, 30, and 35 eV, respectively. The MRM transitions monitored were m/z 332.11>231.06 (ciprofloxacin), 322.08>155.03 (clopidogrel), 362.11>234.05 (levofloxacin), and 338.13>296.1 (linezolid). The collision gas, argon, was 1.96×10^{-3} Torr. Quantitative data processing was obtained through Waters MassLynx software (Milford, MA, USA). Calibration curves were generated by taking the ratio of sample peak area to the internal standard peak area.

5.3.4 Endothelial Cell Culture onto Inserts

Bovine pulmonary artery endothelial cells (ECs) were used in all cell studies. The vials were thawed to room temperature and added to a T-75 tissue culture flask containing 9 mL of endothelial growth media (EGM) that had been equilibrated to 37 °C. The EGM consists of a low glucose (5.5 mM) Dulbecco's Modified Eagles Medium (DMEM, MIDSCI, St. Louis, MO, USA) supplemented with 2.5% v/v adult bovine serum (Sigma-Aldrich, St. Louis, MO, USA), 7.5% fetal bovine serum (Lonza, Walkersville, MD, USA), penicillin, streptomycin, and amphotericin B (MIDSCI, St. Louis, MO USA). bPAECs were allowed to grow in a humidified incubator at 37 °C and 5% CO_2 until they were determined as confluent by optical microscopy. Media was changed the day after plating and then every 2 days thereafter. The ECs were subcultured when the cells reached >80% confluence as visualized by optical microscopy. ECs were then seeded onto 6.5 mm cell inserts that contain a permeable polycarbonate membrane (0.4 um pore diameter, Corning Incorporated, Corning, NY, USA). In short, T-75 flasks of ECs were washed with 10 mL of HEPES and then treated with 5 mL of 0.25% trypsin/EDTA, which was then removed and the cells suspended in 10 mL of media. The cell suspension was removed from the flask and centrifuged at 1500 *g* for 5 min. The supernatant was removed and the pellet was resuspended in approximately 2 mL of equilibrated media. Then 100 µL of concentrated cell solution was pipette onto the inserts with 600 µL of media in the lower chamber. The cells were allowed to grow to confluence for 24 hours as visualized by optical microscopy. Cell inserts were then clicked into place above the channels on the 3D printed device and 100 µL of HBSS was pipetted onto the insert.

5.3.5 Sample Preparation and Experimental Procedure for Cell Viability Study

Saponin (Sigma Aldrich) was used to permeabilize EC membranes in order to induce death. A 0.25% solution of saponin was made by dissolving 13.2 mg into 5.28 mL of water. A portion of the 0.25% solution was then diluted to 0.025% in Hank's balanced salt solution (HBSS, Sigma Aldrich). This solution, or HBSS, was then loaded into syringes and flowed through the 3D printed device underneath the cell insert containing cultured ECs, for 30 min. at 1 µl/min using a dual syringe pump. The inserts were then removed from the device and placed into a 24 well plate containing 600 µL HBSS in the lower chamber.

The nucleic acid stain Sytox Green (Invitrogen, Grand Island, NY, USA), which only labels cell with compromised membranes, was used to determine whether or not saponin had killed ECs. Its excitation excitation and emission maxima are 504 and 523 nm, respectively when bound to DNA. After saponin or HBSS was flowed under the cells, 4 µL of 1 µM Sytox Green was added to the cell insert, resulting in a concentration of 40 nM above the cells. The probe was allowed to incubate at 37 ˚C for 30 min. and then imaged using fluorescence microscopy. An Olympus MVX10 macroscope (Olympus America, Melville, NY, USA) was used to collect fluorescence images for each insert and using the MicroSuite Biological Suite software (Olympus America) average pixel intensities of the fluorescence image were obtained. The data from corresponding to the saponin treated cell insert was normalized to the data from the control cell insert with HBSS flowing through the channel.

5.4 Preliminary Results with 3D Printed Device

The device design used in these studies consisted of 8 channels with inlets allowing for sample introduction/syringe pump integration, analytical wells for membrane containing cell culture inserts and outlets for waste as shown in figure 5.3. The side profile of one channel (figure 5.4) shows how each channel will address the membrane allowing for diffusion of analytes from the channel, through the membrane, to the area above the insert. Once printed, the device was used to study drug transport across the membrane.

5.4.1 Drug Transport across a Membrane

Standard samples containing linezolid and levofloxacin were prepared in PSS no BSA buffer. Concentrations of 1.1 and 2 µM standard solutions were introduced to the 3D device through syringes and soft Teflon tubing. The 3D device included a 3 mm channel which lay directly under an open well that was fitted to the cell insert. Upon insertion of the cell insert, buffer was added to the insert and the standard solutions were flowed through the channels for an hour at 1 µL/min. After an hour, liquid was sampled from the insert and added to a vial containing a solution of acetonitrile and the internal standard, ciprofloxacin. The samples were then analyzed using LC/MS/MS to monitor the diffusion of linezolid and levofloxacin from the channel, across the porous membrane into the cell insert. After an hour of flow, the 1.1 µM and 2 µM samples had between

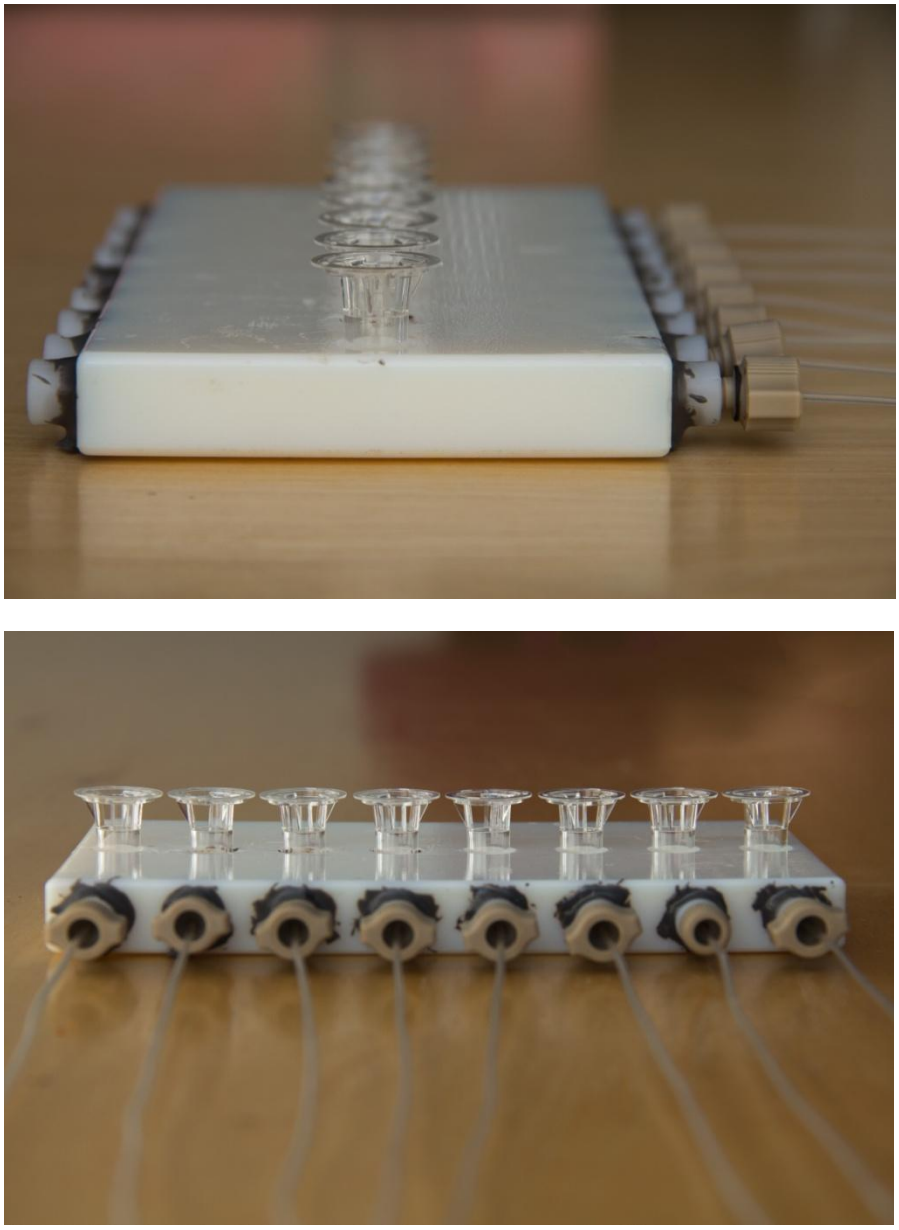

Figure 5.3: 3D printed device. The final 3D printed device contains adapters for syringe based pumps, channels, membrane insertion port and outlets. The top image shows a side view of the device where sample is pumped though the channel via tubing where it flows under the membrane where molecules can diffuse. The bottom image shows the device from the angle of sample entry where all 8 channels of the device can be used simultaneously to address 8 membranes.

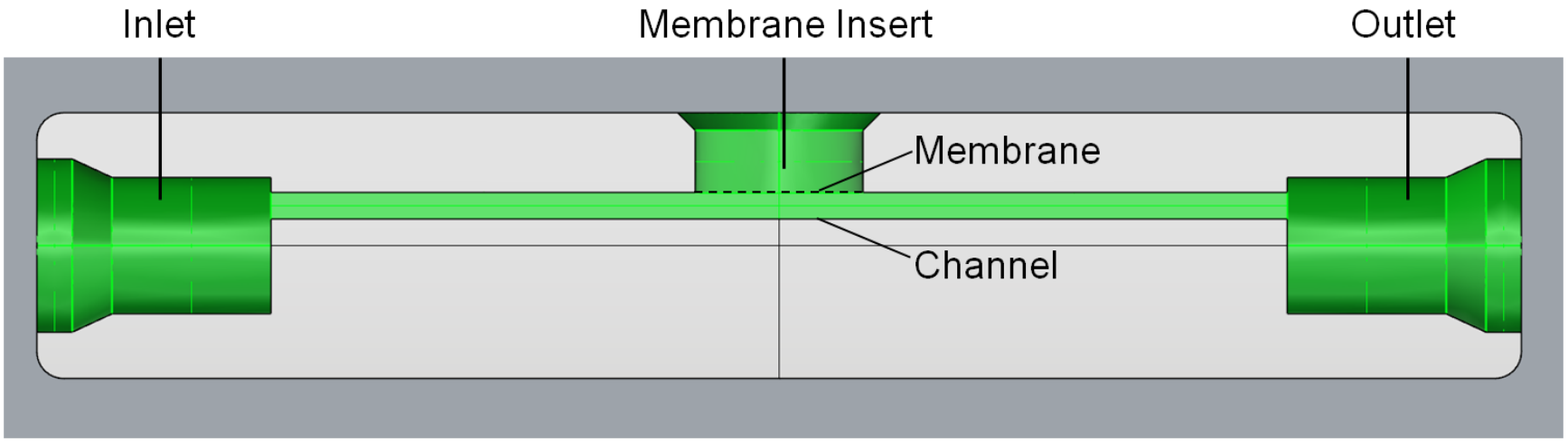

Figure 5.4: 3D printed device side view. The side view of the device shows how the inlet addresses the channel and allows fluid to flow under the membrane. The membrane is part of a commercially available cell insert that is manually inserted into the port on top of the device. Finally, there is an outlet to allow fluid to leave the device.

18.4 % and 20.5% drug transport across the polycarbonate membrane (figure 5.5). Moreover, results yielded reproducible drug transport concentrations between runs furthering the reusability of the device.

In other polymer based devices reusability is not an option due to issues with maintaining seals or the need for resealing devices thought the experiment. Contamination is also a concern due to challenges cleaning devices or absorption of materials into the polymer base. The use of a new device for each experiment can lead to high variability between runs. Also the incorporation of a membrane into the polymer based device, typically reversibly sealed between two pieces, can be easily compromised due to the flexibility of the support material. Cleaning and extended use can also weaken the fragile membrane. The aforementioned strains on conventional fluidic membranes lend virtue to the cell culture insert, which can easily be replaced for additional runs on the same device. The cell insert has a rugged base which supports the membrane and can be easily discarded after use. The rigidity of the 3D device when used simultaneously with the disposable cell insert offers a supportive platform for a reusable fluidic device.

5.4.2 Cell Viability Assessment

Commercially available cell culture inserts were used to integrate the 3D printed device with cultured cells. In this design, the insert clicks into place above the channel and the membrane would contain a layer of cultured cells as visualized in figure 5.6. Furthermore, the ECs were stained with Hoechst dye (ex. 350 nm, em. 460 nm), a simple nucleic acid stain to confirm the presence of a confluent layer of cells on top of the

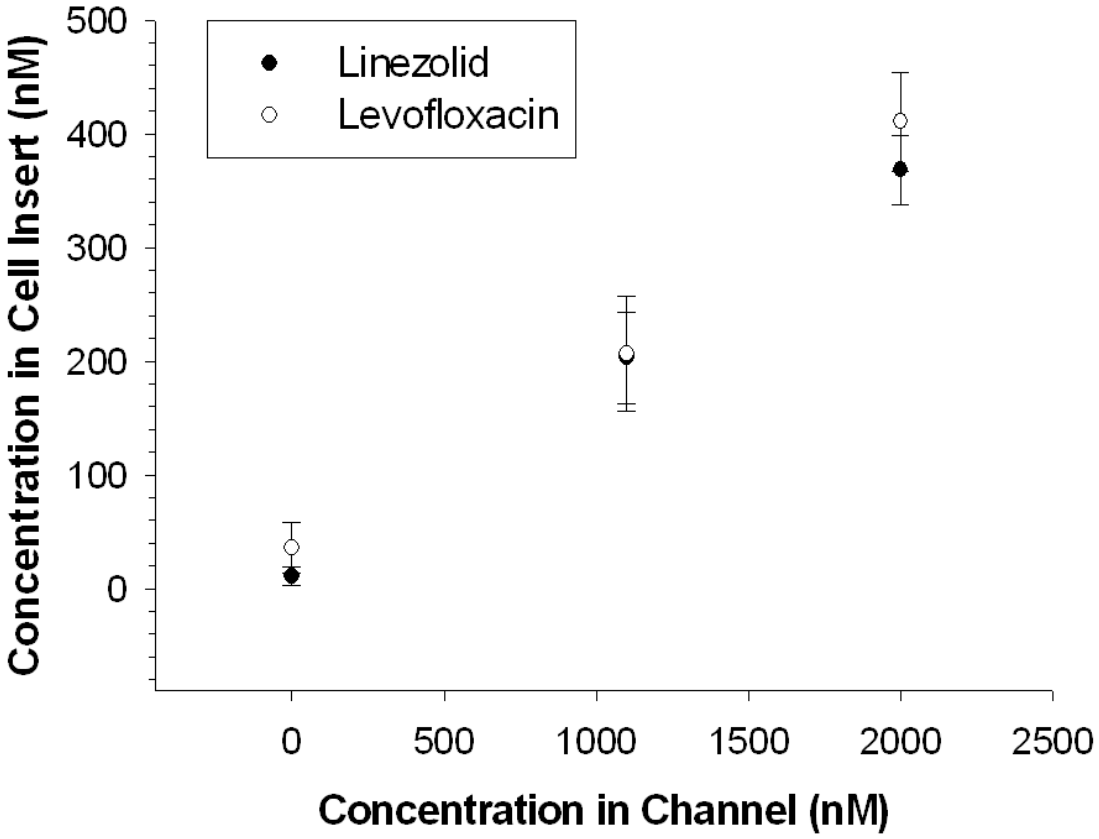

Figure 5.5: Drug transport across a membrane. Standards of the drugs linezolid (N = 4) and levofloxacin (N = 5) were flowed through the channels of the device; samples were collected above the membrane and analyzed via MS. As concentration of the drug increased so, did transport across the membrane with each concentration being statistically different from the previous. (p value < 0.001).

membrane. The image in figure 5.6 was taken from a fluorescence microscope with a DAPI filter and the stained cells are visualized on top of the membrane.

In order to determine whether or not this 3D printed device could be used to study cell activity, a simple viability study was performed. Either HBSS or saponin (kills cells by forming a complex with cholesterol and forming pores in the membrane) was delivered through the channel under the membrane that contained cultured ECs. It was expected that saponin would diffuse through the polycarbonate membrane and come into contact with the ECs. As shown in figure 5.7 A, the ECs that were treated with saponin had almost 5 times more fluorescence than the cells treated with HBSS. The Sytox Green does not stain live cells so; the increased fluorescence indicates a higher population of dead cells. The images from the fluorescence microscope (figure 5.7 B) confirm this fact, as the image of the saponin treated ECs show more fluorescence than the image of ECs treated with HBSS alone.

5.5 Conclusions on 3D Printing

The 3D printed device was capable of studying drug transport and cell viability in a high throughput manner. Furthermore, the device was rugged and reusable, which gives it an advantage over devices made out of soft polymers. Additionally, the ability to rapidly modify and print prototypes is advantageous when optimizing a device design. Experiments on these 3D printed devices are ongoing in the Spence lab with the latest prototype being in 24-well format with threads directly printed on the device in order to integrate pumping mechanisms as shown in figure 5.8.

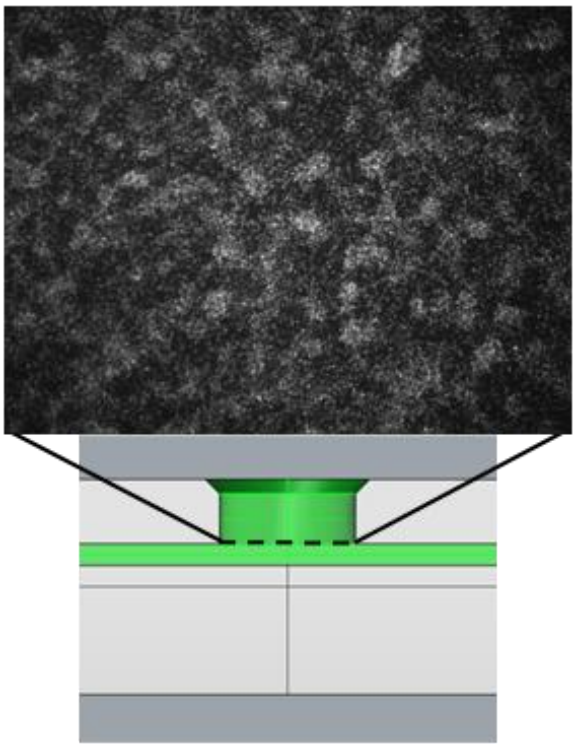

Figure 5.6: Incorporation of endothelial cells on 3D printed device. Endothelial cells were incorporated onto the 3D printed device by culturing them onto the membrane insert. These are commercially available cell inserts well suited for cell culture. Cells were cultured on the inserts and stored in an incubator (37 ˚C, 5% CO_2) until experiments were performed. Cells were labeled with Hoechst dye, a nucleic acid stain, to confirm their presence on the membrane as evidenced in the fluorescent image. Cell inserts were then clicked into place on the device and samples flowed through the channel under the membrane containing cells.

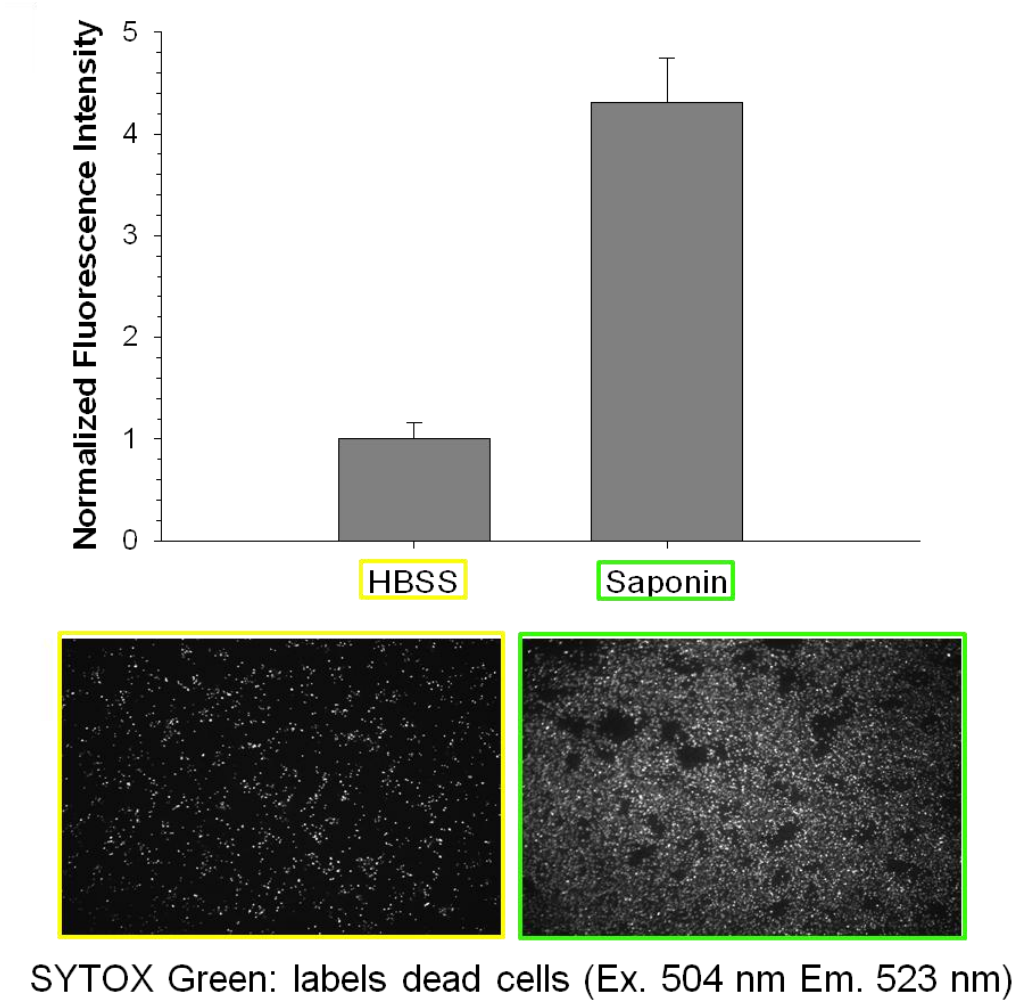

Figure 5.7: Cell viability experiment**.** Saponin, a known cell detergent, was flowed under endothelial cells to induce cell death. Sytox Green, which does not label live cells, was used in order to determine the extent of cell death. The bar graph in part A shows an increase in Sytox Green fluorescence when cells were treated with saponin compared to buffer alone. The fluorescence images in part B represent cells treated with HBSS (left) and cells treated with saponin (right) with the Sytox Green label.

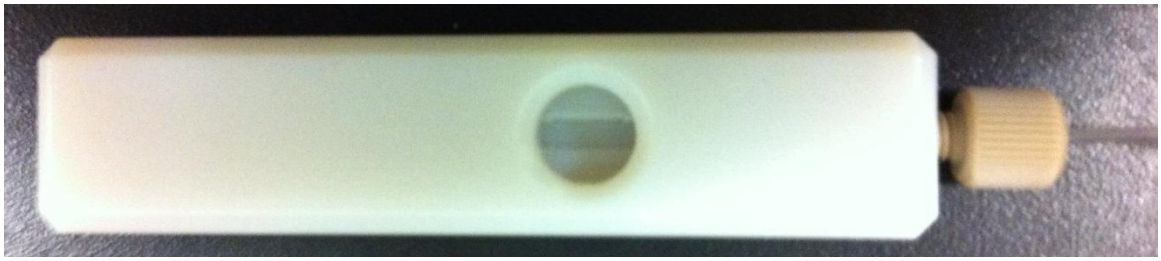

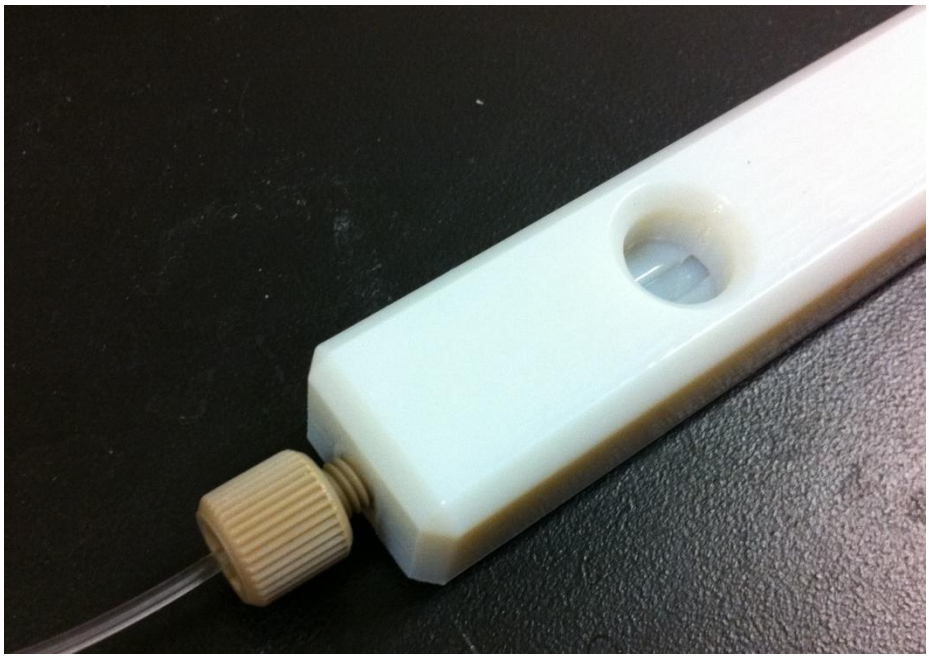

Figure 5.8: Single channel 3D printed device prototype**.** The prototype shown in the top image has the port situated in "24-well plate" format to enable future handling by automated systems. Additionally, the bottom image shows the ability to print threads directly into the device so adapters can be screwed in without the need of an additional adapter or to seal with epoxy.

REFERENCES

REFERENCES

1. C. Y. Fung, C. A. Brearley, R. W. Farndale, M. P. Mahaut-Smith, A major role for P2X1 receptors in the early collagen-evoked intracellular Ca2+ responses of human platelets. *Thromb Haemost* 2005, *94*. 37-40.

2. C. Y. E. Fung, A. J. Marcus, M. J. Broekman, M. P. Mahaut-Smith, P2X1 Receptor Inhibition and Soluble CD39 Administration as Novel Approaches to Widen the Cardiovascular Therapeutic Window. *Trends Cardiovasc. Med.* 2009, *19*. 1-5.

3. W. Karunarathne, C. J. Ku, D. M. Spence, The dual nature of extracellular ATP as a concentration-dependent platelet P2X1 agonist and antagonist. *Integr Biol* 2009, *1*. 655-663, DOI: Doi 10.1039/B909873a.

4. S. Letourneau, L. Hernandez, A. N. Faris, D. M. Spence, Evaluating the effects of estradiol on endothelial nitric oxide stimulated by erythrocyte-derived ATP using a microfluidic approach. *Anal. Bioanal. Chem.* 2010, *397*. 3369-75, DOI: 10.1007/s00216-010-3687-7.

5. H. P. Wright, R. H. Thompson, K. J. Zilkha, Platelet adhesiveness in multiple sclerosis. *Lancet* 1965, *2*. 1109-10.

6. K. I. Ataga, E. P. Orringer, Hypercoagulability in sickle cell disease: a curious paradox. *Am. J. Med.* 2003, *115*. 721-728.

7. R. B. Francis, Jr., Platelets, coagulation, and fibrinolysis in sickle cell disease: their possible role in vascular occlusion. *Blood Coagul Fibrinolysis* 1991, *2*. 341-53.

8. B. P. O'Sullivan, M. D. Linden, A. L. Frelinger, III, M. R. Barnard, M. Spencer-Manzon, J. E. Morris, R. O. Salem, M. Laposata, A. D. Michelson, Platelet activation in cystic fibrosis. *Blood* 2005, *105*. 4635-4641.

9. R. S. Sprague, M. L. Ellsworth, A. H. Stephenson, M. E. Kleinhenz, A. J. Lonigro, Deformation-induced ATP release from red blood cells requires CFTR activity. *American Journal of Physiology* 1998, *275*. H1726-H1732.

10. A. I. Vinik, T. Erbas, T. S. Park, R. Nolan, G. L. Pittenger, Platelet dysfunction in type 2 diabetes. *Diabetes Care* 2001, *24*. 1476-1485.

11. J. Carroll, M. Raththagala, W. Subasinghe, S. Baguzis, T. D. a. Oblak, P. Root, D. Spence, An altered oxidant defense system in red blood cells affects their ability to release nitric oxide-stimulating ATP. *Mol. BioSyst.* 2006, *2*. 305-311.

12. L. Somova, J. Mufunda, Platelet activity and salt sensitivity in the pathogenesis of systemic (essential) hypertension in black Africans. *Clin Exp Hypertens* 1993, *15*. 781-96.
13. R. S. Sprague, A. H. Stephenson, M. L. Ellsworth, C. Keller, A. J. Lonigro, Impaired release of ATP from red blood cells of humans with primary pulmonary hypertension. *Exp. Biol. Med. (Maywood, NJ, U. S.)* 2001, *226*. 434-439.

14. K. B. Anderson, W. Karunarathne, D. M. Spence, Measuring P2X1 receptor activity in washed platelets in the absence of exogenous apyrase. *Anal Methods-Uk* 2012, *4*. 101-105, DOI: Doi 10.1039/C1ay05530e.

15. E. D. Rosen, S. Raymond, A. Zollman, F. Noria, M. Sandoval-Cooper, A. Shulman, J. L. Merz, F. J. Castellino, Laser-induced noninvasive vascular injury models in mice generate platelet- and coagulation-dependent thrombi. *Am. J. Pathol.* 2001, *158*. 1613-1622.

16. H. Matsuno, T. Uematsu, S. Nagashima, M. Nakashima, Photochemically Induced Thrombosis Model in Rat Femoral-Artery and Evaluation of Effects of Heparin and Tissue-Type Plasminogen-Activator with Use of This Model. *J Pharmacol Methods* 1991, *25*. 303-317, DOI: Doi 10.1016/0160-5402(91)90030-9.

17. P. J. Marc, C. E. Sims, M. Bachman, G. P. Li, N. L. Allbritton, Fast-lysis cell traps for chemical cytometry. *Lab on a Chip* 2008, *8*. 710-716, DOI: Doi 10.1039/B719301g.

18. K. B. Anderson, S. T. Halpin, A. S. Johnson, R. S. Martin, D. M. Spence, Integration of multiple components in polystyrene-based microfluidic devices part II: cellular analysis. *Analyst (Cambridge, United Kingdom) 138*. 137-143.

19. A. S. Johnson, K. B. Anderson, S. T. Halpin, D. C. Kirkpatrick, D. M. Spence, R. S. Martin, Integration of multiple components in polystyrene-based microfluidic devices part I: fabrication and characterization. *Analyst (Cambridge, United Kingdom) 138*. 129-136.

20. J. A. Bilello, G. Bauer, M. N. Dudley, G. A. Cole, G. L. Drusano, Effect of 2',3'-Didehydro-3'-Deoxythymidine in an in-Vitro Hollow-Fiber Pharmacodynamic Model System Correlates with Results of Dose-Ranging Clinical-Studies. *Antimicrob Agents Ch* 1994, *38*. 1386-1391.

21. S. L. Preston, P. J. Piliero, J. A. Bilello, D. S. Stein, W. T. Symonds, G. L. Drusano, In vitro-in vivo model for evaluating the antiviral activity of amprenavir in combination with ritonavir administered at 600 and 100 milligrams, respectively, every 12 hours. *Antimicrob Agents Ch* 2003, *47*. 3393-3399, DOI: Doi 10.1128/Aac.47.11.3393-3399.2003.

22. G. L. Drusano, P. A. Bilello, W. T. Symonds, D. S. Stein, J. McDowell, A. Bye, J. A. Bilello, Pharmacodynamics of abacavir in an in vitro hollow-fiber model system. *Antimicrob Agents Ch* 2002, *46*. 464-470, DOI: Doi 10.1128/Aac.46.2.464-470.2002.

23. J. N. H. Shepherd, S. T. Parker, R. F. Shepherd, M. U. Gillette, J. A. Lewis, R. G. Nuzzo, 3D Microperiodic Hydrogel Scaffolds for Robust Neuronal Cultures. *Adv. Funct. Mater.* 2011, *21*. 47-54, DOI: DOI 10.1002/adfm.201001746.

24. Y. B. Lee, S. Polio, W. Lee, G. H. Dai, L. Menon, R. S. Carroll, S. S. Yoo, Bio-printing of collagen and VEGF-releasing fibrin gel scaffolds for neural stem cell culture. *Exp Neurol* 2010, *223*. 645-652, DOI: DOI 10.1016/j.expneurol.2010.02.014.

25. W. Lee, V. Lee, S. Polio, P. Keegan, J. H. Lee, K. Fischer, J. K. Park, S. S. Yoo, On-Demand Three-Dimensional Freeform Fabrication of Multi-Layered Hydrogel Scaffold With Fluidic Channels. *Biotechnol. Bioeng.* 2010, *105*. 1178-1186, DOI: Doi 10.1002/Bit.22613.

26. A. Butscher, M. Bohner, S. Hofmann, L. Gauckler, R. Muller, Structural and material approaches to bone tissue engineering in powder-based three-dimensional printing. *Acta Biomater* 2011, *7*. 907-920, DOI: DOI 10.1016/j.actbio.2010.09.039.

27. J. Stampfl, R. Liska, New materials for rapid prototyping applications. *Macromol Chem Physic* 2005, *206*. 1253-1256, DOI: DOI 10.1002/macp.200500199.

28. D. S. Rangel, Claire; Bielschowsky, Mayra; Farris, Katie; Falconer, Ruth; Baveye, Philippe Rapid Prototyping and 3-D Printing of Experimental Equipment in Soil Science Research *Soil Sci Soc Am J* 2012, *77*. 54-59.

29. B. Y. Ahn, E. B. Duoss, M. J. Motala, X. Y. Guo, S. I. Park, Y. J. Xiong, J. Yoon, R. G. Nuzzo, J. A. Rogers, J. A. Lewis, Omnidirectional Printing of Flexible, Stretchable, and Spanning Silver Microelectrodes. *Science* 2009, *323*. 1590-1593, DOI: DOI 10.1126/science.1168375.

30. D. Therriault, S. R. White, J. A. Lewis, Chaotic mixing in three-dimensional microvascular networks fabricated by direct-write assembly. *Nat. Mater.* 2003, *2*. 265-271, DOI: Doi 10.1038/Nmat863.

31. P. J. Kitson, M. H. Rosnes, V. Sans, V. Dragone, L. Cronin, Configurable 3D-Printed millifluidic and microfluidic 'lab on a chip' reactionware devices. *Lab on a Chip* 2012, *12*. 3267-3271, DOI: Doi 10.1039/C2lc40761b.

32. F. Ilievski, A. D. Mazzeo, R. E. Shepherd, X. Chen, G. M. Whitesides, Soft Robotics for Chemists. *Angew Chem Int Edit* 2011, *50*. 1890-1895, DOI: DOI 10.1002/anie.201006464.

33. E. Sachs, M. Cima, P. Williams, D. Brancazio, J. Cornie, 3-Dimensional Printing - Rapid Tooling and Prototypes Directly from a Cad Model. *J Eng Ind-T Asme* 1992, *114*. 481-488.

34. W. Sun, B. Starly, J. Nam, A. Darling, Bio-CAD modeling and its applications in computer-aided tissue engineering. *Comput Aided Design* 2005, *37*. 1097-1114, DOI: DOI 10.1016/j.cad.2005.02.002.